University of Kentucky
UKnowledge

Theses and Dissertations--Plant Pathology | Plant Pathology

2020

VIRUS-INDUCED CHANGES IN NUCLEAR PROTEINS AND MEMBRANES IN *NICOTIANA BENTHAMIANA* CELLS

Caleb Mathias
University of Kentucky, mathiascaleb@uky.edu
Author ORCID Identifier:
https://orcid.org/0000-0001-9268-3707
Digital Object Identifier: https://doi.org/10.13023/etd.2020.443

Right click to open a feedback form in a new tab to let us know how this document benefits you.

Recommended Citation

Mathias, Caleb, "VIRUS-INDUCED CHANGES IN NUCLEAR PROTEINS AND MEMBRANES IN *NICOTIANA BENTHAMIANA* CELLS" (2020). *Theses and Dissertations--Plant Pathology*. 30.
https://uknowledge.uky.edu/plantpath_etds/30

This Master's Thesis is brought to you for free and open access by the Plant Pathology at UKnowledge. It has been accepted for inclusion in Theses and Dissertations--Plant Pathology by an authorized administrator of UKnowledge. For more information, please contact UKnowledge@lsv.uky.edu.

STUDENT AGREEMENT:

I represent that my thesis or dissertation and abstract are my original work. Proper attribution has been given to all outside sources. I understand that I am solely responsible for obtaining any needed copyright permissions. I have obtained needed written permission statement(s) from the owner(s) of each third-party copyrighted matter to be included in my work, allowing electronic distribution (if such use is not permitted by the fair use doctrine) which will be submitted to UKnowledge as Additional File.

I hereby grant to The University of Kentucky and its agents the irrevocable, non-exclusive, and royalty-free license to archive and make accessible my work in whole or in part in all forms of media, now or hereafter known. I agree that the document mentioned above may be made available immediately for worldwide access unless an embargo applies.

I retain all other ownership rights to the copyright of my work. I also retain the right to use in future works (such as articles or books) all or part of my work. I understand that I am free to register the copyright to my work.

REVIEW, APPROVAL AND ACCEPTANCE

The document mentioned above has been reviewed and accepted by the student's advisor, on behalf of the advisory committee, and by the Director of Graduate Studies (DGS), on behalf of the program; we verify that this is the final, approved version of the student's thesis including all changes required by the advisory committee. The undersigned agree to abide by the statements above.

Caleb Mathias, Student

Dr. Michael M. Goodin, Major Professor

Dr. Rick Bennett, Director of Graduate Studies

VIRUS-INDUCED CHANGES IN NUCLEAR PROTEINS AND MEMBRANES IN *NICOTIANA BENTHAMIANA* CELLS

THESIS

A thesis submitted in partial fulfillment of the
Requirements for the degree of Master of Science in the
College of Agriculture, Food and Environment
At the University of Kentucky

By

Caleb Mathias

Lexington, Kentucky

Director: Dr. Michael M. Goodin, Professor of Plant Pathology

Lexington, Kentucky

2020

Copyright © Caleb Mathias 2020
https://orcid.org/0000-0001-9268-3707

ABSTRACT OF THESIS

VIRUS-INDUCED CHANGES IN NUCLEAR PROTEINS AND MEMBRANES IN *NICOTIANA BENTHAMIANA* CELLS

Viruses rely on host proteins to complete their life cycles. This results in alterations to normal cell physiology to processes which benefit viral processes such as replication and movement to other cells. This may involve the relocalization of host proteins away from their original subcellular targets to sites which may benefit the virus, a process that is not as well understood as it relates to the nucleus. To identify nuclear proteins that may be involved in such processes, a library of random *Nicotiana benthamiana* cDNAs were expressed as GFP fusions in a transgenic marker lines expressing a histone 2B:RFP nuclear marker. Of the 1,087 proteins screened, 355 were found to be associated with the nucleus. These nuclear proteins were then expressed in plants infected with sonchus yellow net virus (SYNV), a betanucleorhabdovirus which forms its replication complex in the nucleus. Of the 355 nuclear-associated proteins, 16 were found to relocalize in response to SYNV infection, and to test if this phenomenon was virus-specific, these proteins were then expressed in plants infected with tobacco etch virus (TEV), a potyvirus which replicates in the cytoplasm. Of these 16 proteins, 6 were found to show both general and virus-specific localization patterns between the two viruses. To gain insight into the cellular tropism of SYNV, a cell map was generated in order determine the effect of this virus on membranes in *N. benthamiana* tissues. Finally, sowthistle yellow vein virus (SYVV), another betanucleorhabdovirus and classical model virus, was identified in the wild for the first time in over 30 years. Sequence and phylogenetic analysis confirmed the identity of this virus with historical laboratory isolates. The availability of SYVV will facilitate future studies that compare the effect of rhabdovirus infection on host nuclear proteins and membranes.

KEYWORDS: Rhabdovirus, plant viruses, protein localization, relocalization, nuclear proteins, microscopy

Caleb Mathias

11/23/2020

Date

VIRUS-INDUCED CHANGES IN NUCLEAR PROTEINS AND MEMBRANES IN *NICOTIANA BENTHAMIANA* CELLS

By
Caleb Mathias

Dr. Michael M. Goodin
Director of Thesis

Dr. Rick Bennett
Director of Graduate Studies

11/23/2020
Date

ACKNOWLEDGEMENTS

I have several individuals to express my gratitude towards for the completion of this thesis. First and foremost, to my academic advisor, Dr. Michael M. Goodin for his insight, instruction, and time for the duration of my research. I am grateful for the opportunity to have worked and learned under his direction on this project and to further the important work conducted in his laboratory. Similarly, I would like to recognize my committee: Dr. Rebecca Dutch, Dr. Arthur Hunt, and Dr. Peter Nagy, for their time and knowledge.

Next, I would like to thank Dr. Renyuan Wang for his phenomenal assistance and guidance as a laboratory technician, both in preparation of laboratory materials and advice in procedural setup. My education has been enriched in part because of how generously he shared his scientific expertise. Additionally, I would like to thank any faculty staff, and students who provided help during experimentation.

I would like to especially thank the laboratories of Dr. David Zaitlin (KTRDC) and Dr. Drake Stenger (USDA ARS) for the resources and opportunities they provided during my project.

Finally, I would like to thank my family for their support and encouragement over the course of my education. I would not be where I am without them.

TABLE OF CONTENTS

LIST OF TABLES

LIST OF FIGURES

Chapter 4

Chapter 1

Literature review

An overview of nuclear structure

Nucleocytoplasmic transport involves the exchange of macromolecules across the nuclear envelope and is a critical function of eukaryotic cells. It plays a central role in signaling, gene expression, and stress response. The nuclear envelope (NE) serves as a barrier between the nucleoplasm and cytoplasm and is comprised of the inner nuclear membrane (INM) and outer nuclear membrane (ONM), the latter of which is contiguous with the endoplasmic reticulum (ER). The INM and ONM are separated by the lumen, or perinuclear space, and they are fused at numerous channels called nuclear pore complexes (NPCs) (Fichtman et al., 2010). These NPCs form a channel which allows for either the active or passive transport of macromolecules between the nucleus and cytoplasm (Cohen et al., 2002; D'Angelo et al., 2006).

While size, number, and individual protein components may vary in different organisms, there are several conserved structural motifs which are as follows: a) eight filaments which extend from an outer ring on the NPC into the cytoplasm, b) another ring on the nuclear end of the pore with another eight filaments which extend into the nucleoplasm and form an enclosed nuclear basket, and C) an octagonal channel linking the two rings which contains a central pore ring (Beck and Hurt, 2016; Mohammad and Mofrad, 2008; Panté and Aebi, 1993).

NPCs are the largest macromolecular structures found in cells, upwards of 30 times the size of a ribosome (Tamura and Hara-Nishimura, 2013; Vashu and Forbes, 2001). The

typical NPC mass in nuclei of vertebrates is approximately 112 MDa with a distribution of 60 NPCs per μm^{-2} in *Xenopus laevis* oocytes and 50 NPCs per μm^2 in plants, the former of which is considered to be densely spaced (Boruc et al., 2012; Meier and Brikljacic, 2009). From a dimensional perspective, the outer diameter of the human NPC is ~1,200 Å with an inner diameter of ~425 Å and a height of ~800 Å (Lin and Hoelz, 2019). Yeast (*Saccharomyces cerevisiae)* NPCs are smaller, with a mass of ~52 MDa and similar diameters but a shorter height of ~640 Å (Kim et al., 2018; Meier et al., 2017). Plant NPCs have not received the same attention as their vertebrate and yeast counterparts, though some early work had been done with the likes of sycamore and bean, finding that the plant NPCs are typically 1159x640 Å (Roberts and Northcote, 1970). This was the most recent microscopic data on the plant NPC for nearly four decades until field emission electron scanning microscopy was used to further characterize the ultrastructure, finding much conservation of structure to vertebrate NPCs (Fiserova et al., 2009).

NPCs of all eukaryotes share an eightfold rotational symmetry (Meier et al., 2017). The dimensional differences can largely be attributed to the individual protein subunits of the NPCs, called nucleoporins (Nups), and are central to understanding the underlying mechanisms of how the NPC operates at a functional level. In vertebrates, the NPC is composed of 500-1000 individual Nup subunits, though only around 30 of these are unique, so each subunit is usually present in multiple copies (Vasu and Forbes, 2001). Initial estimates put the repeat numbers in the range of 8-56 copies per pore (Vasu and Forbes, 2001), though more contemporary work has put this at 16 copies for yeast (Rajoo et al., 2018), whereas in humans these copy numbers can vary between 8, 16, or 32 copies depending on the structural region of the pore (Ori et al., 2013). Despite poor sequence

homology between Nups of plants, vertebrates, and yeast, the general structure and shape has led to maps and classes of Nups within the NPC to be created (Albert et al, 2007; Brohawn et al., 2009; Tamura et al., 2010).

While there are variations in how the different components are commonly labeled, there are three general subdomains: 1) membrane Nups, 2) scaffold Nups, and 3) barrier Nups (Onischenko and Weis, 2012). The membrane Nups are sometimes referred to as transmembrane Nups due to their anchoring of the NPC to the pore membrane and nuclear envelope (Tamura et al., 2013). In plants, the 210 kDa glycoprotein (Gp210) (Gerace et al., 1982; Greber et al., 1990) and nuclear division cycle 1 (NDC1) (Wozniak et al., 1994) form an outer transmembrane ring (Temura et al., 2013). Vertebrate Nups are quite similar to plant Nups in this regard (Hallberg et al. 1993).

The scaffold subdomain connects the membrane and barrier layers while serving as a Nup-rich skeletal structure (Onischenko and Weis, 2012; Temura et al., 2013). In addition, there are three complexes comprising the scaffold, which include the outer rings (cytoplasmic and nuclear), inner ring, and linker Nups, which are often classified as part of the inner ring (Hayama et al., 2017; Temura et al., 2013). The inner ring of plant NPCs is composed of Nup205, Nup188, Nup155, and Nup35 (Temura et al., 2010; 2013). The outer ring of plant NPCs contains Nup160, Nup133, Nup107, Nup96, Nup85, Nup43, Sec13, and SEH1 (“Y-complex” in yeast and vertebrates) (Tamura et al., 2010; 2013; Wiermer et al., 2012; Xu and Meier, 2008). Lastly, the linker Nups include Nup93 and Nup88 in both plants and vertebrates (Alber et al., 2007; Temura et al., 2013).

The final group to consider are the barrier Nups, which are arguably some of the most important as they mediate the selective transport of the NPC (Temura et al., 2013). These

Nups contain phenylalanine-guanine-rich (FG)-repeats and form specific interactions with karyopherins (Onischenko and Weis, 2012; Weis, 2007). A suggested model for the selectivity of the FG-Nups in the inner pore form an 'oily spaghetti' model, which predicts that the FG-Nups take a somewhat disordered accumulation that can be pushed aside by active transport complexes (Macara, 2001; Weis, 2007). There are also three subdomains of this group, which include the cytoplasmic and nuclear FG-Nups as well as the central FG-Nups (Temura et al., 2013). The central FG-Nups are fairly conserved across plants and vertebrates, including Nup98, Nup62, Nup58 (Nup58/45 in vertebrates), Nup54, and Nup35 (Alber et al., 2007; Temura et al., 2013). Nup62 (Nsp1 in yeast) has been identified in *Arabidopsis* and is believed to contribute to the auxin signaling pathway after a mutant study revealed growth defects, which suggests that FG-Nups may play important roles in plant development (Boeglin et al., 2016; Temura et al., 2013). Table 1.1 provides a summary of Nups and their locations in plants, yeast, and vertebrates.

Summary of active transport

Active transport of macromolecules into and out of the nucleus is driven by a family of transport factors known as karyopherins, with importin being the karyopherin responsible for nuclear uptake and exportin for nuclear export (Conti and Izaurralde et al., 2001; Görlich et al., 1994). In the classical import pathway, importin-α binds to a cargo protein containing a nuclear localization signal (NLS) in the cytoplasm (Freitas and Cunha, 2009; Lange et al., 2007). NLSs were first identified in the large T antigen of simian virus 40 (SV40), in which the amino acid sequence was PKKKRKV (Kalderon et al., 1984). This would be referred to as a classical NLS (cNLS) in later years (Rihs et al., 1991). Four years after Kalderon et al.

published their work, a bipartite cNLS would be identified and become the second cNLS, KRPAATKKAGQAKKKK (Dingwall et al., 1988).

After cargo binding, importin-α binds to the importin beta binding (IBB) domain of importin-β, resulting in the importin-α/cargo/importin- β trimeric complex (Lange et al., 2007). Importin-β then forms a series of interactions with the Nups in the NPC, starting with Nup358 on the cytoplasmic filaments, Nup153 on the nucleoplasmic side of the NPC, with Nup62 in the central channel mediating the transfer (Ben-Efraim and Gerace, 2001). Once in the nucleus, RanGTP binds to importin-β, which proceeds to induce a conformational change that releases the cargo from importin-α (Riddick and Macara, 2005). One complex, composed of importin-β and RanGTP, gets exported to the nucleus and disassembled via hydrolysis of RanGTP to RanGDP (Kabachinski and Schwartz, 2015). By contrast, the now NLS-free importin-α binds to the exportin cellular apoptosis susceptibility protein (CAS) to be exported back into the cytoplasm with RanGTP as well (Görlich and Kutay, 1999). A kinetic analysis revealed 800 translocations per second of a 100 kDa protein through the NPC (Ribbeck and Gorlich, 2001). For a summary of nuclear import and export, refer to Figure 1.1.

Viral infection and the host nucleus

Viruses have evolved a remarkable ability to target host cell proteins and structures. The hijacking of host cellular machinery serves purposes ranging from replication to inter- and intracellular movement and are essential to the viral life cycle. This is especially true for RNA viruses, which typically have smaller genomes than their DNA counterparts, and thus rely heavily on host factors for facilitating their replication and movement (Hiscox, 2007). It is therefore important to consider that regardless of where a virus may replicate within the

cell, a number of subcellular loci are often targeted by viral proteins and protein complexes in order to subvert host factors in a manner that favors viral processes. With positive-stranded RNA viruses, this often involves forming replication complexes on host cell membranes, which are commonly derived from organelles, resulting in the subversion host cell functions for the purpose of their life cycle (Nagy and Pogany, 2011).

Given that the nucleus serves as the center of genetic regulation, cell signaling, and RNA, it plays a central role many viral processes (Gorski and Misteli, 2005; Guo and Wang, 2014). This is particularly reviewed in the literature for DNA viruses due to the abundance of them that replicate in the nucleoplasm (Cohen et al., 2011; Schmid et al., 2014). While RNA viruses such as retroviruses and those of the family *Orthomyxoviridae* replicate within the nucleus, other RNA viruses which replicate in the cytoplasm may still require a sequestration of nuclear proteins towards regions of cytoplasmic replication, or hijack import machinery in order to gain traverse the nuclear pore complex and enter the nucleus.

While there are a multitude of nuclear host factors which RNA viruses may use upon entry in the host cell, the general function and purposes for targeting such factors can be grouped into several categories. The largest category involves the manipulation of nucleocytoplasmic transport, either for the import and export of viral proteins or to regulate host gene expression via blocking of the NPC (Le Sage and Mouland, 2013). Other categories may include targeting nuclear-associated proteins directly for virus-related purposes (Meng et al., 2019), or taking advantage of substructures within the nucleus (Balinsky et al., 2013; Hiscox, 2007). Thus, it is an important feature of the viral infection cycle that viruses or their individual proteins are able to overcome selective barriers within the cell, such as the NPC.

There are a number of ways in which viruses may gain entry into the nucleus. Certain viruses, such as murine leukemia virus (MLV), bind to host chromatin during mitosis when the nuclear envelope has degraded in order to enter the nucleus and integrate into host genomes (Aydin and Schelhaas, 2016; Di Nunzio et al., 2013; Flatt and Greber, 2015; Lewis and Emerman, 1994; Rein, 2013). This is in contrast to lentiviruses, whose genomes must traverse the selective barrier of the NPC (Flatt and Greber, 2015). This requires interactions with a series of Nups and other host proteins which are involved in uncoating, moving, and integrating the viral genome into their respective hosts. This may also entail altering nuclear pore architecture or sequestering host proteins away from their original locations in a manner in which may benefit viral entry.

HIV-1 is a well-characterized example of a virus which interacts with a variety of Nups as part of its nuclear entry process. The HIV core has been found to bind to Nup153 to facilitate nuclear import of the capsid-nucleocapsid hexamer complex and Nup98, which likely plays a role in integration (Di Nunzio et al., 2013). This interaction is significant as it not only illustrates an example of nuclear protein targeting for viral entry, but also the retroviral requirement for integration into host chromatin (Kane et al., 2018). In more recent years, it has been demonstrated that the kinesin-1 motor protein, KIF5B, is involved in relocalization of Nup358 into the cytoplasm. Though the exact function of Nup358 in HIV-1 NPC entry is not known, it is possible that it serves to link the viral capsid to KIF5B as similar observations have been made in adenoviruses (Dharana et al., 2016; Strunze et al., 2011). One such explanation for this uncoating that has been suggested is the “tug of war” model, which postulates that KIF5B pulls the viral capsid in opposite directions along a microtubule, thus freeing the cargo (Lukic et al., 2014).

Naturally, viruses which require entry into the nucleus may have many conserved Nup targets. For example, HSV-1 has also been found to dock at Nup214 and Nup358, though RNA interference (RNAi) studies have provided more evidence for the latter (Fay and Panté 2015) but has also led some to believe that this may be a sign of a complex interaction between all three (Le Sage et al., 2013; Pasdeloup et al., 2009). As will be demonstrated later, these Nups are common targets in viral infection, and therefore may provide opportunities for the creation of more specific antivirals. This can become especially important when considering viruses which replicate in the nucleus as an inhibition of replication would greatly hamper the infection cycle.

Influenza A virus (IAV) is unique from many other RNA viruses in that it replicates its genome within the nucleus. Because of this, it is heavily dependent on interactions with nuclear import machinery. The viral nucleocapsids contain a genome composed of eight single-stranded negative-sense RNAs (Kobilier et al., 2012; Whittaker et al., 1996). Upon clathrin-mediated endocytosis and pH-dependent release of the viral ribonucleoprotein (vRNP) from the virion into the cytoplasm where it is imported into the nucleus via the classical importin- α/β pathway. (Kobilier et al., 2012; Le Sage and Mouland, 2013; Martin and Helenius, 1991).

While components of the vRNP have been determined to have NLSs, the NP has been found to be the minimal driving factor of the nuclear import process (Kobiler et al., 2012; O'Neill et al., 1995). The NP contains two NLSs, NLS1 and NLS2, with the former being located at the N terminus spanning residues 1-13 and the latter being located in the middle and spanning residues 198-216 (Cros et al., 2005; Wang et al., 1997; Wu et al., 2017). NLS1 binds weakly to the minor NLS-binding pocket of importin-α, and this interaction has been

implicated in facilitating the nuclear import of the vRNP via the importin-α/β pathway (Cros et al., 2005; Nakada et al., 2015; Wang et al., 1997), with Wu et al. (2017) suggesting that NLS2 could function alongside NLS1 to assist in the binding of importin-α and subsequent nuclear import. Additionally, Miyake et al. (2019) recently discovered that the nuclear import factor transportin 1 (TNPO1) binds to the proline-tyrosine nuclear localization signal (PY-NLS) of the matrix protein (M1) to facilitate its removal from the vRNP, adding a second importin-β to the nuclear import process. These types of interactions with nuclear import machinery are vital to host specificity as the NP and PB2 of mammalian and avian influenza viruses have been found to require interactions with different importin-α isoforms (Gabriel et al., 2011).

Much of the work done to identify NPC components involved in the transport of the vRNPs of IAV into the host nucleus have been conducted via RNAi screening. Karlas et al. (2010) conducted a genome-wide RNAi screen and determined that Nup98 and Nup205 were implicated in IAV replication efficiencies. In another study, Nup153 and Nup214 were also found to have a negative effect on IAV viral replication during RNAi, likely due to their role in the import of viral RNA (vRNA) into the nucleus (König et al., 2010). In a manner similar to HIV-1, IAV has also been found to induce the cytoplasmic relocalization of Nup62 from the NPC core for purposes of vRNA export, and has been demonstrated to be required for viral replication (Le Sage and Mouland, 2013; Morita et al., 2013; Monette et al, 2011; Munier et al., 2013).

Relocalization of NPC components are important in viral replication and import/export pathways of which Hepatitis C virus (HCV) provides an example. Neufeldt et al. (2013) found an increase in cytoplasmic signals of Nup358, Nup155, Nup53, Nup153, and Nup98

during HCV infection. Specifically, they are translocated to the membranous web, which is the replication compartment induced by the HCV NS4B protein using the host endoplasmic reticulum (ER) (Egger et al., 2002; Pawlotsky et al., 2007). This recruitment of Nups to the membranous web as implications for membrane curvature and transport of nuclear proteins into and out of the replication compartment, the latter of which is further evidenced by the presence of NLS and NES sequences on some HCV proteins (Germain et al., 2014; Levin et al., 2014; Neufeldt et al., 2013).

Vesicular stomatitis virus (VSV) is a well-studied example of a virus which limits nucleocytoplasmic transport. VSV is a single-stranded RNA virus of the family *Rhabdoviridae*. The VSV matrix protein (M) has an important role in both viral structure and replication. It is responsible for packaging the viral RNA and budding, but also inhibits the nuclear export of host cell RNAs (Le Sage and Valerie, 2013; Redondo et al., 2015; von Kobbe et al., 2000). Specifically, the M protein binds to Nup98 to provide an inhibition of nucleocytoplasmic transport (Ahmed and Lyles, 1998; Ennignga et al., 2002; von Kobbe et al., 2000). Later work discovered that the M protein actually contains two additional polypeptides named M2 and M3 encoded from the same ORF, referred to as M1 (Jayakar and Whitt, 2002), and while M2 and M3 are involved in cytopathic effects (CPE), it is M1 that participates in the inhibition of host mRNA transport (Jayakar and Whitt, 2002; Kuss et al., 2013; Redondo et al., 2015). This is accomplished via binding of the M protein to Rae1, an RNA binding protein which forms a complex with Nup98 (Kuss et al., 2013). Further investigation has demonstrated that residues 173-213 of Nup98 are involved, and that the complex formation with M protein induces a translocation from the nuclear side of the NPC to the cytoplasm (Faria et al., 2005). Quan et al. (2014) used biocrytallography to determine

that two globular domains of the M protein act in a finger and thumb fashion to bind to the β-propellor and B-tongue domains/motifs of Rae1 and Nup98 proteins, respectively, to complete the trimeric complex. The authors also used in vitro binding assays to illustrate that the M protein of VSV displaces nucleic acid proxies from the Rae1-Nup98 complex, implying that it serves as a phosphate backbone mimic (Quan et al., 2014).

While one assumption is that the inhibition of nucleocytoplasmic transport is to provide less competition for host translational machinery, others have speculated that this activity may be a form of immune-suppression (Gustin and Sarnow, 2002; Lyles, 2000). Indeed, Rajani et al. (2012) found that in siRae1 cells, many genes that are involved in the antiviral response, such as IL-6, CXCL2, CCL5, CXCL10, and IFIT1,2, and 3, were upregulated. This provides evidence that the M protein is also important for suppressing the host antiviral response. The authors provide the so-called "platform hypothesis," which asserts that the Rae1-Nup98 complex is serving as a platform for the M protein to interact vital host proteins instead of simple interference with Rae1 function, as Rae1 was found to not be required for host gene expression (Babu et al., 2003; Sitterlin, 2004) and that siRae1 cells were less sensitive to M protein effects due to less available interaction with host targets (Rajani et al., 2012).

Characterization of these interactions have important clinical implications, especially given the conserved nature of viral infection. Recently, affinity-purification mass spectrometry (AP-MS) was used to identify 332 high-confidence interactions between severe acute respiratory syndrome coronavirus 2 (SARS-CoV-2) and host proteins (Gordon et al., 2020). In a manner similar to VSV, SARS-CoV-2 ORF6 was found to form an interaction with the Nup98-Rae1 complex, which also involves a buried methionine residue that buries

into a hydrophobic pocket of Rae1 (Gordon et al., 2020; Quan et al., 2014). In addition to ORF6, various nonstructural proteins were also found to interfere with nuclear transport. NSP9 forms interactions with Nup88, Nup54, Nup62, Nup214, and Nup58, while NSP15 interacts with NUTF2 (Gordon et al., 2020), which is a nuclear transport factor that mediates the entry of GDP-bound RAN to the nuclear pore complex from the cytosol (Paschal and Gerace, 1995). It is hopeful that these data may provide potential drug targets for the inhibition of SARS-CoV-2.

Some viruses utilize proteolytic cleavage towards host proteins. The picornaviruses Human Rhinovirus (HRV) and poliovirus have both been shown to target Nup153 and Nup62 for degradation to block host macromolecular import and export (Gustin and Sarnow, 2001, 2002; Park et al., 2008). This is likely a result of cleavage by the viral 2A protease (Castelló et al., 2011; Le Sage and Mouland, 2013; Park et al., 2008). In addition, Nup98 is also targeted by poliovirus by 2A-induced cleavage (Park et al., 2008). Later work suggested that the protease 3C may work in conjunction with 2A in the degradation of Nup153 (Ghildyal et al., 2008; Walker et al., 2013).

Post-translational modification is another strategy for subverting nucelocytoplasmic transport employed by viruses. Cardioviruses are known to hyperphosphorylate FG-containing Nups, including Nup62, Nup98, Nup153, and Nup214 through activity of the Large (L) protein zinc finger (Bardina et al., 2009; Porter et al., 2010; Porter and Palmenberg, 2009; Ricour et al., 2009). It was further characterized that this is the result of activation of two mitogen-activated protein kinases (MAPKs), extracellular signal-regulated receptor kinase (ERK) and p38 MAPK, by the L protein (Porter et al., 2010). Once again, an

inhibition of immune function is observed due to transcriptional antagonism of the type 1 interferon (IFN) response (Ricour et al., 2009).

Interference of immune function by binding to karyopherins directly also occurs. Ebolavirus (EBoV) viral protein 24 (VP24) binds to importin-α5, which inhibits the nuclear import of signal transducer and activator of transcription 1 (STAT1) (Mateo et al., 2009; Reid et al., 2006; Xu et al., 2014; Yarbrough et al., 2013). As a result, a major step in the interferon signaling pathway is antagonized. SARS-CoV-1 similarly targets the STAT1 response by using its ORF6 protein to tether import machinery to the rough ER (Frieman et al., 2007). This is possibly a selective mechanism for viruses to modulate immune inhibition.

One class of proteins commonly targeted by viral proteins are heterogeneous ribonucleoproteins (hnRNPs). These RNA-binding proteins (RBPs) are involved in the processing of mRNA precursors into mature mRNAs and also have roles in localization and stability (Chaudhury et al., 2010; Dreyfuss et al., 1993). These are attractive targets for viruses due to their ability to serve similar functions when hijacked (Gustin, 2003; Meng et al., 2019). An example of a common hnRNP used by viruses is hnRNP A1, which has a multitude of functions including NPC export, splicing, processing, and gene expression (Jean-Philippe et al., 2013).

Cells acutely infected with Junín virus (JUNV), a single-stranded negative sense RNA virus in the Arenaviridae family, contain cytoplasmic concentrations of hnRNP A1 (Maeto et al., 2011). This was also observed in the presence of the nucleoprotein (N) (Maeto et al., 2011). Thus, it is implied that hnRNP A1 serves a positive role in the early stages of vRNA transcription and replication (Kaur and Lal, 2020; Maeto et al., 2011). In SARS-CoV-1-infected cells, the N protein was also demonstrated to bind to hnRNP A1, though evidence

suggests that other interacting partners may be recruited in the form of a replication complex (Jiang et al., 2005). Due to the VSV M-Rae1-Nup98 complex, hnRNP A1 has been found to accumulate in the cytoplasm of VSV-infected cells. While it is unlikely that hnRNP A1 is involved in the replication of VSV, apoptotic signaling was found to be delayed in cells where cytoplasmic relocalization was inhibited, illustrating that hnRNP A1 serves different purposes for different viruses (Pettit et al., 2009). HIV-1 uses NPC blocking to accumulate hnRNP A1 in the cytoplasm for IRES-mediated translation (Le Sage and Mouland, 2013; Monette et al., 2009). Specifically, Nup62 is found to localize to the nucleoplasmic side of the NPC in HIV-1 infected cells, likely providing a mechanism in which nuclear import of hnRNP A1 is halted (Monette et al., 2009).

In dengue virus (DENV)-infected cells, both hnRNP C1/C2 and hnRNP H have been found to interact with NS1 and have a positive effect on replication (Dechtawewat et al., 2015; Diwaker et al., 2016). HRV serotype 2 showed more efficient replication than HRV-16, which corresponded with HRV-2 relocalizing hnRNP-C1/C2 into the cytoplasm sooner than HRV 16 (Walker et al., 2015).

Sindbis virus (SINV) was found to have hampered growth kinetics in hnRNP mutational work involving hnRNP K and viral subgenomic RNA (sgRNA), though this work has also highlighted that the other cytological effects of hnRNPs may also be a complicating factor in determining the precise mechanism by which they regulate viral replication (Burnham et al., 2007; LaPonte et al., 2017).

Another nuclear-associated RBP that is relocated to the nucleus following viral infection is the lupus autoantigen (La) protein. While usage of this protein is often associated with the RNAs produce by DNA viruses, such as Epstein-Barr virus (EBV) and adenoviruses (Meng

et al., 2019), poliovirus is able to relocalize La to the cytoplasm (Shiroki et al., 1999). This occurs after the 3C protease cleaves a 50 aa sequence from the C-terminal of the La protein, which is found to be able to localize to the nucleus, suggesting its role in nuclear retention (Shiroki et al., 1999). Once in the cytoplasm, La serves to enhance IRES-mediated translation through recruitment of the 40S ribosomal subunit (Costa-Mattioli et al., 2004; Shiroki et al., 1999).

As previously discussed, the immune system may be inhibited by viral manipulation of nuclear import. Many proteins involved in the host immune response are associated with the nucleus, and viruses may have more direct interactions with these proteins to stop them from completing their signaling pathways. One of the first lines of defense for a cell against viral invasion are interferons (IFNs). Often, this is based around the IκB kinase-nuclear factor- κB (IKK/NF-κB) pathway, which is involved in a number of cell-signaling cascades including the inflammatory, growth, stress, and antiviral responses (Deng et al., 2018; Liu et al., 2017; Luo et al., 2005). The canonical NF-κB pathway starts with the activation of IKK in the cytoplasm, which phosphorylates the IκBα leading to its degradation and the release of NF-κB into the nucleus where it activates the transcription of appropriate antiviral gene targets (Deng et al., 2018; Liu et al., 2017; Sun, 2011).

The NS1 protein of IAV has been shown to prevent the activation of NF-κB by way of the dsRNA binding activity of NS1, which ultimately serves as an antagonist to IFN-α/β synthesis (Gao et al., 2012; Wang et al., 2000). Similar observations have been made in Middle East respiratory syndrome coronavirus (MERS-CoV), in which the 4b accessory protein localizes to the nucleus of infected cells and binds to an importin-α isoform to prevent translocation of NF-κB to the nucleus (Canton et al., 2018). This escape of host

immunity by subversion of nuclear-associated immune factors may provide powerful options for the clinical production of antivirals.

While plants lack the sophisticated immune system that animals have, they still possess signaling pathways and resistance responses to counteract pathogen infection (Jones and Dangl, 2006). For example, post-transcriptional gene silencing (PTGS) is a commonly utilized mechanism against viral infection in plants by targeting RNA for degradation in the cytoplasm (Vaucheret et al., 2001). Cucumber mosaic cucumovirus (CMV) 2b protein localizes to the nucleus and thwarts PTGS regulation (Lucy et al., 2000).

Viral functions within the nucleolus

The nucleolus is a vital subcomponent of the nucleus where ribosomal RNA (rRNA) is synthesized and ribosome biogenesis takes place (Lam et al., 2005). There are three structural compartments within the nucleolus: the fibrillar centers (FCs), the dense fibrillar component (DFC), the granular component (GC), along with the perinucleolar region (PNR) (Sirri et al., 2008; Hiscox et al., 2007). In terms of gaining access to the nucleolus, the criteria are not quite as well characterized as with nuclear import and export, though there may be some overlap with NLSs and nucleolar targeting sequences (NoLSs) in addition to passive import (Dang and Lee, 1989; Martin et al., 2015).

Similar to NLSs and the nucleus NoLSs direct proteins to the nucleolus, though the function is somewhat different due to the lack of active transport mechanisms into the nucleolus and the fact that there is not as strong of a consensus with their amino acid composition as with NLSs (Martin et al., 2015; Scott et al., 2010). Despite this, some general features are as follows: 1) current projections are that over half of the amino acids are basic,

often containing arginine and lysine motifs, and 2) some sequences are bipartite and may overlap with NLSs (Martin et al., 2015; Scott et al., 2010). As an example, the N protein of porcine reproductive and respiratory syndrome virus (PRRSV) contains two NLSs, and within the second NLS was found a domain which could direct EGFP into the nucleolus (Rowland et al., 2003). Still, much work is left to be done in characterizing these sequences.

There are three major proteins in the nucleolus often targeted by viruses: nucleolin, a phosphoprotein which is involved in processes such as rRNA maturation and DNA/RNA metabolism (Tajirishi et al., 2011); fibrillarin, which is involved in rRNA processing (Newton et al., 2003); and B23.1 (nucleophosmin), a ribosomal assembly factor (Hiscox, 2007). Curiously, many of the viruses discussed in the literature regarding interactions with the nucleolus are plant viruses and viroids (Hiscox, 2007; Kalinina et al, 2018).

Potato mop-top virus (PMTV), a single-stranded positive-sense RNA virus, encodes a movement protein named triple gene block (TGB1) (Lukhovitskaya et al., 2015). It has been determined that there are two regions which are responsible for nucleolar targeting, and that targeting of the nucleolus is required for systemic movement of the virus, though the specifics of this requirement are unknown (Lukhovitskaya et al., 2015; Wright et al., 2010). This association with the nucleolus is seen in other plant viruses, including the NIa protein of potato virus A (PVA) (Rajamäki and Valkonen, 2009), ORF3 of groundnut rosette virus (GRV) (Kim et al., 2007), p2 of rice stripe tenuivirus (RSV) (Zheng et al., 2015), TGB1 of barley stripe mosaic virus (BSMV) (Zheng et al., 2018), p23 of citrus tristeza virus (CTV) (Ruiz-Ruiz et al., 2013), MP of turnip vein clearing virus (TVCV) (Levy et al., 2013), p14 of beet necrotic yellow vein virus (BNYVV) (Chiba et al., 2013), and CP of alfalfa mosaic virus

(AMV) (Harranz et al., 2012). Despite extensive observations, more work is needed in all cases to understand the exact requirements of this nucleolar localization for viral movement.

Once again, replication enhancement is also important for subcellular targeting. Nucleolin is often hijacked by viruses. siRNA knockdown of nucleolin was shown to have a negative effect on both replication and assembly of DENV (Balinsky et al., 2013). In both poliovirus and HCV, the amino terminal domain of nucleolin was found to stimulate IRES-mediated translation, though this effect may become inhibitory due to excessive binding (Izumi et al., 2001).

Similar effects are seen with B23.1. The core protein of Japanese encephalitis virus (JEV) is found to interact with B23.1 and induce its relocalization to the cytoplasm (Tsuda et al., 2013), which serves to provide a more complete image as to why the core protein shows partial localization to the nucleolus in past work (Mori et al., 2005). Given its interactions with both RNA and DNA viruses alike regarding transport, replication, and assembly, it has become a candidate for an antiviral drug target (Lobaina and Perera, 2019).

Finally, fibrillarin has been utilized by the PRRSV N protein, which interacts with a glycine-arginine-rich (GAR) region on fibrillarin in the fibrillar compartment of the nucleolus, and it is possible that it may be subverting host cell rRNA process or ribosome biogenesis (Yoo et al., 2003). This work also suggested that B23.1 and nucleolin are responsible for shuttling N into the nucleolus, meaning that all three of these nucleolar proteins can be required for efficient PRRSV infection (Yoo et al., 2003).

Rhabdoviruses

Rhabdoviruses are a family of viruses in the order *Mononegavirales* and currently have been found to encompass 30 genera and 191 species (Dietzgen et al., 2017; Walker et al., 2018). The members of this family have a wide host range including vertebrates, invertebrates, and plants (Dietzgen et al., 2017; Jackson et al., 2005; Redinbaugh and Hogenhout, 2005; Walker et al., 2018). The genus *Lyssavirus* (rabies virus) has mainly evolved to spread from individual to individual via biting, though the majority of rhabdoviruses are vectored by arthropods including plant hoppers, mosquitos, leaf hoppers, and aphids (Dietzgen et al., 2017; Rupprecht et al., 2017; Walker et al., 2018). These viruses pose significant threats to both public health and agriculture, with viruses such as VSV (genus *Vesiculovirus*) serving as an important model in RNA virus biology (Dietzgen et al., 2017; Payne, 2017; Singh et al., 2017, Wollmann et al., 2013), and in fact was the first rhabdovirus to be undergo morphological study (Bradish et al., 1956; Chow et al., 1954).

Structurally, rhabdoviruses are bullet-shaped but some which infect mammals and most of the plant members have a bacilliform morphology (Walker et al., 2018). The enveloped virions are 100-460 nm in length and 45-100 nm in width (Jackson et al., 2005; Nakai and Howatson, 1968; Walker et al., 2018). The outer surface of the virion is decorated with transmembrane glycoprotein (G) spikes of roughly 5 to 10 nm in length and mediates the binding to host cell receptors (Hummeler et al., 1967; Jackson et al., 2005). The single-stranded, negative-sense RNA genome (10-16 kb) is coated by the nucleoprotein (N) and associates with the phosphoprotein (P) and large protein (L), which is the RNA-dependent RNA polymerase (RdRp) (Dietzgen et al., 2017; Nakai and Howatson, 1968). Together, the N, P, and L proteins form a helical ribonucleoprotein complex (RNP), or nucleocapsid core,

which is the minimal replicative (infectious) unit (Healy et al., 2013; Pattnaik et al., 1997). The N protein encapsidation also serves the purpose of protecting the viral genome from host cell nucleases (Ivanov et al., 2011). Serving as a link between the G protein and RNP is the matrix (M) protein, which condenses the nucleocapsid core (30-70 nm wide) (Dietzgen et al., 2017; Healey et al., 2015; Walker et al., 2018).

Apart from the addition of potential accessory proteins, these five structural proteins are conserved across all genera of rhabdoviruses along with flanking untranslated leader (*l*) and trailer (*t*) sequences, as summarized by the following: 3'-*l*-N-P-M-G-L-*t*-5' (Ivanov et al., 2011; Jackson et al., 2005). These sequences may also be overprinted, overlapping, or contain accessory proteins which aid in pathogenesis or cell-to-cell movement, the latter pertaining to plant viruses (Dietzgen et al., 2017; Jackson et a l., 2005; Walker et al., 2011). This ultimately means that rhabdovirus genomes may encode more than 10 proteins (Dietzgen et al., 2017). The relative molar concentration of each protein is dictated by the stop-start mechanism of transcription, whereby the RdRp binds to the 3' end of the template and continues to a U7 sequence at the 5' end of each ORF, resulting in the slippage of the polymerase and generation of a poly(A) tail (Barr et al., 1997; Iverson and Rose, 1981; Schnell et al., 1996). Following this transcription termination/polyadenylation (TTP) sequence is an untranscribed intergenic dinucleotide (C/GA), and finally a conserved transcription initiation (TI) sequence, which is UUG in VSV and many plant rhabdoviruses (Barr et al., 2002; Jackson et al., 2005; Schnell et al., 1996; Stillman and Whitt, 1997; Walker et al., 2011). A consequence of this mechanism is molar gradient of protein expression such that N>P>M>G>L (Abraham and Banerjee, 1976; Dietzgen et al., 2017). The resulting accumulation of N and P proteins is an important regulatory mechanism which

causes the polymerase to switch from transcription to replication during infection (Burrell et al., 2017; Wagner et al., 1987).

The general life cycle of rhabdoviruses is fairly conserved amongst its members and can be summarized by the following: i) endocytic entry mediated by binding of G protein to cell surface receptors ii) uncoating via fusion of viral envelope and endosome iii) release of the RNP into the cytoplasm iv) replication and transcription of viral genome v) accumulation of G proteins on host membranes vi) the M protein of assembled virions buds through membranous regions embedded with G protein to form enveloped virions and are released to infect neighboring cells (Blondel et al., 2015; Payne, 2017; Walker et al., 2018). Plant-infecting rhabdoviruses, however, present important exceptions to both this life cycle and rhabdoviral biology.

Plant-associated rhabdoviruses

Until recently, there were four genera of plant-infecting rhabdoviruses: *Nucleorhabdovirus, Cytorhabdovirus, Varicosavirus,* and *Dichorhavirus*, with the latter two being 2015 additions to the family *Rhabdoviridae* (Walker et al., 2018). However, as of the International Committee on the Taxonomy of Viruses (ICTV) 10th Report (www.ictv.global/report/rhabdoviridae) the genus *Nucleorhabdovirus* has been abolished and its 16 species split into three new genera: Alphanucleorhabdovirus, Betanucleorhabdovirus, and Gammanucleorhabdovirus. This has been proposed due to the fact that L protein sequence alignments of new rhabdovirus genomes do not form monophyletic clades during phylogenetic analysis (ICTV nucleorhabdovirus splitgen proposal online 2019.031 M).

These genera of plant-infecting rhabdoviruses have several key distinctions from their vertebrate and invertebrate counterparts. Varicosa- and dichorhaviruses both possess bipartite genomes with dichorhaviruses containing the L gene on RNA2 and varicosaviruses having the coat protein (CP, N homolog) and four unknown ORFs on its RNA2 (Dietzgen et al., 2017; Walker et al., 2018). Varicosaviruses are also unique in that they lack and envelope and form flexuous rod-shaped virions that are transmitted by the chytrid fungus *Olpidium virulentus* (Colariccio et al., 2005; Dietzgen et al., 2017). Alphanucleorhabdoviurses, betanucleorhabdoviruses, gammanucleorhabdoviruses, and dichorhaviruses are distinct from other rhabdoviruses due to the formation of replication complexes in the nucleus of host plant cells with assembled virions budding into the INM (Jackson et al., 2005). Other considerations when comparing the plant-associated rhabdoviruses to animal-associated genera are a) the requirement of an accessory movement protein (MP) for cell-to-cell movement and b) penetration of the cell wall via mechanical damage or insect stylet piercing, the latter being the most common in nature (Bandyopadhyay et al., 2010; Jackson et al., 2005; Redinbaugh and Hogenhout, 2005). Common insect vectors include planthoppers, leafhoppers, aphids, and mites (Jackson et al., 2005; Walker et al., 2018). The MP is located between the P and M genes and facilitates transport through the plasmodesmata to neighboring cells (Jackson et al., 2005; Walker et al., 2011; Zhou et al., 2019). Plant rhabdoviruses may also encode RNA silencing suppressors (RSS) that interact with the host plant's RNA silencing machinery, including the P protein of sonchus yellow net virus (SYNV), the P6 protein of rice yellow stunt virus (RYSV), and the P protein of lettuce necrotic yellows virus (LNYV) (Guo et al., 2013; Jackson et al., 2005; Mann et al., 2015; Martin et al., 2012).

Sonchus yellow net virus

SYNV is a model virus in the genus *Betanucleorhabdovirus* and was initially isolated from *Sonchus oleraceous* and *Bidens pilosa* (Christie et al., 1974). The 13,752 nt genome encodes the five canonical rhabdovirus proteins in addition to the movement protein, sc4, which has been demonstrated to localize to the cell periphery and maintain specificity to the SYNV nucleocapsid (Figure 1.2) (Goodin et al., 2002; Scholthof et al., 1994; Zhou et al., 2019). The virus is commonly vectored by aphids and completes a life cycle within its insect host while spreading from the hemolymph, gut, and salivary glands before being transmitted to plants (Hogenhout et al., 2003). The transmission process is persistent and propagative, with each insect vector showing differential preferences for monocots versus dicots (Whitfield et al., 2018).

Upon stylet penetration into the host cell, the virions are uncoated at the ER and the nucleocapsid core is released into the cytoplasm where it is imported into the nucleus via interaction with importin-α (Dietzgen et al., 2017). The RdRp-produced viral transcripts are then exported into the cytoplasm where they are translated, and the newly formed proteins then localize to the nucleus. The N protein contains a bipartite NLS while the P protein was demonstrated to contain a karyophilic region (Goodin et al., 2001). Nuclear concentrations of N and P protein likely regulate the switch between genomic replication and transcription (Jackson et al., 2005). The M protein proceeds to condense the nucleocapsids and bud into the G protein lined INM where they accumulate in the inner nuclear envelope (INE) and form intranuclear spherules filled with mature virions (Figure 1.3) (Goodin et al., 2005; Jackson et al., 2005). While mature virions do not participate in cell-to-cell movement, the nucleocapsids associate with the sc4 movement protein, which cause a remodeling of

microtubules at the plasmodesmata to allow for systemic movement and subsequent infection of new cells (Jackson et al., 2005).

Future perspectives and concluding remarks

It is clear that viruses have evolved the ability to take advantage of many nuclear proteins during various stages of their life cycle for purposes such as replication, nuclear entry, or immune evasion. However, it is relevant to consider this fact in the context of the entire plant cell. A consortium led by Pascal Braun in 2011 generated a high-quality interactome map for *A. thaliana* which included ~6,200 interactions between ~2,700 proteins (Arabidopsis Interactome Mapping Consortium, 2011). This was further extrapolated to an estimated 75,000 to 299,000 interacting pairs in plants containing 30,000 to 40,000 proteins (Sheth and Thaker, 2014; Vanderyken et al., 2018). Adding to this, the physiological purpose for nearly 90% of *Arabidopsis* gene products is unknown (Braun et al., 2013). Thus, studying viral usage of host proteins not only provides a better understanding of pathogen-host relationships but also allows a method of elucidating host protein function through manipulation of complex interaction networks within the cell. Examining protein relocalizations induced by viruses in organelles such as the nucleus are therefore a starting point in potentially identifying proteins which important for both viral and plant function.

Table 1.1: Current List of nucleoporins grouped by NPC location and organism

NPC Location	Plants	Yeast	Vertebrates
Cytoplasmic region	Nup214	Nup159	Nup214
	CG1	Nup42 (CG1)	Nup42 (CG1)
	-	-	Nup358
	-	Nup82	Nup88
	Aladin	-	Aladin
	Gle1	Gle1	Gle1
	-	-	DDX19
	Nup62	Nsp1	Nup62
	Rae1	Gle2	Rae1
Outer ring (Y-complex)	Nup75	Nup85	Nup75
	Nup160	Nup120	Nup160
	Nup107	Nup84	Nup107
	Nup96	Nup145C	Nup96
	Nup133	Nup133	Nup133
	Sec13	Sec13	Sec13
	Seh1	Seh1	Seh1
	-	-	Nup37
	Nup43	-	Nup43
	ELYS	-	ELYS
Transmembrane Nups	Ndc1	Ndc1	Ndc1
	-	Pom152	-
	Pom210	-	Pom210
	-	Pom34	-
	-	-	Pom121
	-	Pom33	TMEM33
	Cpr5	-	-
Inner ring (Nup93/Nic96 Complex)	Nup93	Nic96	Nup93
	Nup188	Nup188	Nup188
	Nup205	Nup192	Nup205
	Nup155	Nup157/170	Nup155
	Nup35	Nup53/59	Nup35
	Nup88	-	-
FG Nups	Nup98	-	Nup98
	Nup62	Nsp1	Nup62
	Nup58	Nup49	Nup58/45
	Nup54	Nup57	Nup54
Nuclear Basket	NUA	Mlp1/2	Tpr
	ESD4	-	-
	MAD1	-	-
	MAD2	-	-
	Nup50	Nup2	Nup50
	-	Nup60	-
	Nup1/136	Nup1	Nup153

Yeast and vertebrate Nups compiled from: Knockenhauer and Schwartz, 2016; Lin and Hoelz, 2019.

Plant Nups compiled from: Boruc et al., 2012; Meier et al., 2017; Tamura et al., 2010; Tamura and Hara-Nishimura, 2013; Tang et al., 2020.

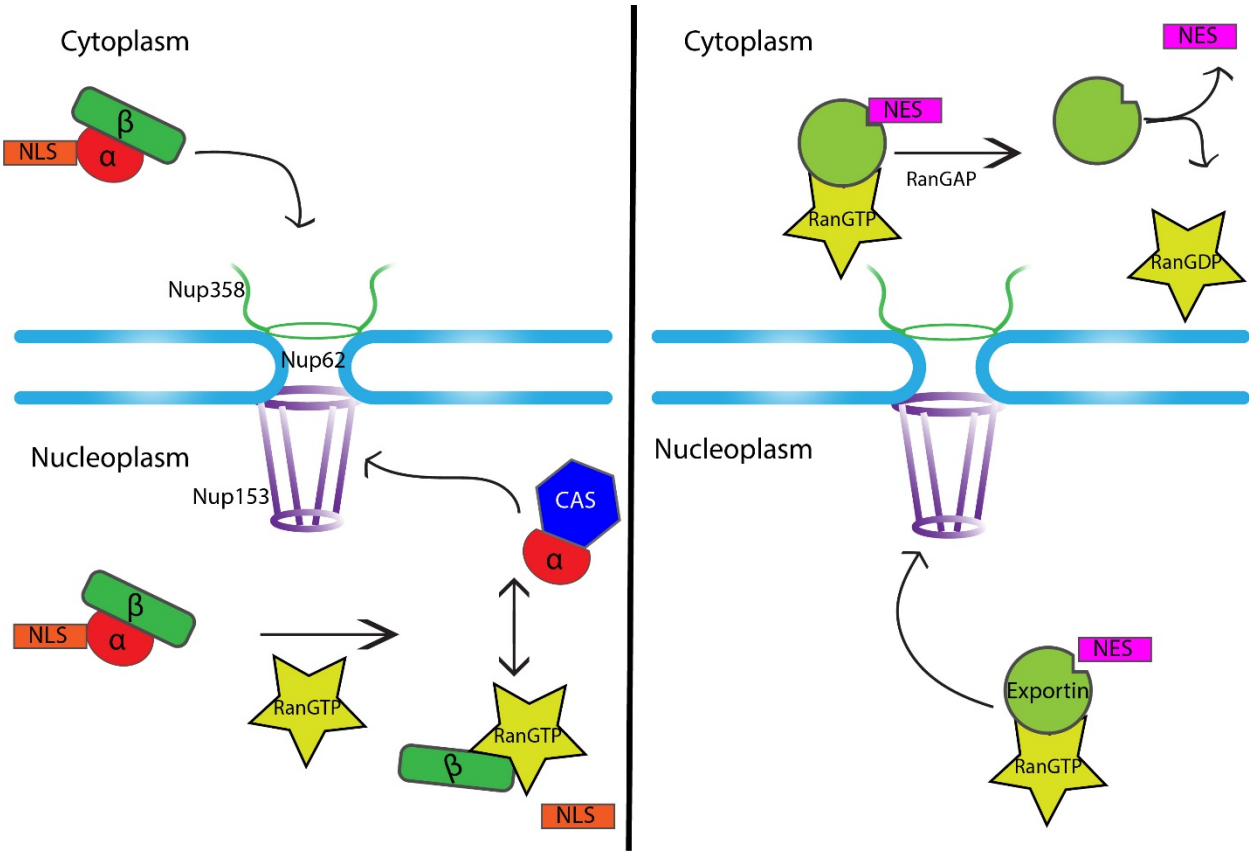

Figure 1.1: Summary of nuclear import (left) and export (right). NLS-containing cargo proteins bind with importin-α, which is also bound to importin-β and this trimeric complex passes through the NPC through binding of importin-β with nucleoporins such as Nup358, Nup62, and Nup153. Once in the nucleoplasm, the association of importin-β with RanGTP leads to the dissociation of the NLS-containing cargo protein and importin-α, the latter of which binds to CAS and is transported back out the NPC where it can begin a new cycle of import. For export, a NES-containing cargo protein binds to exportin, which in turn binds to RanGTP. Upon entry into the cytoplasm, RanGAP induces the hydrolysis of RanGTP into RanGDP, thus releasing the cargo protein into the cytosol.

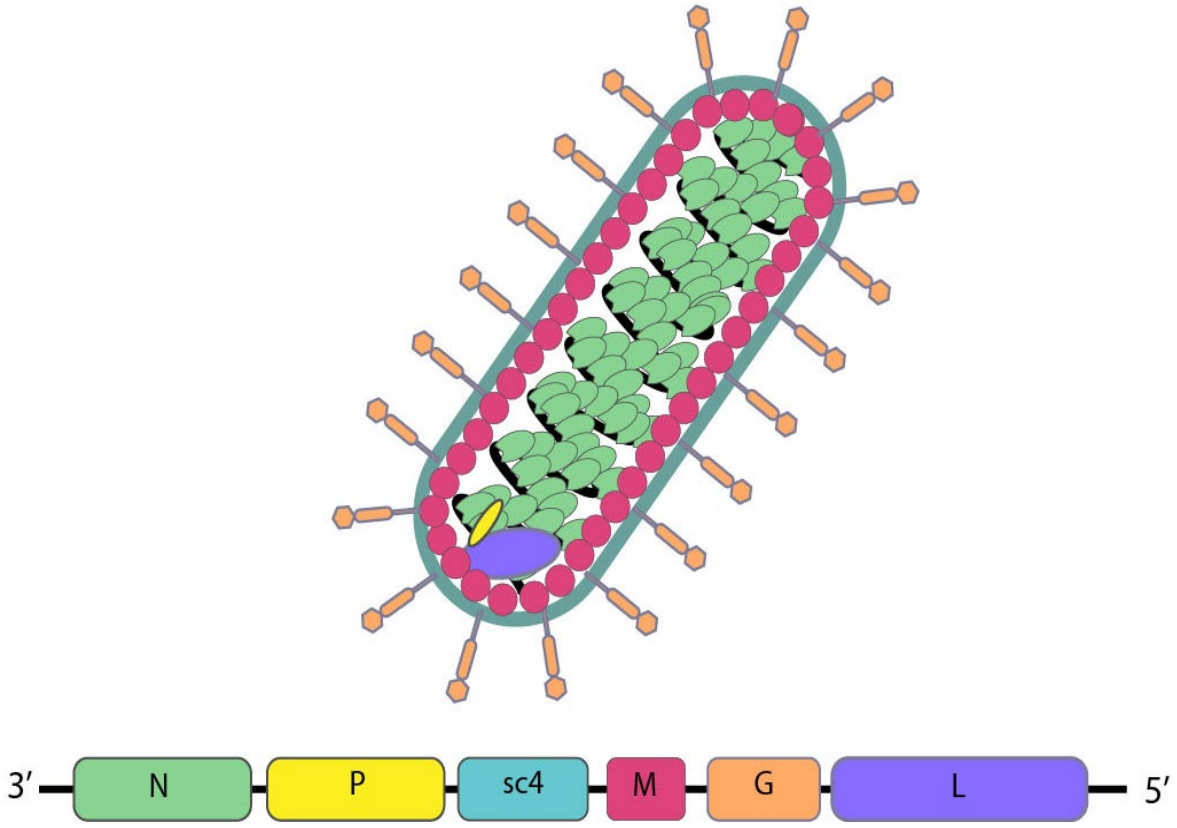

Figure 1.2: Viral structure and genomic organization of SYNV. The negative-sense RNA genomic RNA, nucleocapsid protein (N), and polymerase protein (L) form the nucleocapsid core and minimal infectious unit. This core is condensed by the matrix protein (M) and is involved with budding into the INM. The lipid envelope is derived through this process, as well as the transmembrane glycoproteins (G) which decorate the outside as they accumulate on the IME. While the animal-infecting counterparts take a bullet-shaped morphology, plant rhabdoviruses typically are bacilliform.

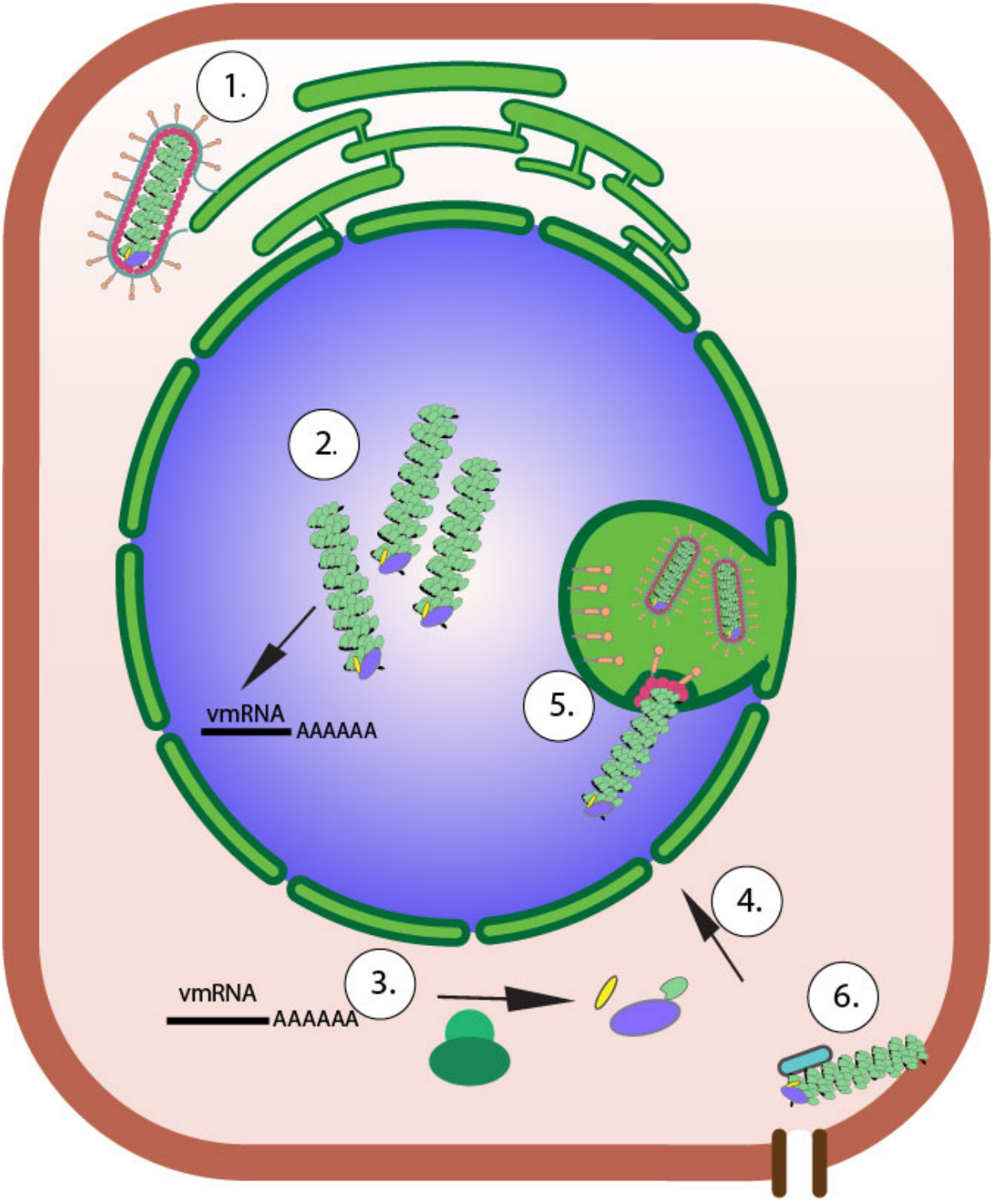
1.
2.
vmRNA
AAAAAA
5.
4.
3.
vmRNA
AAAAAA
6.

Figure 1.3: Replication cycle of SYNV. Upon insect-mediated entry or mechanical wounding, uncoating of SYNV virions occurs on the ER (1). The nucleocapsid cores are imported into the nucleus where the replication complex is formed, where viral mRNAs (vmRNA, depicted as poly(A) transcripts) are produced by the L protein and exported into the cytoplasm (2) where they are translated by host ribosomes (3). The newly synthesized viral proteins are then imported back into the nucleus (4) where viral replication and assembly takes place within viroplasms. The M protein then condenses then nucleocapsid cores and promote budding into the INM where they obtain the viral lipid envelope that is embedded with G proteins (5). The movement protein sc4 together with host factors mediate the cell-to-cell transport of nucleocapsid cores via the plasmodesmata for the purpose of infecting new cells (6).

Chapter 2

Virus-Induced Changes in Host Nuclear Protein Localization

Introduction

Upon entry into a host cell, viruses must evade host defense responses and redirect host cell machinery in order to replicate and establish systemic infections. Viruses target subcellular foci, such as membranes, microtubules, and organelles, as part of the infection process. Viruses also disrupt the protein interaction networks in host cells, a significant number of which are yet to be characterized given that there are upwards of 30,000 proteins in a eukaryotic cell (Brito and Pinney, 2017; Nagy and Pogany, 2011). Much of this remodeling results in a subversion of organellular structure and function, as exemplified by citrus leprosis virus (CLV), which traffics its proteins across a long network of organelles and actin filaments upon manipulating the cellular structures in favor of its own spread (Leastro et al., 2018). Viruses may also induce changes in the localization of proteins in ways that are beneficial to it, as is the case with rotaviruses, which induce the localization of both nuclear and cytoplasmic proteins to sites of viral replication and assembly (Dhillon et al., 2018). The genomic RNA of both dengue and Zika viruses has also been found to associate with hundreds of host proteins (Li et al., 2020; Ooi et al., 2019). Logically, viruses may serve as probes to understand protein interaction networks and other aspects of cellular biology.

The manner by which viruses utilize of targeting various organelles and rerouting host proteins is critically understudied in regard to the nucleus. One such example of how viral proteins target the nucleus is potato virus A (PVA), whose nuclear inclusion protein a (NIa) which has been implicated to play a role in overcoming the host antiviral response (Rajamäki

and Valkonen, 2009). Some viruses, like sonchus yellow net virus (SYNV), a plant-associated rhabdovirus in the genus *Betanucleorhabdovirus*, establish their replication complexes within the host nucleus. Mature virions bud through the inner nuclear envelope (INE), producing large, membranous spherules (Goodin et al., 2005). Therefore, SYNV can serve as a powerful tool to better understand potential interaction networks between viruses and nuclear proteins.

The goal of this study was to determine how viruses impact the localization of nuclear-associated proteins, which is significant as these proteins comprise 25% of the host cellular proteome (Huh et al., 2003). These changes in localization may indicate a role that a host protein has during the viral infection. This effect was investigated here using a combination of fluorescently tagged proteins and laser scanning confocal microscopy (LSCM). To accomplish this, we have screened a *Nicotiana benthamiana* cDNA library with GFP fusions of random proteins for nuclear localization using *N. benthamiana* marker lines expressing RFP to histone 2B (H2B), which serves as a nuclear reference marker (Martin et al., 2009). cDNA constructs encoding the protein-GFP fusions were delivered into the plants via agroinfiltration. Proteins found to localize within subnuclear loci were then expressed in SYNV-infected transgenic *N. benthamiana* plants expressing RFP on the endoplasmic reticulum (ER) in order to visualize virus-induced membrane proliferations within nuclei. To demonstrate if this is a virus-specific phenomenon, the potyvirus TEV was also used in the same manner. It was concluded that the two viruses could induce both general and virus-specific relocalization of host nuclear proteins.

Materials and Methods

Growth, maintenance, and inoculation of plants

N. benthamiana plants were maintained in greenhouse conditions as described by Martins et al. (1998). Transgenic *N. benthamiana* RFP-H2B and RFP-ER marker lines were generated as outlined by Chakrabarty et al. (2007). One set of plants was inoculated with SYNV and another with TEV, following the mechanical inoculation procedure described by Hull (2009), which provides several options for the chelating agent and abrasive substance to be used on the leaves. In this study, 0.02 M sodium sulfite was used as the reducing agent and celite as the abrasive. Four to six SYNV-infected *N. benthamiana* leaves were ground in this mixture via mortar and pestle and used to inoculate three-week-old transgenic RFP-ER plants. TEV was inoculated following the same procedure, however, *N. rustica* plants were used to maintain the virus as they were able to withstand infection longer. The SYNV-infected plants were used for imaging experiments roughly 14 days after inoculation (DAI), which is when symptoms are most prevalent, whereas the TEV-infected plants showed peak symptoms at roughly six DAI due to the more aggressive nature of the virus.

Construction of cDNA library and transformation into Agrobacterium

Protein-of-interest:GFP (POI:GFP) fusions were expressed in plant cells using Agroinfiltration (Chakrabarty et al., 2007). A high-quality *N. benthamiana* cDNA library was constructed using the Clonminer II kit (Thermo Fisher) with pDONR222 as the vector with an average insert size of 1.5 kb. To verify the inserts as *bona fide N. benthamiana* clones, 40 plasmids were randomly selected and sequenced to confirm no contamination from non-cDNA sources. The resulting library was then mobilized into the pSITE-2CA vector (Supplementary Figure 2.1), resulting in the fusion of cDNA-encoded polypeptides with GFP and under regulation of a 2x35S promoter. These constructs were then transformed into Agrobacterium

strain LBA4404 following the procedure provided by Goodin et al. (2002). The transformants were then plated onto LB media containing rifampicin, gentamicin, and spectinomycin, at a 1:1000 dilution. Colonies were left to grow for two days at 27°C. Colonies were agroinfiltrated into the leaf epidermal cells of *N. benthamiana* and those found to contain GFP fusions which localized to the nucleus were stored at -80°C in a 50% glycerol stock solution to be used for further study. Plasmid isolation for sequencing was performed using a Qiagen Spin Miniprep Kit according to manufacturer's instructions.

Protein expression in plant cells and slide preparation

Transformed LBA4404 cells were suspended in MES buffer (10 mM MgCl2, 10 mM MES, pH 5.6) with acetosyringone added to a final concentration of 150 µm and a bacterial OD_{600} of 0.6-1.0 for two hours prior to infiltration of leaves. A 1-ml syringe was then used to infiltrate the suspensions into the abaxial side of a leaf (Goodin et al., 2007). These plants were incubated in growth room for 48 hours under ambient conditions with an 8/16-hrs light/dark cycle. Triangular sections with roughly 1.5 cm sides were then placed on glass slides with a droplet of water on top before being covered with a coverslip. Samples were then imaged using LSCM.

Microscopy

Live cell imaging was conducted using an FV1000 scanning confocal microscope (Olympus). GFP and RFP were excited at 488 and 543 nm, respectively. GFP laser intensity was set to 1% power with high voltage (HV) values in a range between 500-700 V to the

photomultiplier tube (PMT). RFP laser intensity was around 20% with HV values also in a range of 500-700 V to the PMT, depending on what required to avoid over/under saturation of light. Images were acquired using the FluoView^{TM} software v1.5 by Olympus. These images were taken using the 40x objective at a scan speed of 10 µs/pixel with a 512-by-512-pixel resolution. These were exported into a JPEG format and assembled in PowerPoint.

Results

Nuclear proteins exhibit a variety of localization patterns at subnuclear foci

In order to identify proteins localized to subnuclear loci, LSCM was used to screen the cDNA library in transgenic RFP-H2B *N. benthamiana* marker lines. A total of 1,087 proteins were screened, with 355 of the proteins exhibiting localization patterns associated with the nucleus. The remaining either did not show any visible expression in cells, or localized exclusively within the cytoplasm, on membranes, or other subcellular structures.

A variety of localization patterns associated with the nucleus were observed. These were broadly organized into six categories: nucleolar (74; 20.9%), nucleoplasm (95; 26.8%), subnuclear (39; 11.0%), nuclear envelope (10; 2.8%), perinuclear (42; 11.8%), and both nuclear and cytoplasmic (95; 26.8%). A collection of micrographs taken during this project in their appropriate localization categories is provided in Figure 2.1 which displays 259 of the nuclear-associated proteins and which represents the "localisome" for this study. Also of note is that some images, such as 8-57, only a GFP image is available. Table 2.1 provides a list of every nuclear-associated protein as categorized by their respective nuclear localization pattern, with the protein codes listed in bold having available images in Figure 2.1.

For the purpose of scientific rigor, each protein found to localize to the nucleus was imaged on at least two separate occasions, with at least 100 cells examined to determine the most frequent localization pattern. In addition, full cells were imaged to see if there were any GFP accumulation in the cytoplasm or on cellular membranes. Thus, the classification of proteins presented in both Table 2.1 and Figure 2.1 is largely informed by these data, though some met criteria for assignment to multiple groups. For example, some of the proteins in the "Nucleolar" category also displayed localization throughout the nucleoplasm, such as with 2-45 panel E2i and 4-23 panel H2i, but due to the accumulation of GFP in the nucleolus it was placed in this group. Similarly, in the "Subnuclear" category, protein 3-69 showed strong nucleolar localization, but punctate aggregations of GFP were found in the nucleoplasm as can be clearly seen by the exclusions of RFP in panel Yii, so the protein was categorized as subnuclear. Proteins in the "Nuclear envelope" category were found to have a strong presence in the nuclear envelope, whereas those defined as "Perinuclear" similarly showed expression in the envelope but also had GFP accumulation on cellular membranes. Protein 4-55 is a particularly challenging case as it consistently showed expression in the nucleolus but also in the envelope and on membranes, so it was placed in the "Perinuclear" category. Also challenging to categorize was protein 3-76 in the "Nuclear and cytoplasmic" group. Punctate GFP accumulations were consistently observed to associate with the outer nuclear membrane with rare GFP presence inside of the nucleus. Due to this association along with the presence in the cytoplasm, it was placed into this category.

A subset of nuclear proteins relocalize within the nucleus in response to virus infection

To determine if any of the nuclear proteins would relocalize during SYNV infection, the GFP fusions of nuclear-localized proteins were agroinfiltrated into virus-infected plants at peak

symptom expression post inoculation. These transgenic *N. benthamiana* plants expressed RFP to the ER (Figure 2.2A) in order to visualize the virus-induced membrane spherules (Figure 2.2B). Each fusion was expressed in six to nine leaves divided amongst two separate plants which were infected with SYNV in order to ensure consistency in localization pattern, using mock H2B and ER plants to verify that the proteins maintained the same expression in healthy plants as previously defined in the previous section.

Of the 355 nuclear localized proteins, 120 were found to express in the SYNV-infected plants. The majority of these proteins which did have visible expression remained consistent with the localization seen in healthy plants, however, 16 proteins did show a clear change in localization, as shown in Figure 2.3. These changes are summarized in Table 2.2.

Some of the observed relocalizations, such as for RC-534, Nb-18, and Nb71, were found to shift from subcellular loci to what appears to be the nucleolus. By contrast, proteins RC-238, RC-396, 3-69, and 4-8 relocalized from the nucleolus to elsewhere in the nucleus. Proteins RC-51, Nb-287, and 2-18 appear to wrap around the membranous spherules induced by the virus, while protein 3-69 formed punctate aggregations which seemed to also associate with the spherules. Other observed relocalizations were from the nucleoplasm to the perinuclear space, such as for proteins 2-25, 2-43, and 2-45, while protein 8-42 showed perinuclear localization in healthy plants but was more distributed in the nucleoplasm in SYNV-infected plants.

Table 2.3 shows the sequencing results for a small subset of the proteins used in this project, with underlined protein codes indicating those which show relocalization in virus-infected plants, and some clear patterns have emerged. Proteins Nb-18, Nb-71, and 2-45 were all found to be ribosomal subunits, with the former two showing similar localization and relocalization patterns. Two of the proteins, RC-238 and 3-69, were revealed to be histones, both

of which showing some level of accumulation in the nucleolus but exhibiting different relocalization patterns in the presence of SYNV. Protein 2-18, which clearly resides in the nuclear envelope and accumulates in the SYNV spherules, was uncharacterized. Several other ribosomal proteins and histones were found during sequencing, though were not found to relocalize during viral infection.

Virus-specific changes in subnuclear localization

Generalized protein relocalization in response to virus infection

To determine if these relocalizations were virus-specific, proteins which relocalized in the presence of SYNV were expressed in plants challenged with TEV infection, along with a random selection of proteins which did not in order to see if any were only affected by TEV. Table 2.4 provides a summary of the results found in these experiments. It is important to note that, much like with the SYNV-infected plants, not every protein showed expression in the TEV-infected plants, potentially due to alterations in steady-state physiology.

Figure 2.4A shows localization patterns which differed from the mock in both SYNV- and TEV- infected plants. For RC-238, distribution throughout the nucleoplasm was observed, compared to the nucleolar localization pattern found in the mock plants. Nb-243 localizes within punctate foci throughout the nucleoplasm in mock plants but is more evenly distributed in the SYNV-infected plants. In the TEV-infected plants, there is accumulation in both the nucleoplasm and the viral proliferation in the nuclear envelope. The localization of 2-43 in the mock plants was throughout the nucleoplasm whereas in SYNV-infected plants the localization was in the

nuclear envelope. In TEV-infected plants, 2-43 had localized in the membranous proliferation in a manner similar to Nb-243, though 2-43 did not show localization in the nucleoplasm.

SYNV-specific protein relocalization

Another observation were relocalizations in SYNV infected plants but not TEV infected plants. Figure 2.4B shows protein Nb-287, which was found to localize as punctate bodies, particularly near the nuclear envelope. In SYNV-infected plants, localization was limited to the nuclear envelope, which was found to wrap around the membranous spherules caused by the virus. With protein 3-69, localization was largely found within the nucleolus in both mock and TEV-infected plants, but in SYNV-infected plants a combination of localization to the nuclear envelope and punctate loci was observed.

TEV-specific protein relocalization

The final observation was a relocalization in TEV infected plants, but not in SYNV-infected plants. This was indeed the rarest as only one of the screened proteins had demonstrated this phenomenon. Figure 2.4C illustrates the localization patterns of 8-43, which was found to localize in the nucleoplasm with clear accumulation in the NE, which was consistent with the localization in SYNV-infected plants. However, in TEV-infected plants the protein lacked any nucleoplasmic localization and instead relocalized to punctate foci throughout the viroplasm.

Discussion

In this study, fluorescent tagging of host proteins was used in conjunction with LSCM in order to identify proteins which localized within the nucleus of transgenic marker line *N. benthamiana.* These nuclear host proteins were then expressed in plants infected with SYNV, a virus which forms its replication complex in the nuclei of host plants, to see if any localization changes could be observed. The final step was to determine if these induced relocalizations were virus specific. For this, we used a second and genetically distinct virus, TEV, to see if the changes were consistent with what was found with SYNV. It was determined that some of these changes were, in fact, unique to each virus, thus illustrating that two genetically distinct viruses were able to induce virus-specific relocalizations. Further, TEV forms its viral replication complex in the cytoplasm of host cells, which also demonstrates that regardless of where a virus replicates it may require nuclear proteins to complete its life cycle

Examining the proteins identified in Table 2.3 leads to some interesting implications. For example, nine ribosomal subunit proteins were identified. Three of these, Nb-18, Nb-71, and 2-45, were found to relocalize during SYNV infection (Figure 2.3). It has been known for some time that viruses such as vaccinia virus (Kaerlein and Horak, 1976), as well as pseudorabies virus and herpes simplex virus (Kennedy et al., 1981), phosphorylate ribosomal proteins in the cytoplasm and nucleus, though the exact function of this has not been elucidated (Li, 2019; Meyuhas, 2008). More recent work has found that potato leaves (*Solanum tuberosum* L.) infected with PVA had a comparatively higher amount of ribosomal proteins in the nuclei of compared with healthy plants (Rajamäki et al., 2020). Further, there are nearly 80 ribosomal proteins which are found in the nucleus and these proteins often traffic to the cytoplasm (Lam et al., 2007; Hiscox, 2007). Thus, these data, along with the data provided in this study, suggest that

there is much work to be done in further understanding the diverse roles ribosomal proteins play during viral infection.

Two of the proteins, RC-238 and 3-69, were identified as histones. While the exact localization patterns in mock plants differed, both seemed to show an association with the nucleolus. Histones have been demonstrated to be enriched in the nucleolus, and higher expression levels have been found to also induce nucleolar localization (Sen Gupta et al., 2018), which could be potential explanations for these observed localization patterns. Both of these proteins relocalized in response to SYNV (Figure 2.4A), but only RC-238 showed relocalization in response to both SYNV and TEV (Figure 2.4B). Further investigations should be conducted to understand both the discrepancy in these localization patterns and the mechanisms by which RNA viruses would induce, directly or indirectly, the relocalization of histones. Given the role that histone modifications have in epigenetic regulation (Alaskhar Alhamwe et al., 2018), further investigation into the mechanisms surrounding these localization changes is warranted, both in the context of host cell physiology and in viral processes. This is especially pertinent as there has been an increase in studies which examine the impact of pathogen infection on epigenetics (Bierne et al., 2012; Fischer, 2020; Nehme et al., 2019; Saha and Tomar, 2018).

What is also apparent is that some of the sequences in Table 2.3 are chloroplastic-like proteins. These include 1-6, 2-25, 2-43, 2-45, and 2-50. Indeed, 2-43 and 2-50 were relocalized within the nucleus during viral infection, suggesting that these proteins are serving a functional role in the nucleus, especially given that 2-50 is a DNA damage repair protein, which have been shown to be activated during RNA virus infection (Ryan et al., 2016). What must also be considered is that proteins associated with one organelle may also “cross-talk” with other organelles, particularly for stress responses (Bobik and Burch-Smith, 2015; Chan et al., 2010;

Krupinska et al., 2020) For example, Whirly1 is a DNA binding protein implicated in systemic acquired resistance and found in both the nucleus and chloroplast (Desveaux et al., 2004; Krause et al., 2012). These data provide evidence for why studying localization by visualization is important, as proteins may not always localize where expected based purely where expected.

Two other relocalized proteins, Nb-243 and Nb-287, were found to be glyoxylate/succinic semialdehyde reductase 1 (GLYR1) and a probable kinase, respectively. GLYR1 detoxifies harmful aldehydes during the plant stress response and preferentially reduces glyoxylate to glycolate in an NADPH-dependent manner (Allan et al., 2009; Brikis et al., 2017; Simpson et al., 2008; Zarei et al., 2017). The role in photorespiration is intriguing, as viruses are known to exploit metabolic pathways, such as glycolysis and fermentation, particularly for ATP generation (Hyodo and Okuno, 2020; Nagy and Lin, 2020; Sanchez and Lagunoff, 2015). Given that both SYNV and TEV induced its relocalization, especially compared to in mock plants, it is possibly important for infection. Nb-287 being a kinase has implications in the SYNV life cycle as both the P and sc4 movement proteins are phosphoproteins and hijacking of kinases is common in many viruses, particularly those of medical importance (Barik and Banerjee, 1992; Gupta et al., 2000; Keating and Striker, 2012). It is also worth noting that Nb-287 only showed relocalization in SYNV-infected plants (Figure 2.4B), further adding to this hypothesis.

Another consideration is the topic of liquid-liquid phase separation (LLPS). LLPS is a thermodynamically driven process in which membraneless organelles, such as the nucleolus, form within cells (Feng et al., 2019). These membraneless organelles, or condensates, are involved in both the sequestration and modification of biomolecules, and thus have gained interest in recent years for roles they perform in vital cellular processes such as enzymatic reactions and signaling pathways, many of which are only beginning to be elucidated (Hondele

et al., 2020). This is particularly true in the context of the nucleolus, in which the structure and function can be altered based on the non-equilibrium state that dictates interactions between the nucleolus and the nucleus (Lafontaine et al., 2020). Thus, this developing field of research presents an exciting avenue for further exploring how the complex biochemical process of LLPS can affect protein modification and, in a broader sense, subcellular localization. It may also help inform about the formation of the subnuclear bodies which were quite prevalent in this work.

Taken together, the images presented in this study illustrate both general and virus-specific relocalizations of host nuclear proteins. The generation of the localisome (Figure 2.1) illustrates a collection of protein localizations which may be of interest for future work, even if they did not relocalize during viral infection in this study. For the proteins which did show relocalization, generation of transgenic marker lines expressing the full-length proteins used in this work along with the usage of an SYNV minireplicon (Ganesan et al., 2013) would be helpful for further verification of this phenomena. Additionally, further studies such as gene silencing, which can be applied to characterize what happens to both host and virus in the absence of these proteins, could be employed. This would lead to not only a better understanding of the virus-host interactome, but also the general interactome of the healthy host. Finally, it would be interesting to use RNA-Seq technology to see the types of genes upregulated during SYNV or TEV infection to see if there are any correlations with the data presented in this study. Given the sometimes dramatic relocalizations of nuclear proteins shown, there is a lot to yet be characterized surrounding the physiological significance of such changes, which provides plenty of options for further work. In this way, we have demonstrated the relocalization of nuclear proteins, many of which were classified into distinct groups and have implications in important

regulatory roles. This work will be continued in order to explore a mechanistic understanding of how viruses modify nuclear localized proteins and virus-induced cellular modifications.

Acknowledgements

The author would like to express gratitude towards Renyuan Wang for their assistance during the experimental procedures, Rowan Calkins for the isolation of *N. benthamiana* proteins, and Amy Crume for their greenhouse work.

Table 2.1: Localization of every nuclear-associated protein screened. Proteins listed in bold have images provided in Figure 1.

Nucleolar	Nucleoplasm	Subnuclear	Nuclear Envelope	Perinuclear (with membranes)	Nuclear and cytoplasmic
RC-17	RC-7	**RC-32**	**RC-51**	**RC-34**	RC-194
RC-28	**RC-55**	RC-33	**RC-71**	**RC-64**	**RC-339**
RC-70	**RC-88**	**RC-121**	RC-132	**RC-128**	**RC-345**
RC-75	**RC-178**	RC-189	**Nb-271**	**RC-332**	**RC-363**
RC-133	**RC-303**	**RC-315**	**Nb-311**	**RC-337**	**RC-391**
RC-139	**RC-353**	**RC-379**	1-19	**RC-675**	**RC-477**
RC-173	RC-394	**RC-442**	**7-4**	**RC-749**	**RC-555**
RC-193	**RC-420**	**RC-446**	**7-19**	**RC-753**	**RC-733**
RC-210	**RC-428**	**RC-534**	**8-43**	**RC-766**	**RC-747**
RC-238	RC-447	**RC-804**	**10-57**	**RC-911**	**RC-752**
RC-244	RC-448	**RC-847**		**Nb-32**	RC-758
RC-249	**RC-463**	**RC-869**		**Nb-240**	**RC-775**
RC-322	RC-496	**RC-919**		**Nb-245**	**RC-845**
RC-396	**RC-498**	RC-948		**Nb-272**	**RC-890**
RC-398	**RC-499**	**Nb-18**		**Nb-281**	**Nb-244**
RC-539	**RC-533**	Nb-103		**Nb-294**	**Nb-249**
RC-553	**RC-536**	**Nb-121**		**Nb-295**	**Nb-251**
RC-557	RC-547	**Nb-243**		**Nb-422**	**Nb-256**
RC-698	RC-708	**Nb-248**		1-25	**Nb-264**
RC-734	RC-712	**Nb-253**		**2-2**	Nb-265
RC-763	**RC-756**	**Nb-285**		2-23	**Nb-289**
RC-834	**RC-921**	**Nb-287**		2-30	**Nb-297**
RC-846	RC-927	**1-2**		2-56	**Nb-302**
RC-863	RC-991	**2-18**		2-70	**Nb-308**
RC-897	Nb-23	2-33		3-3	**1-17**
RC-974	Nb-33	**2-35**		**4-55**	1-42
Nb-27	Nb-65	3-33		**4-58**	1-67
Nb-55	**Nb-312**	3-44		**4-61**	**2-25**
Nb-71	**Nb-428**	3-49		**5-9**	**2-47**
Nb-117	**1-5**	3-54		**7-30**	**2-49**
Nb-120	**1-6**	3-57		**8-22**	**2-53**

Table 2.1 (continued)

Nucleolar	Nucleoplasm	Subnuclear	Nuclear Envelope	Perinuclear (with membranes)	Nuclear and cytoplasmic
Nb-198	2-40	**3-64**		**8-36**	2-62
Nb-202	**2-43**	**3-69**		9-39	2-66
Nb-203	2-44	**4-20**		**9-42**	3-28
Nb-212	**2-46**	**4-41**		**9-49**	3-32
Nb-222	**2-50**	**7-10**		**9-50**	3-61
Nb-239	2-54	**7-33**		**9-52**	**3-76**
Nb-266	2-58	**8-13**		**9-59**	**3-80**
Nb-300	2-60	**8-54**		**9-78**	**4-1**
Nb-321	2-73			**9-80**	**4-7**
Nb-379	2-75			10-41	**4-27**
Nb-425	2-76			**10-52**	**4-39**
1-3	3-6				**4-48**
2-34	3-7				**4-63**
2-38	3-8				**4-67**
2-41	3-15				**5-19**
2-42	3-16				**5-25**
2-45	3-17				**7-2**
2-55	3-19				**7-11**
2-61	3-20				**7-22**
3-24	3-34				**7-25**
3-25	3-42				**7-28**
3-26	3-47				**7-29**
4-8	**3-50**				**7-31**
4-19	**3-51**				**7-34**
4-23	**3-70**				**7-56**
4-36	**3-71**				**8-1**
7-1	3-73				**8-6**
7-32	**3-75**				**8-8**
7-42	**3-78**				8-26
7-43	3-81				8-29
8-20	**4-10**				8-40
8-27	**4-24**				**8-42**
8-44	**4-51**				**8-45**
8-58	**4-53**				**8-52**
8-63	**4-60**				**8-65**
8-66	**5-8**				**8-67**
8-79	**7-9**				**8-68**
9-1	**7-18**				**8-73**
9-64	**8-32**				**8-81**

Table 2.1 (continued)

Nucleolar	Nucleoplasm	Subnuclear	Nuclear Envelope	Perinuclear (with membranes)	Nuclear and cytoplasmic
9-67	8-35				**9-2**
9-72	**8-46**				**9-6**
10-19	**8-57**				**9-8**
10-21	**8-64**				**9-14**
	8-75				**9-20**
	8-78				**9-31**
	9-21				**9-32**
	9-23				**9-47**
	9-24				**9-61**
	9-30				**9-66**
	9-33				**9-69**
	9-35				**9-73**
	9-48				**9-77**
	9-55				**9-81**
	9-63				**9-82**
	9-71				**9-83**
	10-25				**10-6**
	10-34				**10-45**
	10-35				**10-54**
	10-43				**10-55**
	10-58				**10-68**
	10-81				**10-73**
	10-82				**10-74**
	10-87				**10-75**
	10-88				**10-80**
74	**95**	**39**	**10**	**42**	**95**
20.85%	**26.76%**	**10.99%**	**2.82%**	**11.83%**	**26.76%**

Table 2.2: Summary of the proteins which were relocalized in SYNV-infected plants.

Protein	Pattern in Mock-H2B	Pattern in SYNV-ER
RC-51	Envelope and Membranes	Envelope around spherules
RC-238	Nucleolus	Subnuclear (not nucleolus)
RC-396	Nucleolar	Subnuclear (not nucleolus)
RC-534	Subnuclear (not nucleolus)	Nucleolus
Nb-18	Subnuclear (not nucleolus)	Nucleolus
Nb-71	Subnuclear (not nucleolus)	Nucleolus
Nb-243	Subnuclear (not nucleolus)	Nuclear
Nb-287	Subnuclear (not nucleolus)	Perinuclear (with membranes)
2-18	Subnuclear (not nucleolus)	Nuclear envelope
2-25	Nuclear and cytoplasmic	Perinuclear (with membranes)
2-43	Nuclear and cytoplasmic	Perinuclear (with membranes)
2-45	Nucleoplasm	Perinuclear (with membranes)
2-50	Nucleolar	Nuclear
3-69	Nucleolar	Perinuclear (with membranes)
4-8	Nucleolar	Subnuclear (not nucleolus)
8-42	Perinuclear (with membranes)	Nucleoplasmic

Table 2.3: Sequencing results obtained during study using the BLAST algorithm. Underline protein codes indicate proteins which had relocalized during viral infection.

Protein Code	Identity
RC-33	Histone H4
RC-51	Proteinase inhibitor precursor (PI)
RC-70	Aquaporin TIP2-1
RC-238	Nicotiana sylvestris histone H2B.3
RC-332	Nicotiana attenuata uncharacterized
RC-379	60S ribosomal protein L27a-3
RC-804	Nicotiana sylvestris protein pxr1
RC-834	60S ribosomal protein L15
Nb-18	40S ribosomal protein S23
Nb-32	Trypsin proteinase inhibitor precursor (PI)
Nb-71	60S ribosomal protein L35-like, transc. V. X2
Nb-121	Tabacum zinc finger CCH domain-containing protein 37-like
Nb-243	Glyoxylate/succinic semialdehyde reductase 1
Nb-287	Probable inactive receptor kinase
Nb-312	HMG1/2-like protein
1-2	40S ribosomal protein S25
1-3	50S ribosomal protein L6, chloroplastic
1-5	Sm-like protein LSM7, mRNA
1-6	Triose phosphate/phosphate translocator, chloroplastic-like
2-18	Uncharacterized protein, transc. V. X3
2-25	Nicotiana undulata chloroplast clone pCK2-6, complete sequence
2-34	Auxin-binding protein ABP19a-like
2-35	Serine/arginine repetitive matrix protein 2 transc. V. X4
2-40	TIFY 6B-like, transc. V. X2
2-43	chlorophyll a-b binding protein 21, chloroplastic-like
2-45	50S ribosomal protein L11, chloroplastic
2-50	DNA-damage-repair/toleration protein DRT111, chloroplastic-like
2-55	Probable 60S ribosomal protein
3-49	HGV2, transc. V. X2
3-54	Transcription factor AS1-like
3-64	40S ribosomal protein S11-like
3-69	Histone 2b
4-20	Fructose-bisphosphate aldolase
4-36	EIN3-binding F-box protein 1-like
8-43	Replication factor C subunit 1-like

Table 2.4: Summary of the proteins which were relocalized in N. benthamiana plants infected with SYNV and those infected with TEV.

Protein	Mock-H2B	Localization in SYNV-ER	Localization in TEV-ER
RC-238	Nucleoloar	Nucleoplasmic	Nucleoplasmic
Nb-243	Subnuclear loci	Nucleoplasmic	Nucleoplasm and NE
2-34	Nucleoplasmic	Perinuclear and membranes	Nuclear envelope
Nb-287	Subnuclear loci	Nuclear envelope	Subnuclear loci
3-69	Nucleolar	Subnuclear loci	Nucleolar
8-43	Nucloplasm and NE	Nucleoplasm and NE	Punctate loci in nuclear envelope

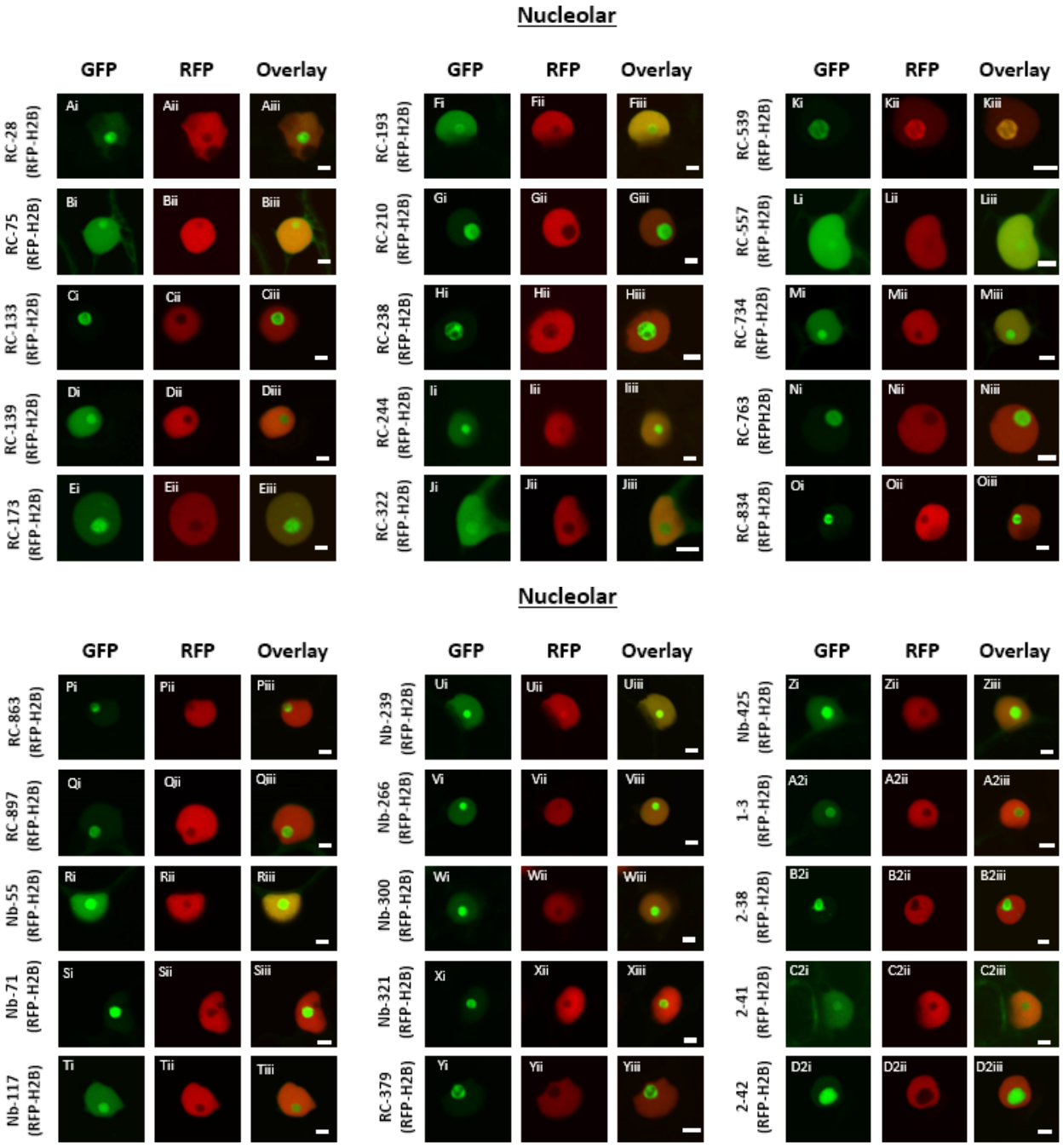
Nucleolar
GFP
RFP
Overlay
RC-28 (RFP-H2B)
RC-75 (RFP-H2B)
RC-133 (RFP-H2B)
RC-139 (RFP-H2B)
RC-173 (RFP-H2B)
RC-193 (RFP-H2B)
RC-210 (RFP-H2B)
RC-238 (RFP-H2B)
RC-244 (RFP-H2B)
RC-322 (RFP-H2B)
RC-539 (RFP-H2B)
RC-557 (RFP-H2B)
RC-734 (RFP-H2B)
RC-763 (RFPH2B)
RC-834 (RFP-H2B)
Nucleolar
GFP
RFP
Overlay
RC-863 (RFP-H2B)
RC-897 (RFP-H2B)
Nb-55 (RFP-H2B)
Nb-71 (RFP-H2B)
Nb-117 (RFP-H2B)
Nb-239 (RFP-H2B)
Nb-266 (RFP-H2B)
Nb-300 (RFP-H2B)
Nb-321 (RFP-H2B)
RC-379 (RFP-H2B)
Nb-425 (RFP-H2B)
1-3 (RFP-H2B)
2-38 (RFP-H2B)
2-41 (RFP-H2B)
2-42 (RFP-H2B)

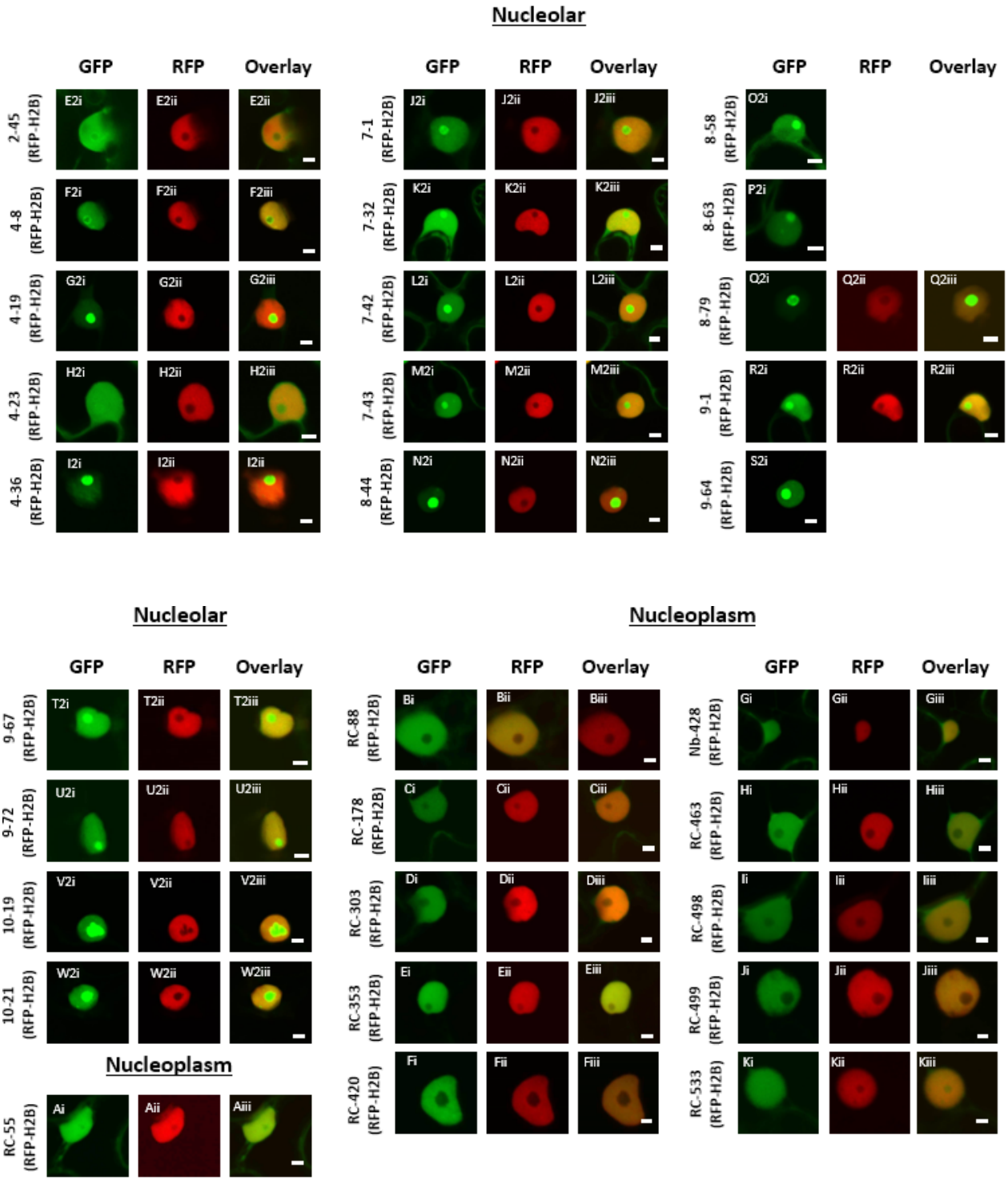
Nucleolar
GFP
RFP
Overlay
2-45 (RFP-H2B)
E2i
E2ii
E2iii
4-8 (RFP-H2B)
F2i
F2ii
F2iii
4-19 (RFP-H2B)
G2i
G2ii
G2iii
4-23 (RFP-H2B)
H2i
H2ii
H2iii
4-36 (RFP-H2B)
I2i
I2ii
I2iii
7-1 (RFP-H2B)
J2i
J2ii
J2iii
7-32 (RFP-H2B)
K2i
K2ii
K2iii
7-42 (RFP-H2B)
L2i
L2ii
L2iii
7-43 (RFP-H2B)
M2i
M2ii
M2iii
8-44 (RFP-H2B)
N2i
N2ii
N2iii
8-58 (RFP-H2B)
O2i
8-63 (RFP-H2B)
P2i
8-79 (RFP-H2B)
Q2i
Q2ii
Q2iii
9-1 (RFP-H2B)
R2i
R2ii
R2iii
9-64 (RFP-H2B)
S2i
Nucleolar
GFP
RFP
Overlay
9-67 (RFP-H2B)
T2i
T2ii
T2iii
9-72 (RFP-H2B)
U2i
U2ii
U2iii
10-19 (RFP-H2B)
V2i
V2ii
V2iii
10-21 (RFP-H2B)
W2i
W2ii
W2iii
Nucleoplasm
RC-55 (RFP-H2B)
Ai
Aii
Aiii
Nucleoplasm
GFP
RFP
Overlay
RC-88 (RFP-H2B)
Bi
Bii
Biii
RC-178 (RFP-H2B)
Ci
Cii
Ciii
RC-303 (RFP-H2B)
Di
Dii
Diii
RC-353 (RFP-H2B)
Ei
Eii
Eiii
RC-420 (RFP-H2B)
Fi
Fii
Fiii
Nb-428 (RFP-H2B)
Gi
Gii
Giii
RC-463 (RFP-H2B)
Hi
Hii
Hiii
RC-498 (RFP-H2B)
Ii
Iii
Iiii
RC-499 (RFP-H2B)
Ji
Jii
Jiii
RC-533 (RFP-H2B)
Ki
Kii
Kiii

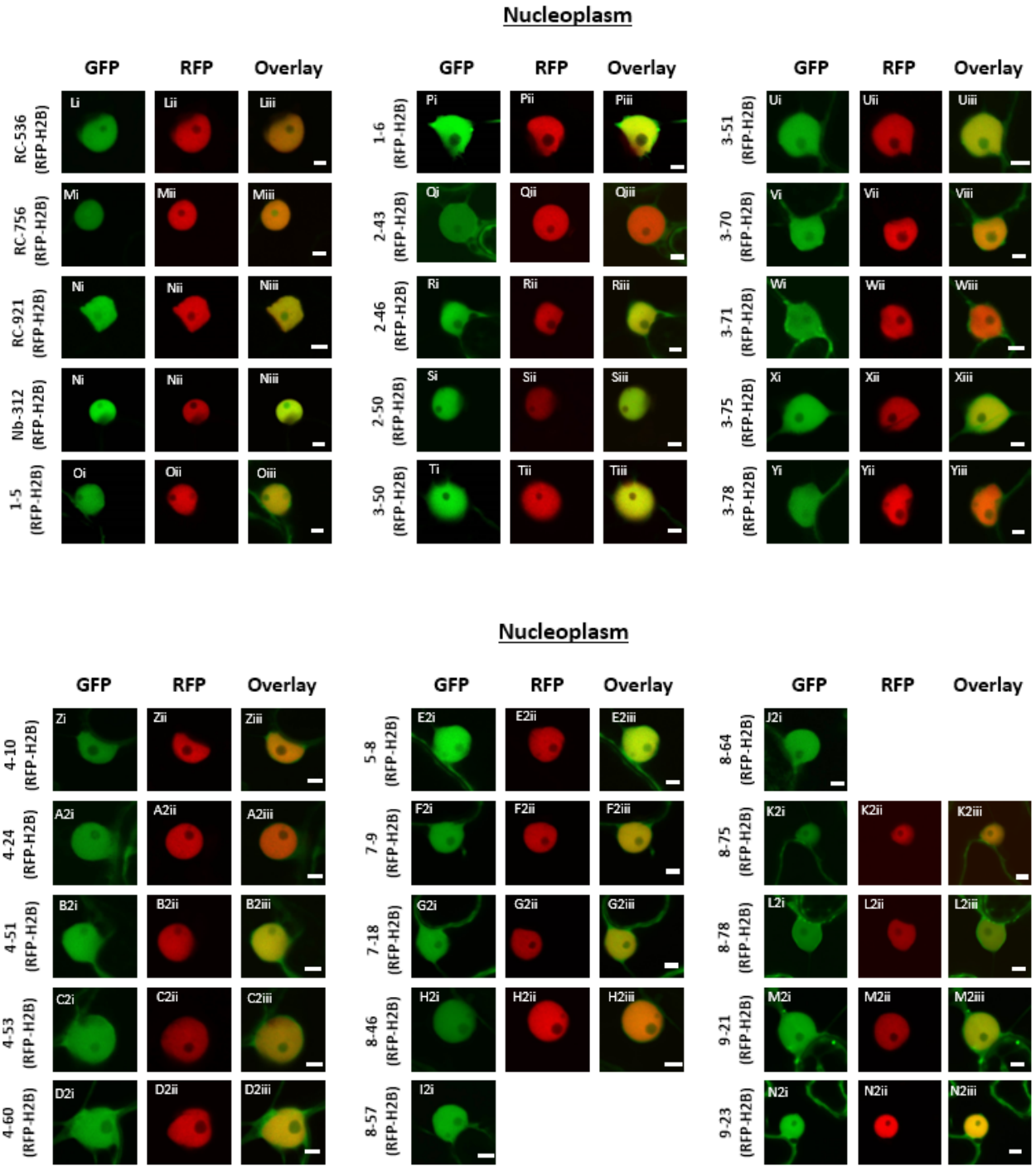
Nucleoplasm
GFP
RFP
Overlay
RC-536 (RFP-H2B)
RC-756 (RFP-H2B)
RC-921 (RFP-H2B)
Nb-312 (RFP-H2B)
1-5 (RFP-H2B)
1-6 (RFP-H2B)
2-43 (RFP-H2B)
2-46 (RFP-H2B)
2-50 (RFP-H2B)
3-50 (RFP-H2B)
3-51 (RFP-H2B)
3-70 (RFP-H2B)
3-71 (RFP-H2B)
3-75 (RFP-H2B)
3-78 (RFP-H2B)
Nucleoplasm
GFP
RFP
Overlay
4-10 (RFP-H2B)
4-24 (RFP-H2B)
4-51 (RFP-H2B)
4-53 (RFP-H2B)
4-60 (RFP-H2B)
5-8 (RFP-H2B)
7-9 (RFP-H2B)
7-18 (RFP-H2B)
8-46 (RFP-H2B)
8-57 (RFP-H2B)
8-64 (RFP-H2B)
8-75 (RFP-H2B)
8-78 (RFP-H2B)
9-21 (RFP-H2B)
9-23 (RFP-H2B)

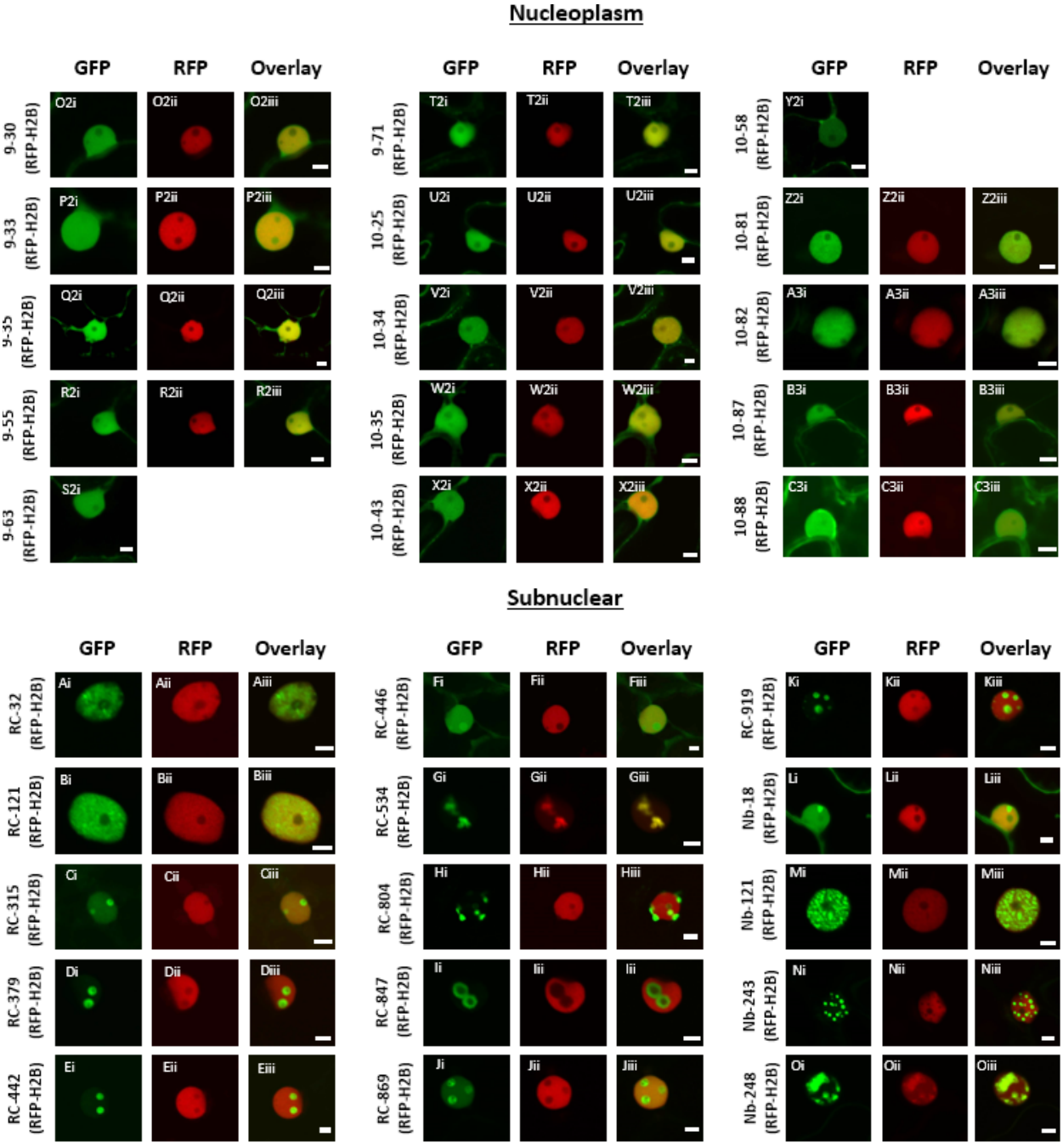
Nucleoplasm
GFP
RFP
Overlay
9-30 (RFP-H2B)
O2i
O2ii
O2iii
9-33 (RFP-H2B)
P2i
P2ii
P2iii
9-35 (RFP-H2B)
Q2i
Q2ii
Q2iii
9-55 (RFP-H2B)
R2i
R2ii
R2iii
9-63 (RFP-H2B)
S2i
9-71 (RFP-H2B)
T2i
T2ii
T2iii
10-25 (RFP-H2B)
U2i
U2ii
U2iii
10-34 (RFP-H2B)
V2i
V2ii
V2iii
10-35 (RFP-H2B)
W2i
W2ii
W2iii
10-43 (RFP-H2B)
X2i
X2ii
X2iii
10-58 (RFP-H2B)
Y2i
10-81 (RFP-H2B)
Z2i
Z2ii
Z2iii
10-82 (RFP-H2B)
A3i
A3ii
A3iii
10-87 (RFP-H2B)
B3i
B3ii
B3iii
10-88 (RFP-H2B)
C3i
C3ii
C3iii
Subnuclear
RC-32 (RFP-H2B)
Ai
Aii
Aiii
RC-121 (RFP-H2B)
Bi
Bii
Biii
RC-315 (RFP-H2B)
Ci
Cii
Ciii
RC-379 (RFP-H2B)
Di
Dii
Diii
RC-442 (RFP-H2B)
Ei
Eii
Eiii
RC-446 (RFP-H2B)
Fi
Fii
Fiii
RC-534 (RFP-H2B)
Gi
Gii
Giii
RC-804 (RFP-H2B)
Hi
Hii
Hiii
RC-847 (RFP-H2B)
Ii
Iii
Iii
RC-869 (RFP-H2B)
Ji
Jii
Jiii
RC-919 (RFP-H2B)
Ki
Kii
Kiii
Nb-18 (RFP-H2B)
Li
Lii
Liii
Nb-121 (RFP-H2B)
Mi
Mii
Miii
Nb-243 (RFP-H2B)
Ni
Nii
Niii
Nb-248 (RFP-H2B)
Oi
Oii
Oiii

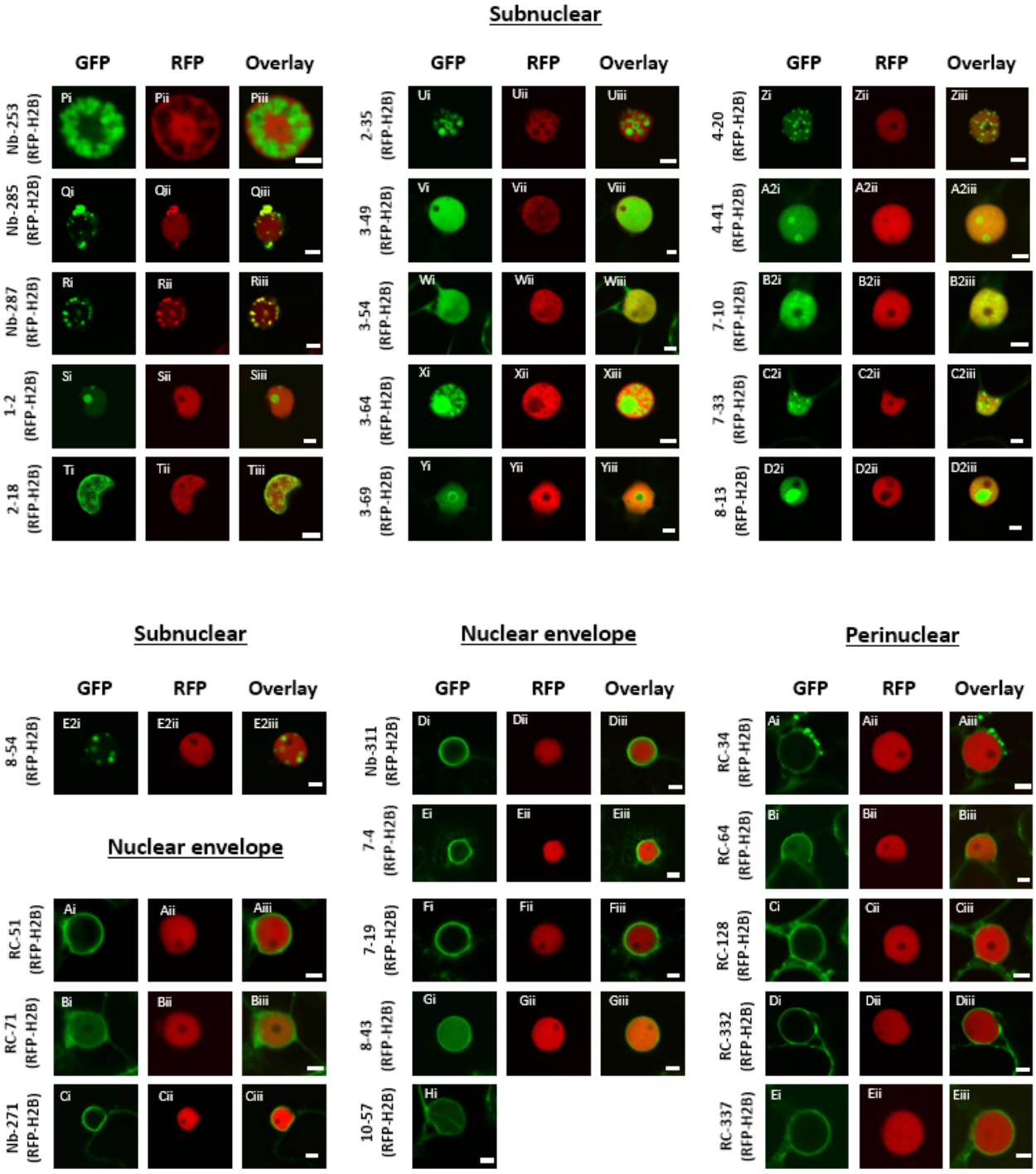
Subnuclear
GFP
RFP
Overlay
Nb-253 (RFP-H2B)
Pi
Pii
Piii
Nb-285 (RFP-H2B)
Qi
Qii
Qiii
Nb-287 (RFP-H2B)
Ri
Rii
Riii
1-2 (RFP-H2B)
Si
Sii
Siii
2-18 (RFP-H2B)
Ti
Tii
Tiii
2-35 (RFP-H2B)
Ui
Uii
Uiii
3-49 (RFP-H2B)
Vi
Vii
Viii
3-54 (RFP-H2B)
Wi
Wii
Wiii
3-64 (RFP-H2B)
Xi
Xii
Xiii
3-69 (RFP-H2B)
Yi
Yii
Yiii
4-20 (RFP-H2B)
Zi
Zii
Ziii
4-41 (RFP-H2B)
A2i
A2ii
A2iii
7-10 (RFP-H2B)
B2i
B2ii
B2iii
7-33 (RFP-H2B)
C2i
C2ii
C2iii
8-13 (RFP-H2B)
D2i
D2ii
D2iii
Subnuclear
8-54 (RFP-H2B)
E2i
E2ii
E2iii
Nuclear envelope
RC-51 (RFP-H2B)
Ai
Aii
Aiii
RC-71 (RFP-H2B)
Bi
Bii
Biii
Nb-271 (RFP-H2B)
Ci
Cii
Ciii
Nuclear envelope
Nb-311 (RFP-H2B)
Di
Dii
Diii
7-4 (RFP-H2B)
Ei
Eii
Eiii
7-19 (RFP-H2B)
Fi
Fii
Fiii
8-43 (RFP-H2B)
Gi
Gii
Giii
10-57 (RFP-H2B)
Hi
Perinuclear
RC-34 (RFP-H2B)
Ai
Aii
Aiii
RC-64 (RFP-H2B)
Bi
Bii
Biii
RC-128 (RFP-H2B)
Ci
Cii
Ciii
RC-332 (RFP-H2B)
Di
Dii
Diii
RC-337 (RFP-H2B)
Ei
Eii
Eiii

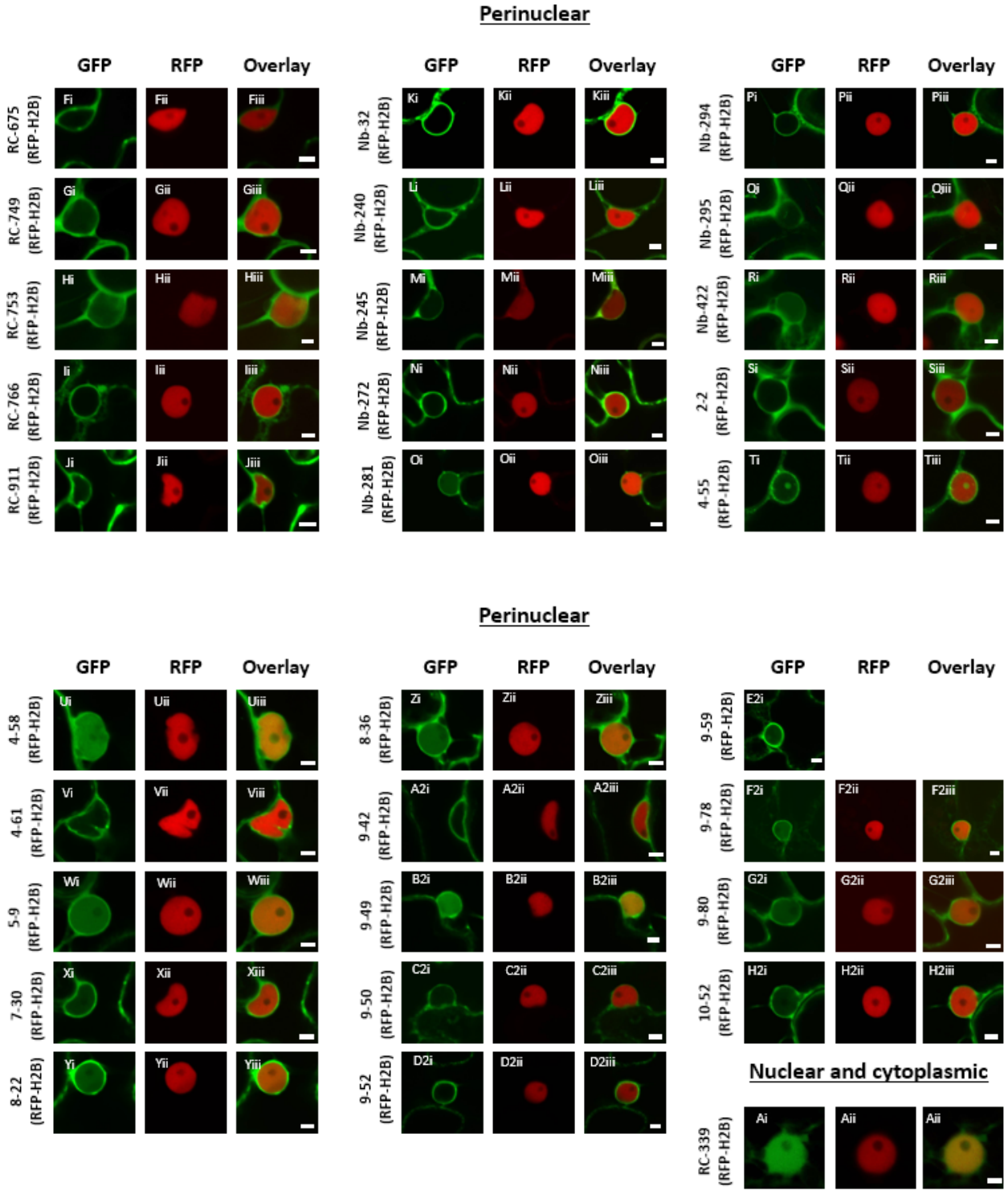
Perinuclear
GFP
RFP
Overlay
RC-675 (RFP-H2B)
Fi
Fii
Fiii
RC-749 (RFP-H2B)
Gi
Gii
Giii
RC-753 (RFP-H2B)
Hi
Hii
Hiii
RC-766 (RFP-H2B)
Ii
Iii
Iiii
RC-911 (RFP-H2B)
Ji
Jii
Jiii
Nb-32 (RFP-H2B)
Ki
Kii
Kiii
Nb-240 (RFP-H2B)
Li
Lii
Liii
Nb-245 (RFP-H2B)
Mi
Mii
Miii
Nb-272 (RFP-H2B)
Ni
Nii
Niii
Nb-281 (RFP-H2B)
Oi
Oii
Oiii
Nb-294 (RFP-H2B)
Pi
Pii
Piii
Nb-295 (RFP-H2B)
Qi
Qii
Qiii
Nb-422 (RFP-H2B)
Ri
Rii
Riii
2-2 (RFP-H2B)
Si
Sii
Siii
4-55 (RFP-H2B)
Ti
Tii
Tiii
Perinuclear
GFP
RFP
Overlay
4-58 (RFP-H2B)
Ui
Uii
Uiii
4-61 (RFP-H2B)
Vi
Vii
Viii
5-9 (RFP-H2B)
Wi
Wii
Wiii
7-30 (RFP-H2B)
Xi
Xii
Xiii
8-22 (RFP-H2B)
Yi
Yii
Yiii
8-36 (RFP-H2B)
Zi
Zii
Ziii
9-42 (RFP-H2B)
A2i
A2ii
A2iii
9-49 (RFP-H2B)
B2i
B2ii
B2iii
9-50 (RFP-H2B)
C2i
C2ii
C2iii
9-52 (RFP-H2B)
D2i
D2ii
D2iii
9-59 (RFP-H2B)
E2i
9-78 (RFP-H2B)
F2i
F2ii
F2iii
9-80 (RFP-H2B)
G2i
G2ii
G2iii
10-52 (RFP-H2B)
H2i
H2ii
H2iii
Nuclear and cytoplasmic
RC-339 (RFP-H2B)
Ai
Aii
Aii

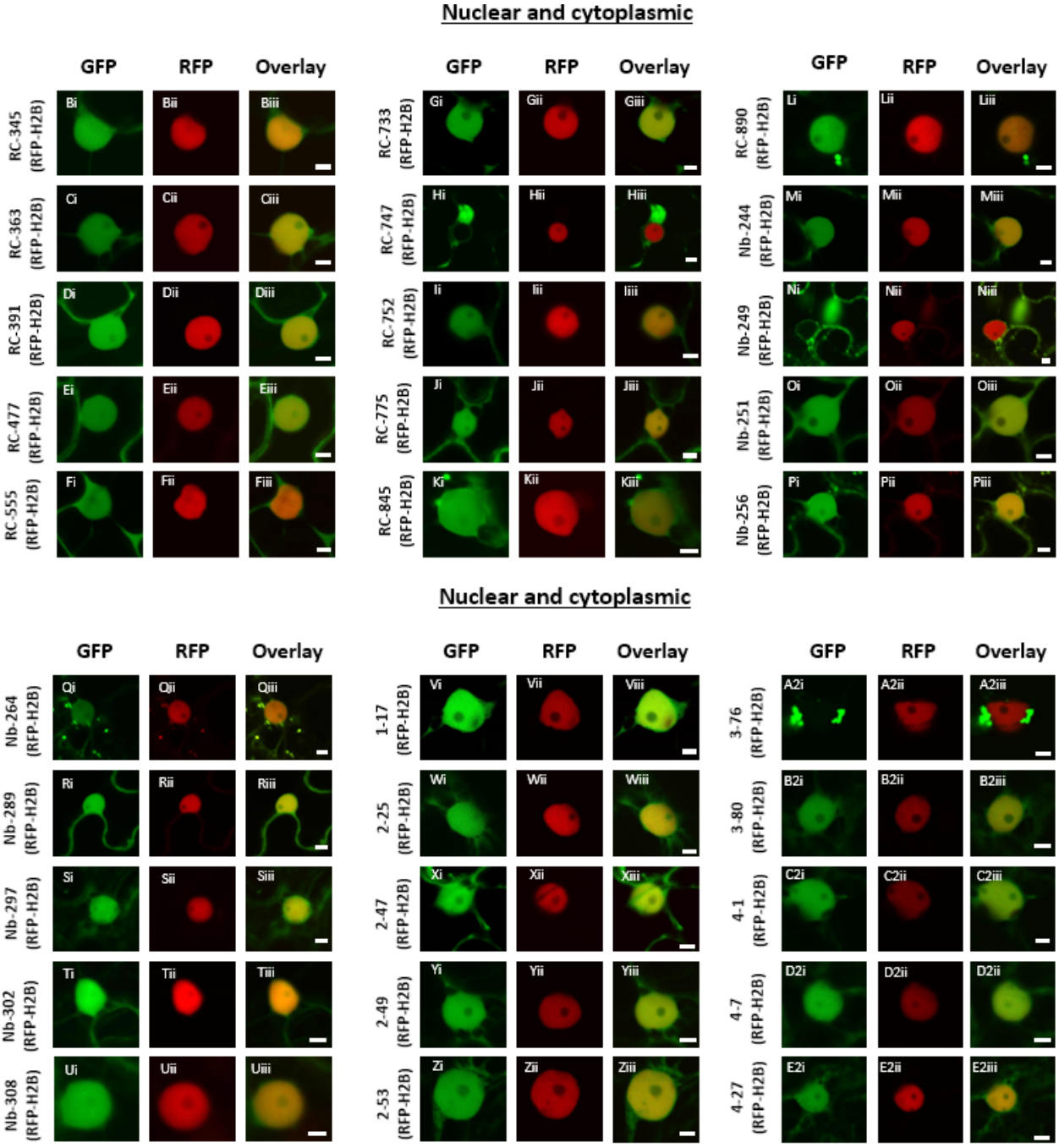
Nuclear and cytoplasmic
GFP
RFP
Overlay
RC-345 (RFP-H2B)
RC-363 (RFP-H2B)
RC-391 (RFP-H2B)
RC-477 (RFP-H2B)
RC-555 (RFP-H2B)
RC-733 (RFP-H2B)
RC-747 (RFP-H2B)
RC-752 (RFP-H2B)
RC-775 (RFP-H2B)
RC-845 (RFP-H2B)
RC-890 (RFP-H2B)
Nb-244 (RFP-H2B)
Nb-249 (RFP-H2B)
Nb-251 (RFP-H2B)
Nb-256 (RFP-H2B)
Nuclear and cytoplasmic
GFP
RFP
Overlay
Nb-264 (RFP-H2B)
Nb-289 (RFP-H2B)
Nb-297 (RFP-H2B)
Nb-302 (RFP-H2B)
Nb-308 (RFP-H2B)
1-17 (RFP-H2B)
2-25 (RFP-H2B)
2-47 (RFP-H2B)
2-49 (RFP-H2B)
2-53 (RFP-H2B)
3-76 (RFP-H2B)
3-80 (RFP-H2B)
4-1 (RFP-H2B)
4-7 (RFP-H2B)
4-27 (RFP-H2B)

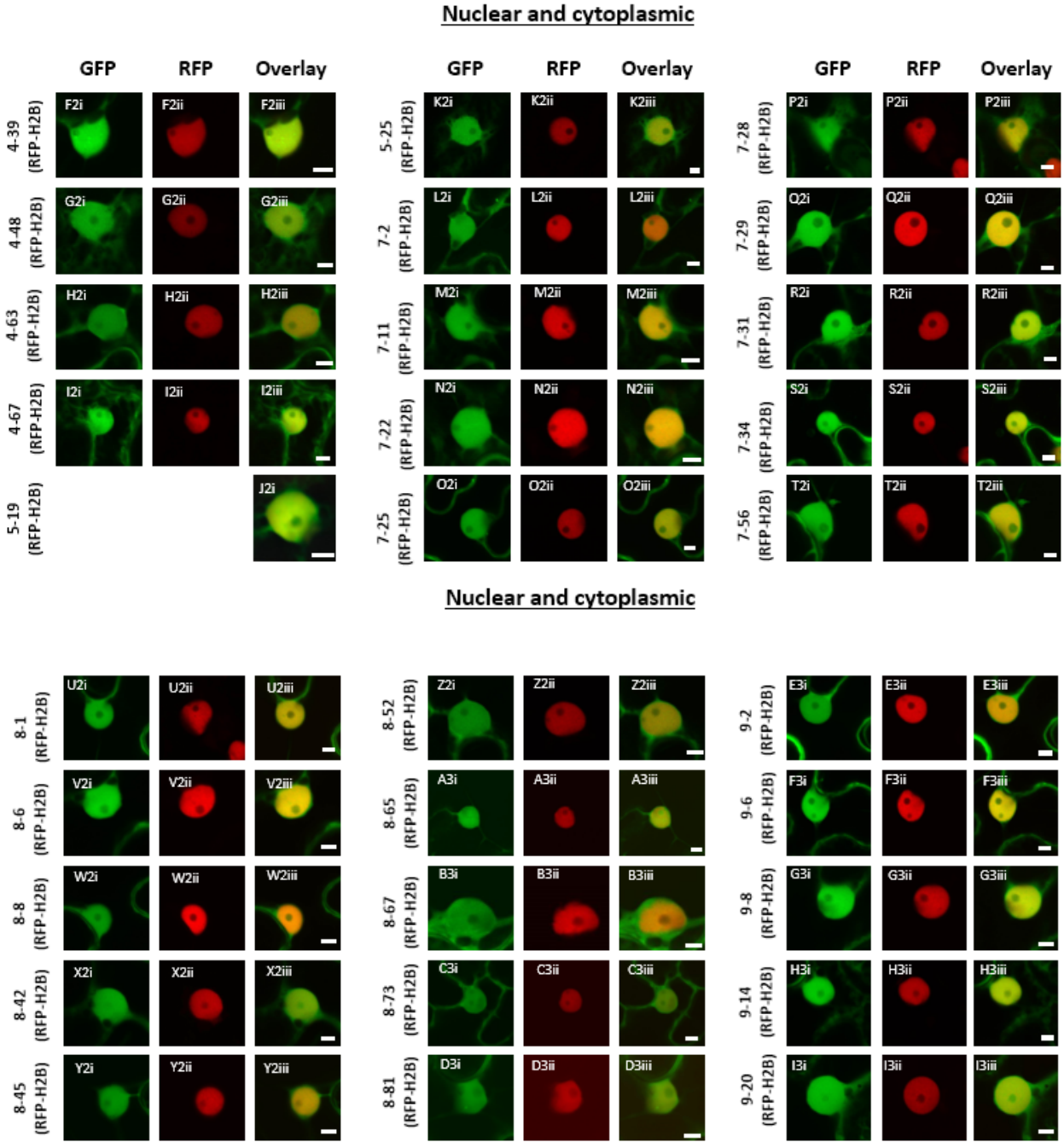
Nuclear and cytoplasmic
GFP
RFP
Overlay
4-39 (RFP-H2B)
F2i
F2ii
F2iii
4-48 (RFP-H2B)
G2i
G2ii
G2iii
4-63 (RFP-H2B)
H2i
H2ii
H2iii
4-67 (RFP-H2B)
I2i
I2ii
I2iii
5-19 (RFP-H2B)
J2i
5-25 (RFP-H2B)
K2i
K2ii
K2iii
7-2 (RFP-H2B)
L2i
L2ii
L2iii
7-11 (RFP-H2B)
M2i
M2ii
M2iii
7-22 (RFP-H2B)
N2i
N2ii
N2iii
7-25 (RFP-H2B)
O2i
O2ii
O2iii
7-28 (RFP-H2B)
P2i
P2ii
P2iii
7-29 (RFP-H2B)
Q2i
Q2ii
Q2iii
7-31 (RFP-H2B)
R2i
R2ii
R2iii
7-34 (RFP-H2B)
S2i
S2ii
S2iii
7-56 (RFP-H2B)
T2i
T2ii
T2iii
Nuclear and cytoplasmic
8-1 (RFP-H2B)
U2i
U2ii
U2iii
8-6 (RFP-H2B)
V2i
V2ii
V2iii
8-8 (RFP-H2B)
W2i
W2ii
W2iii
8-42 (RFP-H2B)
X2i
X2ii
X2iii
8-45 (RFP-H2B)
Y2i
Y2ii
Y2iii
8-52 (RFP-H2B)
Z2i
Z2ii
Z2iii
8-65 (RFP-H2B)
A3i
A3ii
A3iii
8-67 (RFP-H2B)
B3i
B3ii
B3iii
8-73 (RFP-H2B)
C3i
C3ii
C3iii
8-81 (RFP-H2B)
D3i
D3ii
D3iii
9-2 (RFP-H2B)
E3i
E3ii
E3iii
9-6 (RFP-H2B)
F3i
F3ii
F3iii
9-8 (RFP-H2B)
G3i
G3ii
G3iii
9-14 (RFP-H2B)
H3i
H3ii
H3iii
9-20 (RFP-H2B)
I3i
I3ii
I3iii

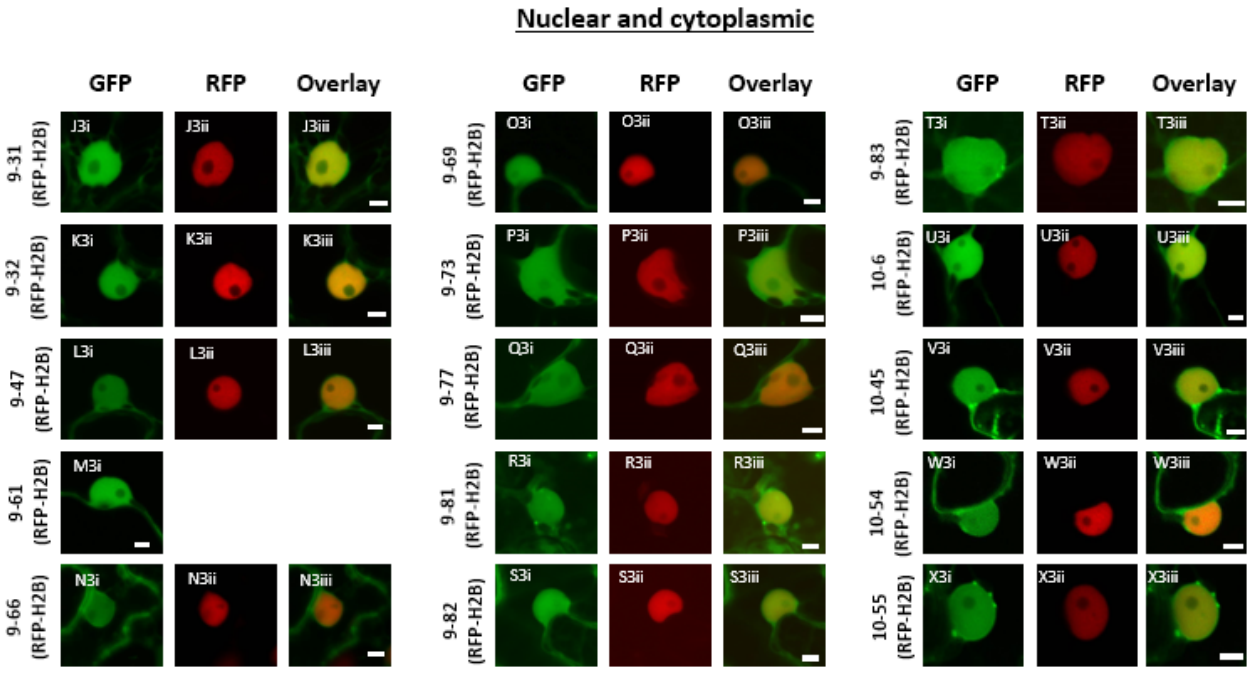
Nuclear and cytoplasmic
GFP
RFP
Overlay
9-31 (RFP-H2B)
J3i
J3ii
J3iii
9-32 (RFP-H2B)
K3i
K3ii
K3iii
9-47 (RFP-H2B)
L3i
L3ii
L3iii
9-61 (RFP-H2B)
M3i
9-66 (RFP-H2B)
N3i
N3ii
N3iii
9-69 (RFP-H2B)
O3i
O3ii
O3iii
9-73 (RFP-H2B)
P3i
P3ii
P3iii
9-77 (RFP-H2B)
Q3i
Q3ii
Q3iii
9-81 (RFP-H2B)
R3i
R3ii
R3iii
9-82 (RFP-H2B)
S3i
S3ii
S3iii
9-83 (RFP-H2B)
T3i
T3ii
T3iii
10-6 (RFP-H2B)
U3i
U3ii
U3iii
10-45 (RFP-H2B)
V3i
V3ii
V3iii
10-54 (RFP-H2B)
W3i
W3ii
W3iii
10-55 (RFP-H2B)
X3i
X3ii
X3iii

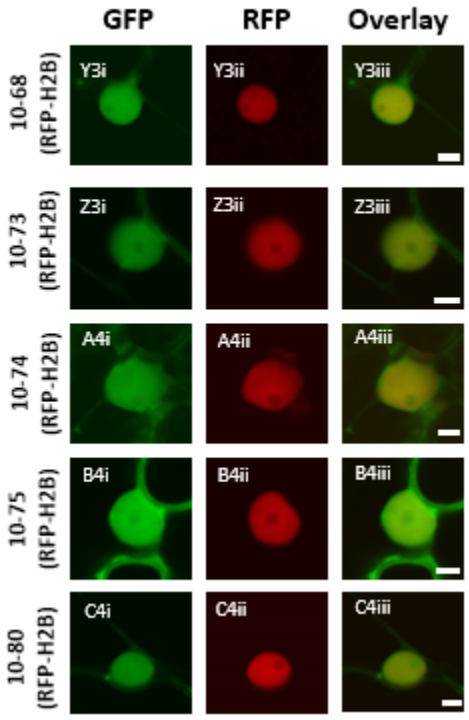
Nuclear and cytoplasmic
GFP
RFP
Overlay
10-68 (RFP-H2B)
Y3i
Y3ii
Y3iii
10-73 (RFP-H2B)
Z3i
Z3ii
Z3iii
10-74 (RFP-H2B)
A4i
A4ii
A4iii
10-75 (RFP-H2B)
B4i
B4ii
B4iii
10-80 (RFP-H2B)
C4i
C4ii
C4iii

Figure 2.1: Localisome showing the collection of micrographs taken during duration of nuclear screening. Patterns illustrate various loci in which nuclear-destined proteins typically localize, including the nucleolus, nucleoplasm, subnuclear loci, nuclear envelope, perinuclear region (including membranes), and the nucleus including cytoplasmic accumulation. Scale bar= 5 μm.

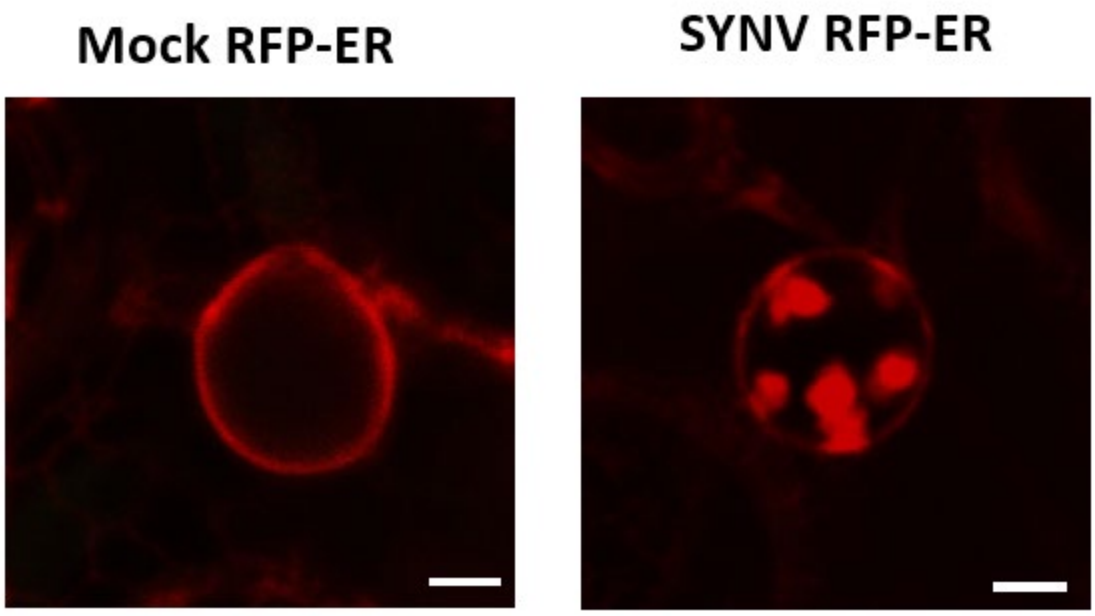

Figure 2.2: N. benthamiana marker line expressing RFP to the ER to visualize the nuclear envelope (left). SYNV viral accumulations in the nuclear envelope induce intranuclear membranous spherules. Scale bar= 5 μm

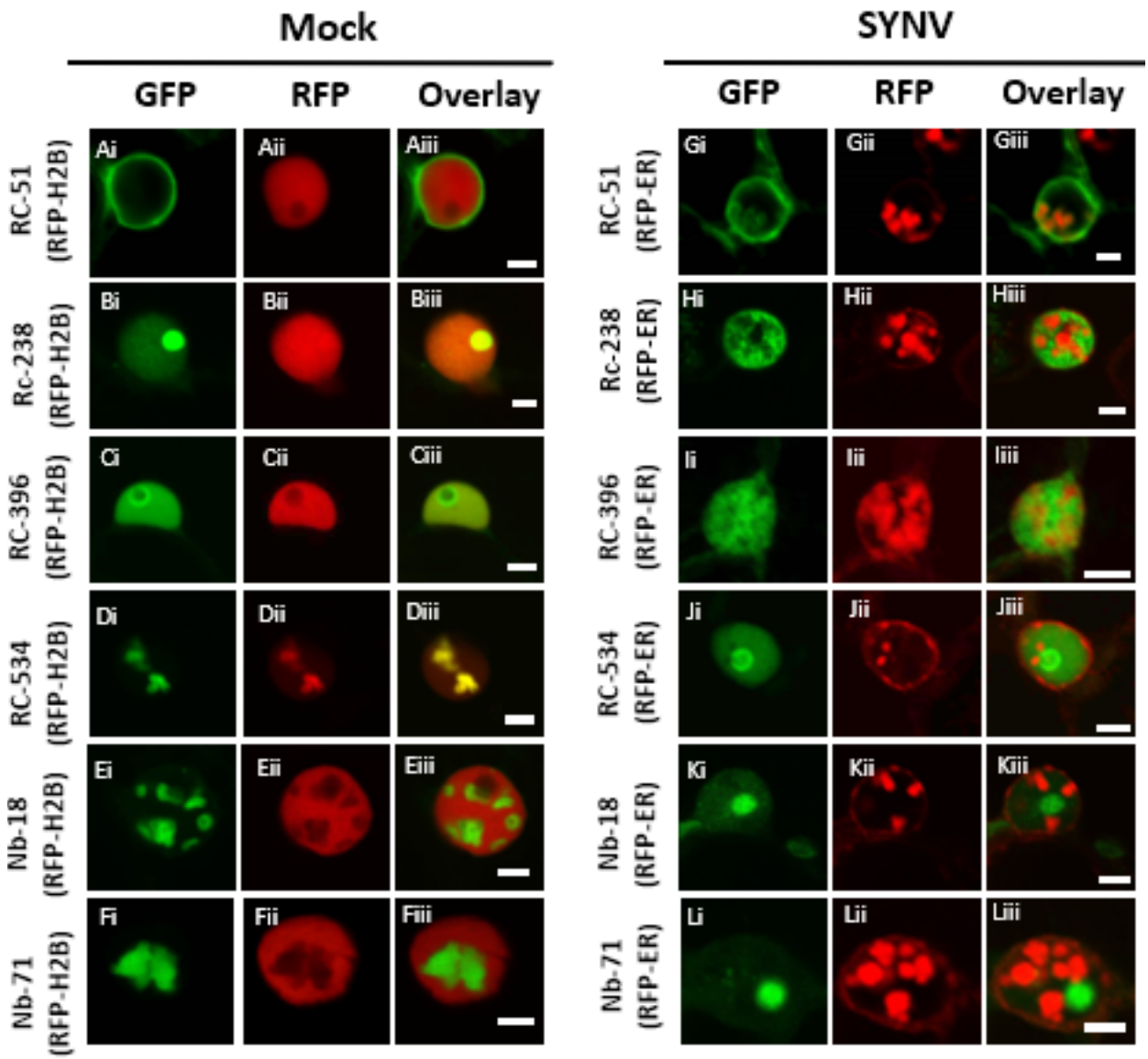
Mock
SYNV
GFP
RFP
Overlay
RC-51 (RFP-H2B)
Rc-238 (RFP-H2B)
RC-396 (RFP-H2B)
RC-534 (RFP-H2B)
Nb-18 (RFP-H2B)
Nb-71 (RFP-H2B)
RC-51 (RFP-ER)
Rc-238 (RFP-ER)
RC-396 (RFP-ER)
RC-534 (RFP-ER)
Nb-18 (RFP-ER)
Nb-71 (RFP-ER)
Ai
Aii
Aiii
Bi
Bii
Biii
Ci
Cii
Ciii
Di
Dii
Diii
Ei
Eii
Eiii
Fi
Fii
Fiii
Gi
Gii
Giii
Hi
Hii
Hiii
Ii
Iii
Iiii
Ji
Jii
Jiii
Ki
Kii
Kiii
Li
Lii
Liii

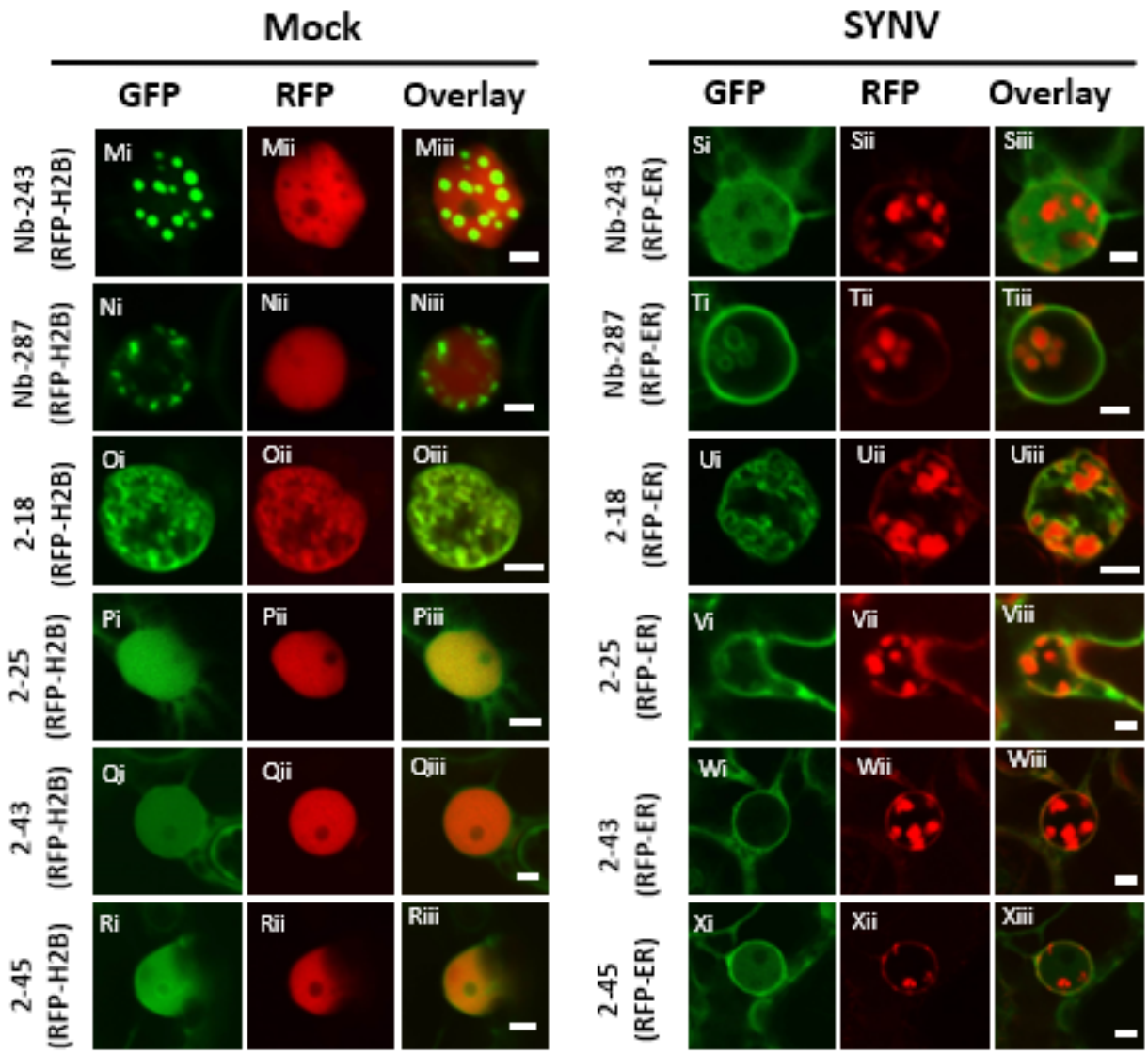
Mock
SYNV
GFP
RFP
Overlay
Nb-243 (RFP-H2B)
Nb-287 (RFP-H2B)
2-18 (RFP-H2B)
2-25 (RFP-H2B)
2-43 (RFP-H2B)
2-45 (RFP-H2B)
Nb-243 (RFP-ER)
Nb-287 (RFP-ER)
2-18 (RFP-ER)
2-25 (RFP-ER)
2-43 (RFP-ER)
2-45 (RFP-ER)
Mi
Mii
Miii
Ni
Nii
Niii
Oi
Oii
Oiii
Pi
Pii
Piii
Qj
Qii
Qiii
Ri
Rii
Riii
Si
Sii
Siii
Ti
Tii
Tiii
Ui
Uii
Uiii
Vi
Vii
Viii
Wi
Wii
Wiii
Xi
Xii
Xiii

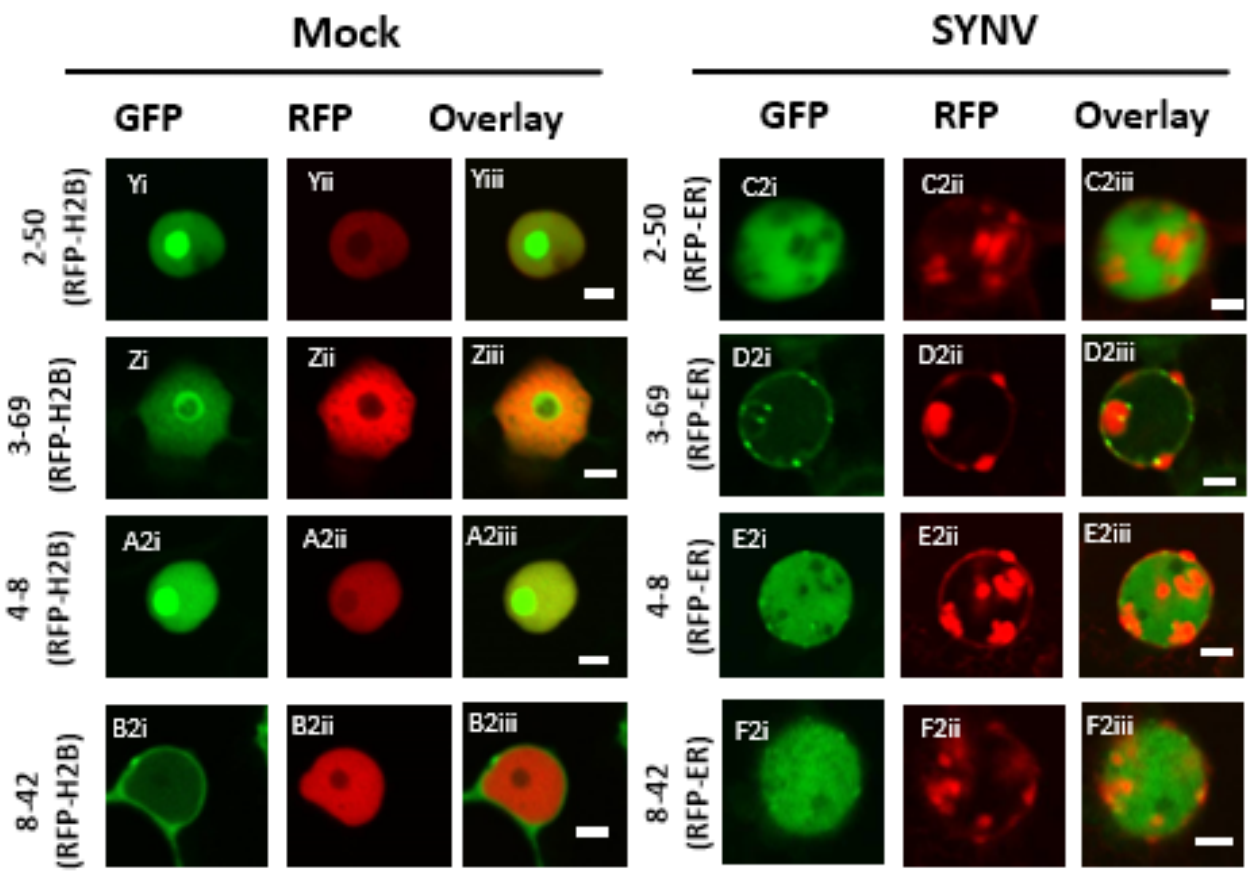

Figure 2.3: Micrographs showing protein relocalizations in response to SYNV-infection in N. benthamiana. Scale bar= 5 µm

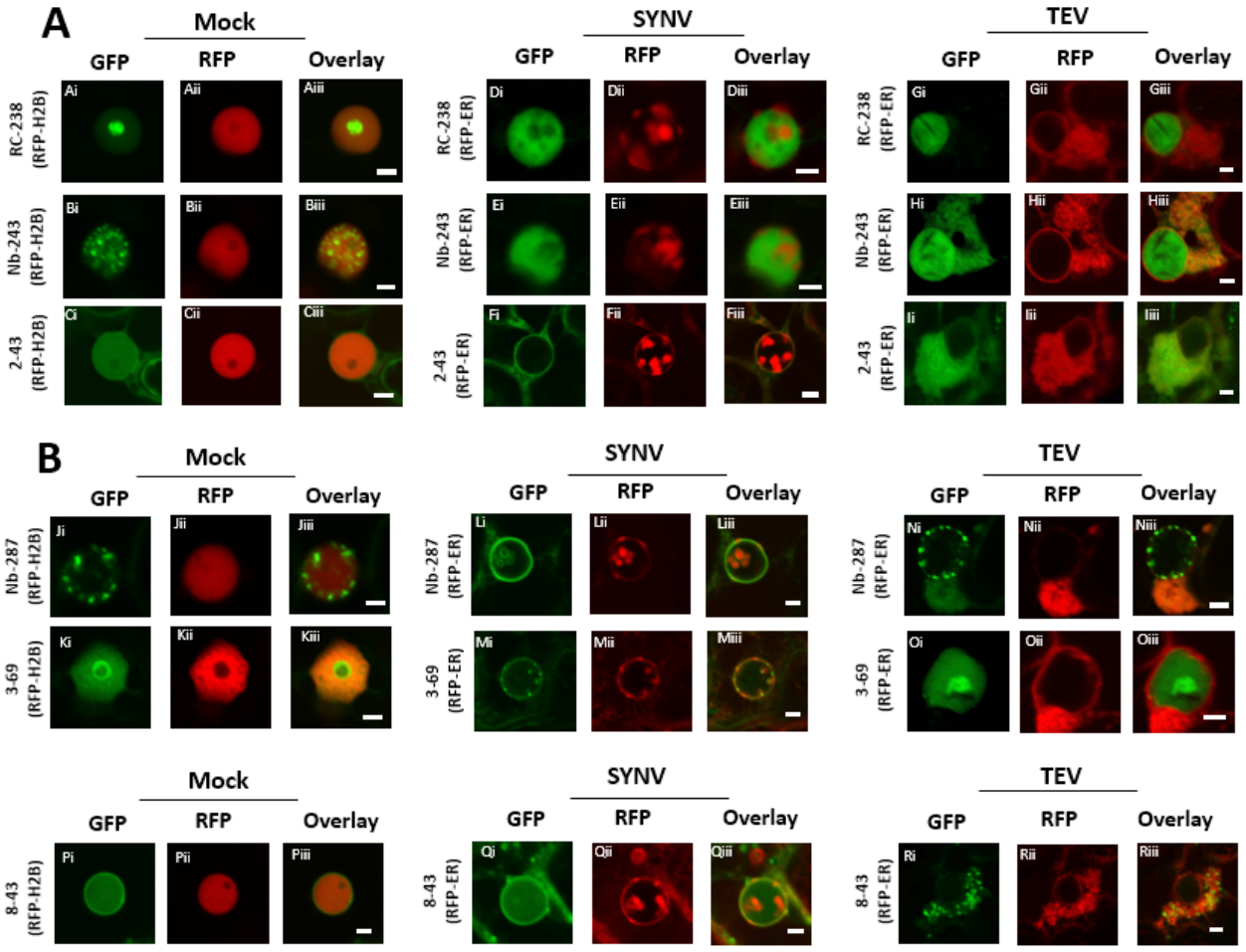

Figure 2.4: Image matrix showing virus-induced changes in nuclear localization. A) Protein localization patterns which changes in response to both SYNV and TEV infection. B) Proteins exhibiting relocalization in response to SYNV infection but not TEV. C) Proteins relocalize in response to TEV infection by not SYNV. Scale bar= 5 µm.

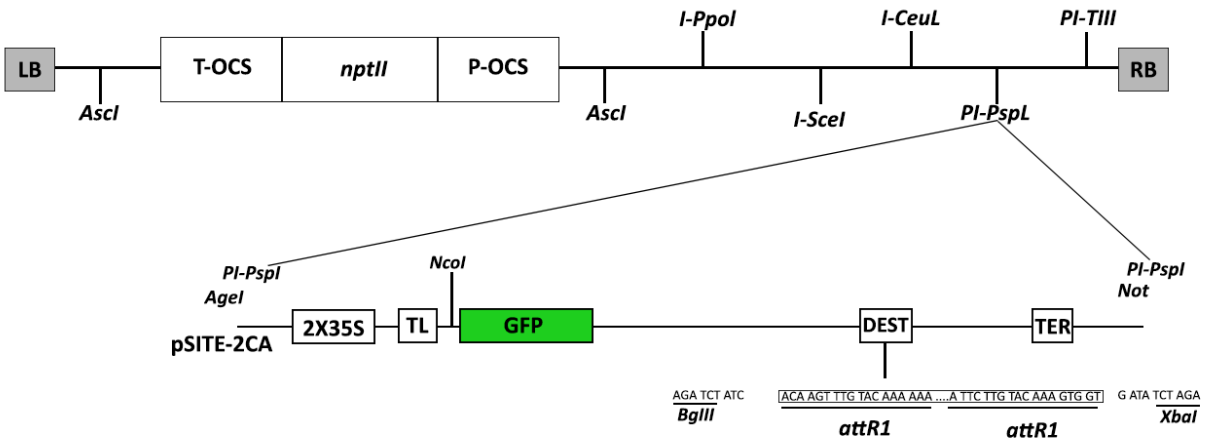

Supplementary Figure 2.1: Map of the binary pSITE-2CA vector. This vector allows for C-terminal fusions of polypeptides to GFP. The backbone is from a commercially available vector and the att sites are where cDNAs are cloned. Average insert size in this library was 1.5 kb.

(Reference: Chakrabarty et al., 2007).

Chapter 3[1]

A cell map of SYNV in *Nicotiana benthamaia*

Introduction

An important consideration in plant virology is understanding the diversity of host factors present in the plant host cell which may promote or inhibit viral processes. The eukaryotic cell contains intracellular components such as membranes, filaments, organelles, and macromolecules which all may be targeted and manipulated during the virus life cycle (Hull, 2014; Schmid et al., 2014). The host cell is not left defenseless as it may employ several strategies as part of an antiviral response, including RNA silencing, hormonal regulation, protein degradation and translational repression, (Calil and Fontes, 2016; Kambham et al., 2017; Wu et al., 2019). Thus, viral infection involves the complex interplay between viral and host factors, and this is the focal point of much of the work occurring in plant virus research, particularly as computational biology progresses and such large scale analyses become more feasible (Ala-Poikela et al., 2019; Cook and Jensen, 2018; Osterbaan and Fuchs, 2019).

What must also be considered is the fact that viruses are not limited to just one cell type. In plants, viruses move their genomes from cell-to-cell through plasmodesmata into adjacent cells where they can initiate new replication cycles. In its simplest form, this involves viral movement proteins (MP) which form a transport complex that modifies the plasmodesmata to facilitate the passage of the complex through the channel (Hipper et al., 2013; Schoelz et al.,

[1]This project was completed in collaboration with Alex Stewart and Taylor Trapp. Micrographs and data interpretation by Caleb Mathias. Additional data by Stewart and Trapp not shown.

2011; Taliansky et al., 2008; Ueki and Citovsky, 2007). In addition to the cell-to-cell movement, viruses also move systemically through their hosts via the vasculature in order to infect the entire plant. This involves translocation from mesophyll cells, bundles sheath, vascular parenchyma, companion cells, and sieve elements where it enters the phloem and spreads to the rest of the plant in a manner similar to photoassimilate distribution (Carrington et al., 1996; Hipper et al., 2013; Navarro et al., 2019; Ueki and Citovsky, 2007). This means that viruses colonize a variety of different cells, tissues, and organs for the duration of infection, which adds a level of complexity in terms of unraveling how viruses manipulate host factors throughout the entire plant. This is especially true when considering differential gene expression (DGE), which not only occurs naturally in different tissue types throughout healthy hosts (Artlip et al., 2019; Birnbaum et al., 2003; Hui et al., 2018; Slotte et al., 2007) but is often changed during the course of pathogen infection (Bouazizi et al., 2020; Kumar and Kirti, 2011; Whitham et al., 2006; Zhang et al., 2019). It is therefore beneficial to study viral infection in all parts of the plant in the context of both virology and plant physiology using a wide range of both integrative omics approaches and microscopy.

Expression maps seek to combine large quantities of both expression and visualization data for purposes such as elucidating genetic function, protein localization, and variations in gene expression (Regev et al., 2017; Rhee et al., 2019). One of the premier examples of expression mapping is the Human Protein Atlas (HPA) (www.proteinatlas.org), which is an open-access database that is the result of a consortium started in 2003 with the goal of mapping and characterizing the complete human proteome throughout single-cells, tissues, and organs (Uhlén et al., 2015). Additional datasets included gene expression data in the blood (Unlén et al., 2019), brain (Sjöstedt et al., 2020), metabolic networks (Unlén et al., 2019), and the proteome of

major cancer types (Unlén et al., 2017). Initial work included antibody-based imaging of subcellular protein localization, systems biology, and immunohistochemistry (Uhlén et al., 2005), but was further expanded to include RNA-seq data from the Genotype-Tissue Expression (GTEx) consortium (Keen and Moore, 2015), and Cap Analysis of Gene Expression (CAGE) data from the Functional Annotation Of the Mammalian Genome (FANTOM) consortium (Lizio et al., 2019). This database has been instrumental in providing researchers with high quality confocal images and expression data for aiding in their work, including research regarding diagnosis of Alzheimer's disease (Khoonsari et al., 2019) molecular characterization of different cancer types (Benfeitas et al., 2017; Lee et al., 2018; Morin et al., 2018), and is currently being used for transcriptome profiling of SARS-CoV-2 (Hikmet et al., 2020).

Of course, expression mapping is not just limited to mammals. Since the sequenced genome of *Arabidopsis thaliana* was completed in 2000, complete sequences of plant genomes have grown rapidly, and in 2005 a transcriptome map of *A. thaliana* developmental stages was generated by Schmid et al. using the Affymetrix ATH1 array platform. Since then, over 40 transcriptome maps have been constructed for 32 plants (reviewed in Klepikova and Penin, 2019), including economically important crops such as rice (Nobuta et al., 2007; Zhang et al., 2010), wheat (Ramírez-González et al., 2018; Schreiber et al., 2009), corn (Sekhon et al., 2011; Stelpflug et al., 2016; Walley et al., 2016), sorghum (Shakoor et al., 2014), and soybean (Libault et al., 2010; Severin et al., 2010). Initially, these maps were based on microarray analysis, though since 2015 RNA-seq-based atlases have become the most prevalent method (Klepikova and Penin, 2019). The data from these studies are often compiled in either new or preexisting databases. Some of these encompass data from multiple organisms, such as the EBI Expression Atlas (ebi.ac.uk/gxa) and GTEx (gtexportal.org) , but there are several plant-specific databases,

such as the eFP browser (bar.utoronto.ca/eplant/), TomExpress (tomexpress.toulouse.inra.fr), TraVA (travadb.org), Melonet-DB (gene.melonet-db.jp), TobEA (solgenomics.net), and *ROSAseq* (iant.toulouse.inra.fr). These databases compile expression data from different parts of the plant and under different environmental conditions and thus fulfill a similar need as the HPA in terms of providing researchers with genomic, transcriptomic, proteomic, and metabolomic data in a convenient location. However, unlike the HPA many of these plant databases lack the breadth of high-quality confocal imaging data provided by the HPA. Further, many plant viruses have not had their localization visualized via microscopy throughout different plant tissues. Therefore, a there is a need for cell mapping not only in healthy plants, but those undergoing viral infection which may be used to complement such databases, particularly regarding the alteration of expression levels which pathogens may cause. It is for this reason that a cell map of the plant-adapted rhabdovirus sonchus yellow net virus (SYNV), a betanucleorhabdovirus which replicates in the nuclei of plants, using laser scanning confocal microscopy (LSCM). To date, no such map exists for SYNV, so this will not only allow for better insight into viral infection in different parts of the plant but also for use in future omics studies which investigate the subcellular alterations created during the virus lifecycle. To accomplish this, we performed live-cell imaging of both healthy (mock) and SYNV-infected *Nicotiana benthamiana* '16c' plants, which express green fluorescent protein (GFP) to the endomembrane system, which leads to the staining of the endoplasmic reticulum (ER) and nuclear membranes (Goodin et al., 2005). This is a useful reference marker for SYNV as the viral accumulation induces the formation of membranous intranuclear spherules.

Materials and Methods

Laser Scanning Confocal Microscopy

Live cell imaging was conducted using an FV1000 scanning confocal microscope (Olympus). GFP was excited at 488 nm. GFP laser intensity was set to 1% power with high voltage (HV) values in a range between 500-700 V to the photomultiplier tube (PMT). Images were acquired using the FluoView™ software v1.5 by Olympus. These images were taken using the 40x objective at a scan speed of 10 μs/pixel with a 512-by-512-pixel resolution. These were exported into a JPEG format and assembled in PowerPoint.

Growth, maintenance, and inoculation of plants

N. benthamiana plants were maintained in greenhouse conditions as described by Martins et al. (1998). Transgenic *N. benthamiana* 16c marker lines were generated as outlined by Ruiz et al., (1998). Plants were inoculated with SYNV following the mechanical inoculation procedure described by Hull (2009), which provides several options for the chelating agent and abrasive substance to be used on the leaves. In this study, 0.02 M sodium sulfite was used as the reducing agent and celite as the abrasive. Several SYNV-infected *N. benthamiana* leaves were ground in this mixture via mortar and pestle and used to inoculate a tray of transgenic 16c plants containing an average of 4-6 leaves. Plants were imaged 2-4 weeks after inoculation to allow for symptoms to fully develop and for all major plant parts to have developed. Plant tissues samples were wet mounted onto slides for imaging.

Results

SYNV remodels host nuclear architecture

In this study, a sampling of major plant tissues where chosen due to ease of access and visibility of cells with viral infection. As can be seen in Figure 3.1A, C, M, N, and P, nuclei in mock 16c *N. benthamiana* plants are characterized as having the nuclear envelope (NE) tagged with GFP as the outer nuclear membrane (ONM) is contiguous with the ER, which is part of the endomembrane system tagged in 16c plants (Goodin et al 2005). The nuclei of plants infected with SYNV exhibit intranuclear spherules induced by viral nucleocapsid budding into and accumulating in the inner nuclear membrane (INM). This is illustrated clearly in Figure 3.1B, D, and Q. This pattern remains fairly consistent in the nuclei of cells in other SYNV-infected tissues. Intriguingly, in some of the cells found in the middle of the flower petals (Figure 3.1R), the membranous spherules were slightly smaller than those found in the nuclei of other cells.

SYNV accumulation at the cellular level

Some images were taken to encompass many cells in order to observe if any patterns existed with the spread of the virus. In the leaf primordia, those in plants infected with SYNV show nuclear viral accumulations in the lower right of the developing leaf where the more mature cells are located (Figure 3.1F) when compared to the mock (Figure 3.1E). Roots of mock plants are shown in Figure 3.1M and N, with the former being the developing root cap. In roots of virus infected plants (Figure 3.1O), nuclei with SYNV symptoms were most common in more developed tissues around the vasculature, as can be seen by the circular accumulations of GFP near the center of the image. Foci closer to the root cap did not have any viral symptoms present,

presumably due to this region being of rapid differentiation. Viral accumulation was also observed in the nuclei of the narrow cells in the style (Figure 3.1G and H). Viral accumulation was not observed in the ovary or other reproductive organs.

SYNV induces alterations in the endomembrane system throughout the cell

Finally, the endomembrane system was imaged in both mock (Figure 3.1I and J) and infected hosts (Figure 3.1K and L). Though the change was not dramatic, there are differences in the appearance of mock and SYNV-infected cell membranes. For example, in the mock plants the strands appear much more ordered than in the virus-infected plant. The reticulate pattern has been replaced by uneven coagulations of ER. Further investigations will be needed to fully determine the extent of the effects of SYNV on membranous networks in the cell.

Discussion

The purpose of this study was to obtain a cellular map of SYNV infection in *N. benthamiana*, which serves as a valuable model host for plant-virus interaction studies (Bally et al., 2018). While not every tissue type is present, leaves, roots, leaf primordia, flower petals, ER, and style were imaged. Despite the smaller sample size, the images presented show representatives from both shoot and root, as well as developing tissue. The later example was particularly interesting as the viral movement followed the expected pattern of being absent from the rapidly dividing cells of the meristem but showing slight presence along the more mature cells near what is likely the growing procambial tissue (Figure 3.1 F, lower right of panel). Further, the likely alteration in ER patterns between mock (Figure 3.1 I, J) and SYNV-infected

(Figure 3.1 K, L) cells warrants more investigation. It would also be intriguing to study more of the reproductive organs as SYNV is known to be horizontally transmitted by insect vectors, so further study could elucidate why there is a lack of vertical transmission.

Studying viral infection from a whole-plant perspective is valuable as it not only allows for tracking the extent of viral systemic spread but also can be used to better characterize the physiological effects of such infection by observing the perturbations in subcellular architecture. Further, in the era of next-generation sequencing (NGS), quantifications of expression levels in plant tissues can make unveil the extent to which viruses in different parts of the plant are altering regulatory networks within cells. For example, viruses like cucumber mosaic virus (CMV), tomato spotted wilt virus (TSWV) and potato virus X (PVX) were found to regulate the expression of 33 differentially expressed genes in chrysanthemums (Choi et al., 2015). The rise of expression mapping over the past two decades has provided a rationale for the complementary relationship between visual phenotypic data and more detailed transcriptomic, proteomic, and metabolomic profiles for the construction of wide-ranging datasets (Caicedo et al., 2017; Pesti et al., 2019).

Further work with regards to cellular mapping of SYNV would involve several factors. First, a wider sampling of tissue types is necessary to further characterize the extent of viral spread. In the same manner, studying spread at different stages of growth would also prove valuable as it would illustrate the relationship between plant development and viral spread. Finally, more extensive imagine techniques such as 3D reconstruction of cells using LSCM "z-stacking" would reveal details that may be hidden, particularly with respect to the cytoskeleton as views of this can be limited by 2D imaging. Using fluorescent markers at different subcellular loci would also aid in this venture. Finally, silencing of prospective host factors important for

replication and/or spread would also be useful to have a collection of visualization data in addition to expression data to better identify potential targets for antivirals.

Acknowledgements

We would like to thank Taylor Trap and Alex Stewart for their assistance during the imaging process.

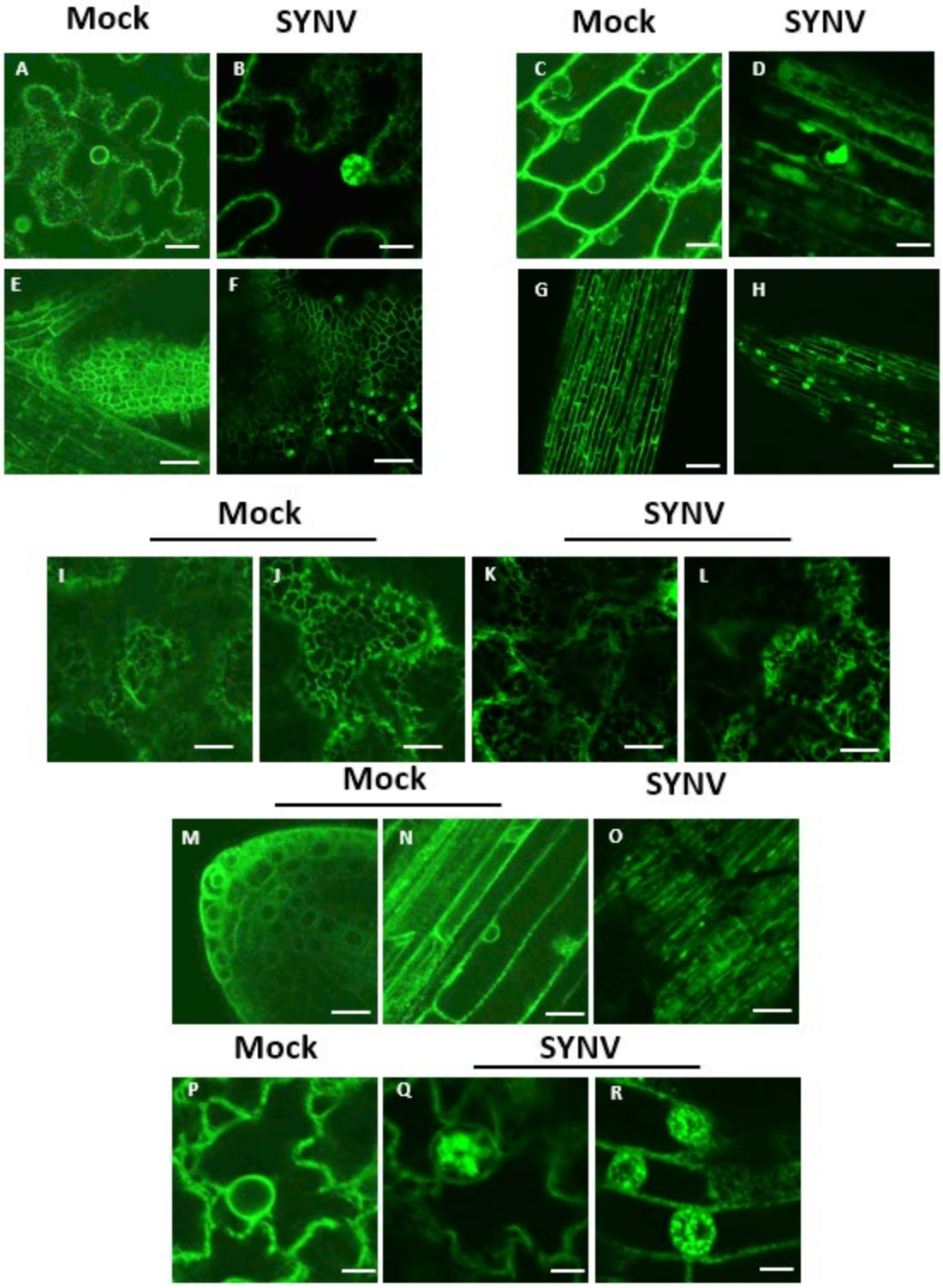
Mock
SYNV
Mock
SYNV
A
B
C
D
E
F
G
H
Mock
SYNV
I
J
K
L
Mock
SYNV
M
N
O
Mock
SYNV
P
Q
R

Figure 3.1: Series of micrographs comparing healthy vs SYNV-infected tissues in the 16c transgenic marker line of Nicotiana benthamiana. A+B Leaf epidermis. C+D Pistil. E+F Leaf primordia. G+H Style. I-L Leaf endomembrane. M-O Root P-R Flower petal.

Scale bars are as follows: Panels A-D, P-R= 10 μm. Panels E-H, O= 50 μm. Panels I-N= 25 μm.

Chapter 4[1]

Lost and found: Rediscovery and genomic characterization of sowthistle yellow vein virus after a 30+ year hiatus

The rhabdovirus sowthistle yellow vein virus (SYVV) was used in a series of elegant experiments to establish a fundamental paradigm of plant virus – vector interactions, in which a plant virus was demonstrated to be propagative in an insect vector. SYVV was first described by Duffus (1963) with a post-acquisition latent period in the aphid vector (*Hyperomyzus lactucae* L.) considerably longer than that of plant viruses known at that time to be retained persistently by the vector. Additional evidence for the propagative nature of SYVV in the aphid was provided by Richardson and Sylvester (1968), who described bacilliform virus particles in the perinuclear space of both sowthistle (*Sonchus oleaceous* L.) and *H. lactucae,* and demonstrated that aphids injected with SYVV from plant extracts transmit the virus to sowthistle. Propagation of SYVV in *H. lactucae* was confirmed by demonstration of transovarial passage at low level (Sylvester, 1969), dosage dependency of latent period following injection inoculation of SYVV to aphids (Sylvester et al., 1970), electron microscopic observation of SYVV particles in multiple organ systems of the insect (Sylvester and Richardson, 1970), infection of a primary cell culture of ovarian and embryonic tissue of *H. lactucae* (Peters and Black, 1970), deleterious effects of SYVV on fitness of *H. lactucae* (Sylvester, 1973), and efficient transmission of SYVV during serial passage from aphid to aphid via injection (Sylvester and Richardson, 1969, 1971). Subsequent research on SYVV was limited to characterization of virion structural components,

[1]This chapter was originally published as: Stenger, D.C., Burbank, L.P., Wang, R., Stewart, A.A., Mathias, C., and Goodin, M.M. (2020). Lost and found: Rediscovery and genomic characterization of sowthistle yellow vein virus after a 30+ year hiatus. Virus Research 284, 197987. Caleb Mathias contributed to the data analysis: see supplemental data.

including proteins (Peters and Kitajima, 1970; Schultz and Harrap, 1976; Ziemiecki and Peters, 1976) and RNA (Stenger et al., 1988).

During the past 30+ years, there has been a paucity of research on SYVV. As molecular cloning techniques became widely applied to plant virology, beginning in the 1980's, researchers studying plant rhabdoviruses focused on more tractable systems, such as sonchus yellow net virus (SYNV), that were mechanically transmissible to *Nicotiana* species (Heaton et al., 1989; Jackson and Li, 2016). More recent advancements in Next Generation Sequence technology made it possible to obtain genome sequences of recalcitrant plant rhabdoviruses (Menzel et al., 2018; Ramalho et al., 2014; Willie and Stewart, 2017; Zhou et al., 2020). Indeed, the Ninth Report of the International Committee on the Taxonomy of Viruses (ICTV) lists nine member species in the genus *Nucleorhabdovirus* (Dietzgen et al., 2012) for which genome sequences were available, with the notable exception of SYVV. The present status of taxonomy for the family *Rhabdoviridae* is presented in the full ICTV Online (10th) Report (www.ictv.global/report/rhabdoviridae) as summarized by Walker et al. (2018).

As the American pioneers of plant rhabdovirus research (Edward S. Sylvester, Jean Richardson and James E. Duffus) retired, their isolates of SYVV were no longer maintained and are, presumably, lost to history. Concurrently, SYVV disappeared from the environment, at least in coastal California. Once commonly observed infecting the cosmopolitan weed sowthistle, displacement of the vector *H. lactucae* by an invasive non-vector (*Uroleucon sonchi* (L.)) aphid colonizing sowthistle is anecdotally considered to be responsible for a decline in incidence of SYVV in California (Sylvester and Richardson, 1992).

In November of 2018, sowthistle plants displaying classic symptoms of SYVV infection (Figure 4.1) and colonized by *H. lactucae* and *U. sonchi* were fortuitously observed in an organic

citrus grove in Kern County, CA while conducting field research on the glassy-winged sharpshooter vector of *Xylella fastidiosa* (Stenger et al., 2019). This serendipitous encounter initiated the research described here, in which genomic sequence of SYVV was determined, first from an archived library of SYVV cDNA clones constructed for the Berkeley lab isolate in 1986 (Stenger et al., 1988), and then from infected plant material collected in 2018.

Genomic RNA extracted from purified virions of the SYVV Berkeley isolate was used as template to construct a library of cDNA clones in 1986 (Stenger et al., 1988). The library consisted of 84 clones (after screening for insert size >450 bp) with inserts up to 1.1 kbp. At the time, each clone was grown separately, with plasmid DNA extracted and stored frozen. Select clones were used as probes in Northern blots of healthy and infected plant and aphid tissues (Stenger et al., 1988) but were not sequenced. The library of cDNA clones remained in frozen storage under the care of Andrew O. Jackson. In 2019, the SYVV cDNA library was returned to D. C. Stenger, who authenticated the library based upon nucleotide sequence of the multiple cloning site of the specific plasmid cloning vector (pUC9) employed in 1986 and presence of homopolymeric G/C tails flanking the inserts, which were added to cDNA and plasmid vector to facilitate insertion. Integrity of the cloned cDNA library was assessed by electrophoresis of native plasmids in 1% agarose. This analysis indicated that the plasmids were intact after >30 years in storage and varied in size between 3.1 and 3.8 kbp, as expected for the combined size of the plasmid vector and inserts, as estimated in 1986.

Each recombinant plasmid from the 1986 library was used to transform Escherichia coli strain JM109 (Life Technologies); plasmids were purified from transformants and used as template in Sanger sequencing reactions primed with universal M13 forward and reverse primers annealing to plasmid vector sequences flanking cDNA insertions. Sequences were determined

using an Applied Biosystems 3130 Genetic Analyzer. Sequence reads were trimmed to remove plasmid vector sequences and homopolymeric tails, and compiled into contigs using Sequencher version 5.4.6 (Gene Codes, Ann Arbor, MI). BLAST X searches were conducted, in which translated coding sequences were used as queries of the non-redundant protein database. Results of the BLAST X search indicated that each of the five contigs derived from the 1986 cDNA library shared homology with known plant rhabdoviruses. Figure 4.2 shows the genomic location of the 1986 cDNA contigs relative to the six open reading frames (ORFs) conserved among nucleorhabdoviruses. Based on sequences determined from the 1986 cDNA library, primers were designed to amplify a series of 16 overlapping RT-PCR products spanning most of the SYVV genome, excluding termini. Template for these RT-PCR reactions was a total nucleic acid sample (designated HWY65) extracted from symptomatic sowthistle leaves collected on Nov. 1, 2018 from an organic citrus orchard located west of Highway 65 in Kern County, CA, approximately 9 miles east of McFarland, CA. For RT-PCR, first-strand cDNA synthesis and polymerase chain reactions were carried out using Superscript reverse transcriptase IV (Thermo-Fisher Scientific) and Phusion high fidelity DNA polymerase (Thermo-Fisher Scientific), respectively. RT-PCR products were cloned into pGEMT-easy (Promega, Madison, WI) and purified from transformed Escherichia coli strain JM109. Inserts from three to five clones of each RT-PCR product were sequenced as described above and compiled into a single contig of 13,335 nts representing >97 % of the SYVV genome.

Oxford Nanopore sequencing was used to obtain terminal sequences, thereby completing the genomic sequence of SYVV RNA from the HWY65 sample. For Nanopore sequencing, infected plant material was ground in liquid nitrogen and total RNA extracted using a CTAB/phenol-chloroform extraction protocol (Hilario and Mackay, 2007). Ribosomal RNA was

removed using a RiboMinus Plant Kit (Thermo Fisher); remaining RNA was purified and concentrated using AMPure XP beads (Beckman Coulter). Poly-A tails were added using E. coli Poly-A polymerase (New England Biolabs) following manufacturer's protocol and the sequencing library was made with 500 ng of poly-A RNA using a direct RNA sequencing kit (SQK-RNA002; Oxford Nanopore). The RNA library was sequenced on a MinION sequencing device until a total of 829,833 reads were obtained. Sequence reads were base-called using Oxford Nanopore software (Guppy version 3.3.0). The 13,335 nt contig previously assembled from Sanger sequenced cloned RT-PCR products was used as a reference for assembly of viral sequence reads with minimap2 (Li, 2018). Mapped reads were sorted with Samtools (Li et al., 2009) and all reads aligning to ends of the reference were pulled out and converted to FASTA format using seqtk (https://github.com/lh3/seqtk). Because of low sequence coverage at the termini, a second round of Nanopore sequencing was conducted on the same RNA sample using a cDNA-PCR Sequencing kit (SQK-DCS109; Oxford Nanopore) for library prep and primers designed based on end sequences obtained from direct RNA sequencing. cDNA sequence reads were base-called, sorted, and assembled as described above.

The resulting Nanopore sequence data extended the 2018 HWY65 contig to 13,719 nts (Figure 4.2B) containing the complete sequence for all six ORFs (nucleoprotein [N], phosphoprotein [P], movement protein [MP,] matrix protein [M], glycoprotein [G], and large [L; RNA dependent RNA polymerase]) conserved among nucleorhabdoviruses and flanked by untranslated Leader (166 nt) and Trailer (148 nt) sequences. The complete nucleotide sequence of SYVV- HWY65 was deposited in GenBank as accession MT185675. Alignment of the HWY65 contig with contigs obtained from the 1986 cDNA library revealed 98.5 % nucleotide sequence identity over all regions for which sequence was available for both (~86 % of the

genome). This indicates that the 2018 HWY65 sequence represents the same virus as the Berkeley lab isolate used as template to construct the 1986 cDNA library.

A BLAST N search was conducted using the complete nucleotide sequence of SYVV-HWY65 as query. Subjects returned with the most significant E values were four nucleorhabdoviruses. Alignment of complete nucleotide sequences indicated SYVV-HWY65 was most closely related to zhuye pepper nucleorhabdovirus (ZPNRV; accession MH323437.1; 56.5 % identity), datura yellow vein virus (DYVV; accession KM823531.1; 56.0 % identity), black currant-associated rhabdovirus (BCaRV; accession MF543022.1; 55.6 % identity), and SYNV (accession L32603.1; 53.0 % identity). Proteins encoded by SYVV were aligned with proteins encoded by representative nucleorhabdoviruses and compared (Table 4.1). Five of six SYVV proteins shared highest amino acid percent identity with the recently described ZPNRV. The SYVV P protein was most closely related to DYVV. The next closest relatives were BCaRV and SYNV.

Most rhabdoviruses package a single, negative-sense RNA serving as template for a series of polyadenylated mRNA transcripts corresponding to each ORF and an untranslated Leader RNA (Dietzgen et al., 2012). Located between each SYVV ORF is a conserved iteron sequence (Figure 4.2C), containing (in positive-sense) a transcript termination/polyadenylation signal (AUAUAAGAAAAA), a non-transcribed dinucleotide (CC), and a transcript initiation motif (AAC). The SYVV intergenic iteron shares 100 % identity with the corresponding iterons of SYNV and BCaRV. The intergenic iterons of DYVV and ZPNRV also were similar to that of SYVV but contained single nucleotide polymorphisms in one (ZPNRV) or two (DYVV) copies of the iteron. Rhabdovirus genomes typically include regions of complementarity of the untranslated Leader and Trailer, at or near the termini, potentially capable of forming a

panhandle structure (Wetzel et al., 1994). For the SYVV 2018 HWY65 sequence, four nucleotides of each end are complementary (Figure 4.2D). A caveat to this analysis is that complementary terminal sequences of SYVV genomic RNA could potentially include additional U(n) and A(n) residues at the 5' and 3' ends, respectively, that could not be distinguished from the poly-A tails added during sample preparation for Next Generation Sequencing.

A phylogenetic analysis was conducted using an alignment of L protein sequences downloaded from NCBI. A Maximum Likelihood tree (1000 bootstrap iterations) was generated (Figure 4.3) using the relevant suite of programs available via the Phylogeny.fr website (http://www.phylogeny.fr/) for sequence alignment (MUSCLE), curation (Gblocks), phylogeny (PhyML), and tree rendering (TreeDyn), respectively (Dereeper et al., 2008). SYVV shared an exclusive node (representing a most recent common ancestor) with several member (SYNV and DYVV) and tentative (ZPNRV, BCaRV, and alfalfa-associated nucleorhabdovirus) species of the genus Nucleorhabdovirus. However, the genus Nucleorhabdovirus is paraphyletic, with the clade containing all member and tentative species of the genus also including bipartite rhabdoviruses (coffee ringspot virus, orchid fleck virus and citrus leprosis nuclear virus). As these three bipartite rhabdoviruses are placed in the recently established genus Dichorhavirus (Dietzgen et al., 2014, 2018), Nucleorhabdovirus constitutes a paraphyletic lineage that does not have a basal node exclusive of other taxa (Fig. 4.3). To address this issue, the ICTV has proposed that the genus Nucleorhabdovirus be abolished with species reassigned to three new proposed genera: Alphanucleorhabdovirus, Betanucleorhabdovirus and Gammanucleorhabdovirus. After this revised taxonomy is adopted, SYVV will be assigned to the genus Betanucleorhabdovirus and given the formal species name Sowthistle yellow vein betanucleorhabdovirus (Figure 4.3). Retention of SYVV as a species is warranted based upon the

proposed revision to the family Rhabdoviridae (ICTV nucleorhabdovirus splitgen proposal online 2019.031 M) in which the threshold for species demarcation within the genus Betanucleorhabdovirus is less than 75 % nucleotide sequence identity of complete genomes.

Rediscovery and genomic characterization of SYVV described here fills a knowledge gap with respect to an historically important plant rhabdovirus. This work also demonstrates that cDNA clones constructed decades ago remain viable if stored properly and may be useful if provenance and chain of custody are documented. As the cohort of scientists who served as the vanguard of the modern molecular era reach the ends of their careers, no doubt numerous collections of viruses and derived clones will be lost. We suggest, to the scientific community at large, that the new and old generations communicate and do a bit of ‘freezer mining’ to revive and analyze archived materials before it is too late.

Table 4.1: Percent amino acid identity of sowthistle yellow vein virus encoded proteins (N, P, MP, M, G, and L) relative to most closely related nucleorhabdoviruses.

Virus	GenBank Accession	N	P	MP	M	G	L
sonchus yellow net virus	L32603.1	50.8	25.7	23.1	26.2	39.6	42.9
datura yellow vein virus	KM823531.1	56.0	32.5	35.9	31.7	47.6	49.1
black currant-associated rhabdovirus	MF543022.1	47.1	27.2	30.0	30.7	41.0	49.1
zhuye pepper nucleorhabdovirus	MH323437.1	58.7	30.4	38.3	41.9	50.2	52.1

Supplementary Table 4.1: Predicted isoelectric points and molecular weights of each SYVV protein.

Protein	pI	MW (kD)
N	7.12	52.5
P	5.33	43.5
MP	8.54	36.4
M	6.91	31.6
G	6.22	70.7
L	7.81	241.8

Supplementary Table 4.2: WoLF PSORT prediction of subcellular localization of each SYVV protein.

Subcellular Localization	Protein					
	N	P	MP	M	G	L
	Chloroplast (4)	Cytosol (7)	Cytosol (6)	Nucleus (7)	Plastid (6.5)	Nucleus (8)
	Nucleus (4)	Chloroplast (3)	Nucleus (4)	Cytosol (5)	Golgi_Plastid (5)	Cytosol (2)
	Cytosol (4)	Nucleus (3)	Peroxisome (2)	Chloroplast (1)	Golgi (2.5)	Chloroplast (1)
	Plastid (1)		Mitochondria (1)		Extracellular (2)	Plastid (1)
					Vacuole (2)	ER (1)

K-nearest neighbor (kNN) used is 14

Figure 4.1. Sowthistle (*Sonchus oleraceus* L.) plant, growing as a weed in an organic citrus orchard located in Kern County, CA (photographed Nov. 1, 2018), displaying yellow vein symptoms typical of sowthistle yellow vein virus infection.

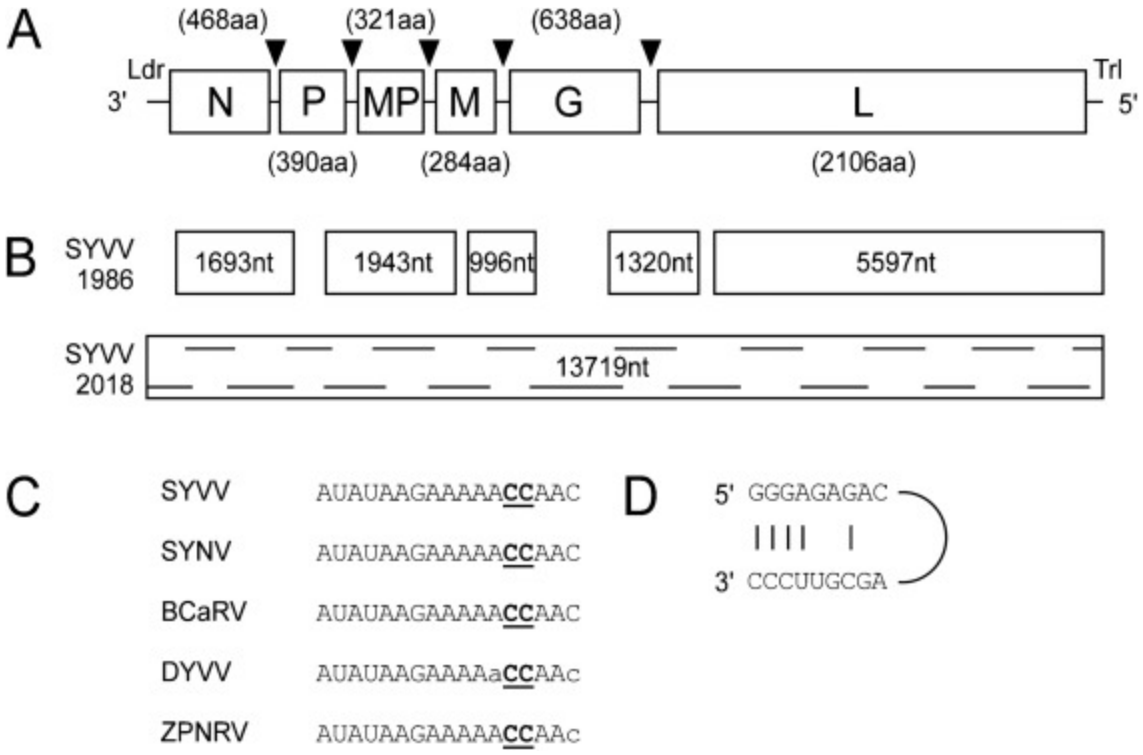

Figure 4.2. The sowthistle yellow vein virus (SYVV) genome. Presented is (A) the genetic map of SYVV showing position of open reading frames encoding proteins (M, P, MP, M, G, and L; in positive sense) with peptide amino acid (aa) lengths denoted parenthetically above or below, position of intergenic iterons denoted by black triangles, and position of untranslated Leader (Ldr) and Trailer (Tlr) regions indicated at the termini; (B) genomic position of sequence contigs (rectangles) derived from the 1986 cDNA library of the historic Berkeley lab isolate and the 2018 HWY65 field sample of SYVV, with lines denoting position of amplicons sequenced for the 2018 HWY65 contig; (C) nucleotide sequence (in positive-sense) of intergenic iterons of SYVV and closest relatives sonchus yellow net virus (SYNV), black currant-associated rhabdovirus (BCaRV), datura yellow vein virus (DYVV), and zhuye pepper nucleorhabdovirus (ZPNRV), with bold/underline denoting the untranscribed dinucleotide spacer and lower case denoting single nucleotide polymorphic sites present in one (ZPNRV) or two (DYVV) iteron

copies; and (D) base pairing of the panhandle structure of SYVV genomic RNA characteristic of rhabdovirus terminal sequences (presented in negative-sense).

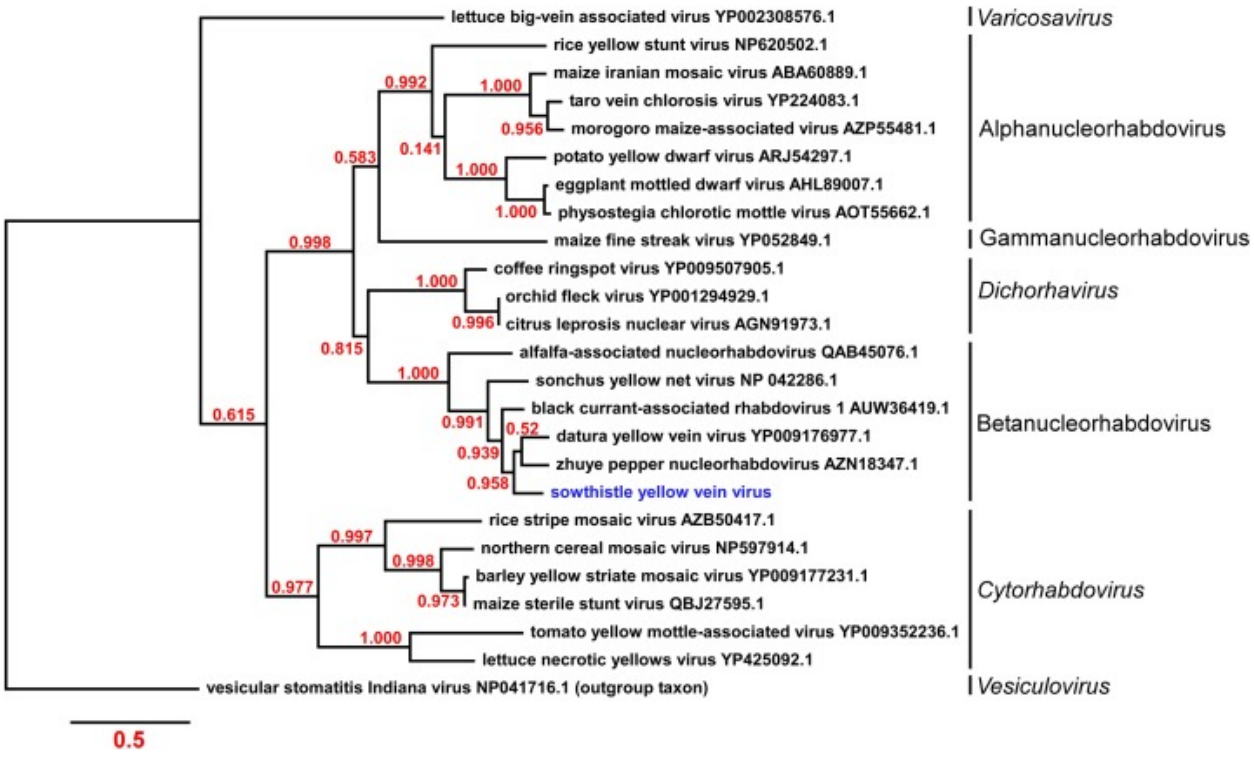

Figure 4.3. Phylogenetic placement of sowthistle yellow vein virus (SYVV) inferred from Maximum Likelihood analysis of RNA-dependent RNA polymerase (L) protein sequences. Taxa compared include representative of plant rhabdoviruses; protein accession numbers corresponding to entries in the NCBI non-redundant protein database are indicated for each taxon following virus name. The SYVV L protein sequence was derived from the complete genome sequence of the 2018 HWY65 sample (GenBank accession MT185675). The vertebrate-infecting rhabdovirus vesicular stomatitis Indiana virus was used as the outgroup taxon to root the tree. Bootstrap values (based on 1000 iterations) are shown to the left of each node; scalebar at bottom left denotes a genetic distance (an estimation of substitution rate per site) of 0.5. Nomenclature for genera are labelled at right and correspond to revised taxonomy of the family *Rhabdoviridae* under consideration by International Committee on the Taxonomy of Viruses. Note that taxa currently in the genus *Nucleorhabdovirus* are expected to be reassigned to three

new genera: Alphanucleorhabdovirus, Betanucleorhabdovirus, and Gammanucleorhabdovirus. In this revised taxonomy, SYVV is classified in the genus *Betanucleorhabdovirus.*

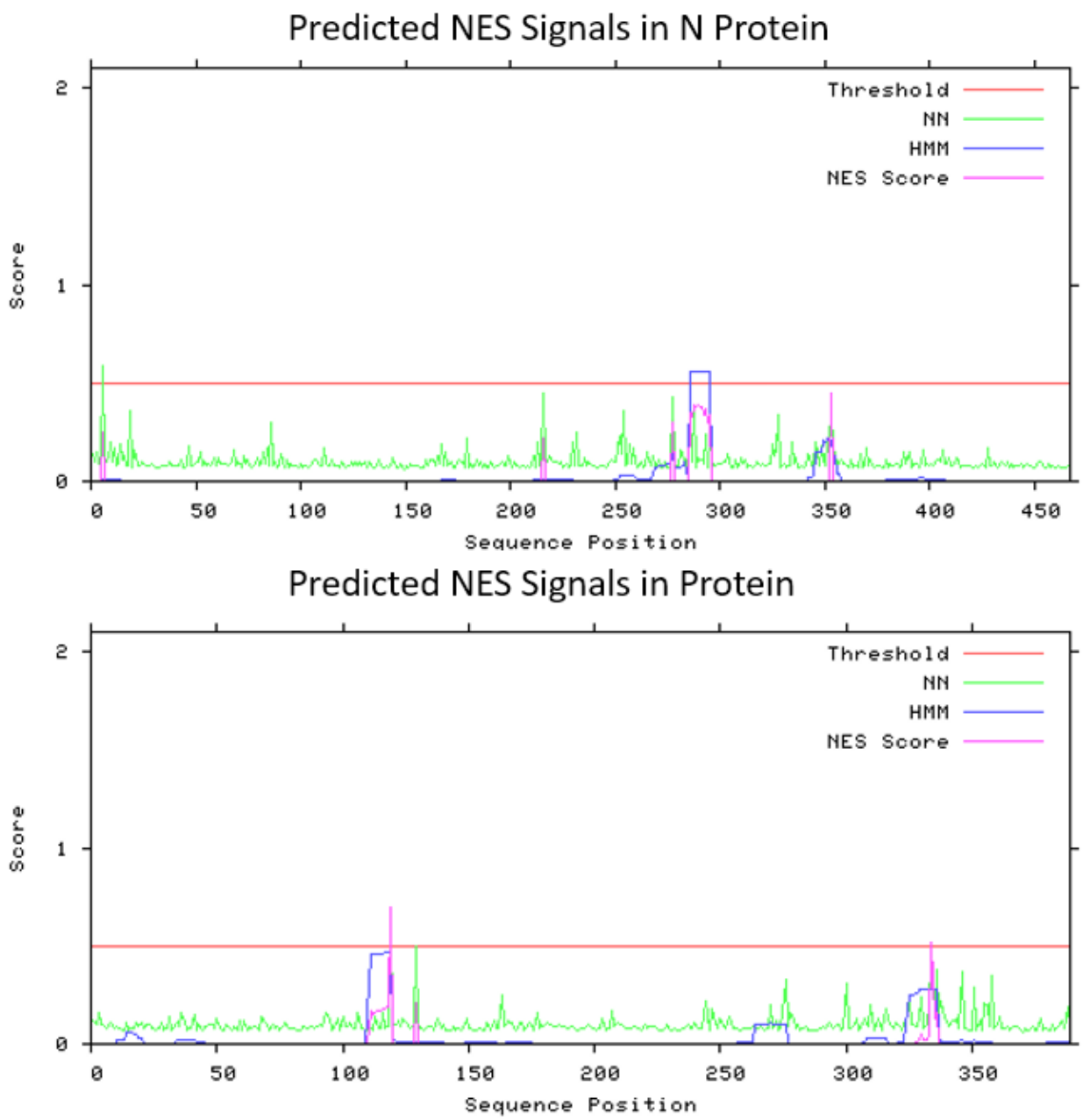
Predicted NES Signals in N Protein
Threshold
NN
HMM
NES Score
Score
Sequence Position
0
1
2
0
50
100
150
200
250
300
350
400
450
Predicted NES Signals in Protein
Threshold
NN
HMM
NES Score
Score
Sequence Position
0
1
2
0
50
100
150
200
250
300
350

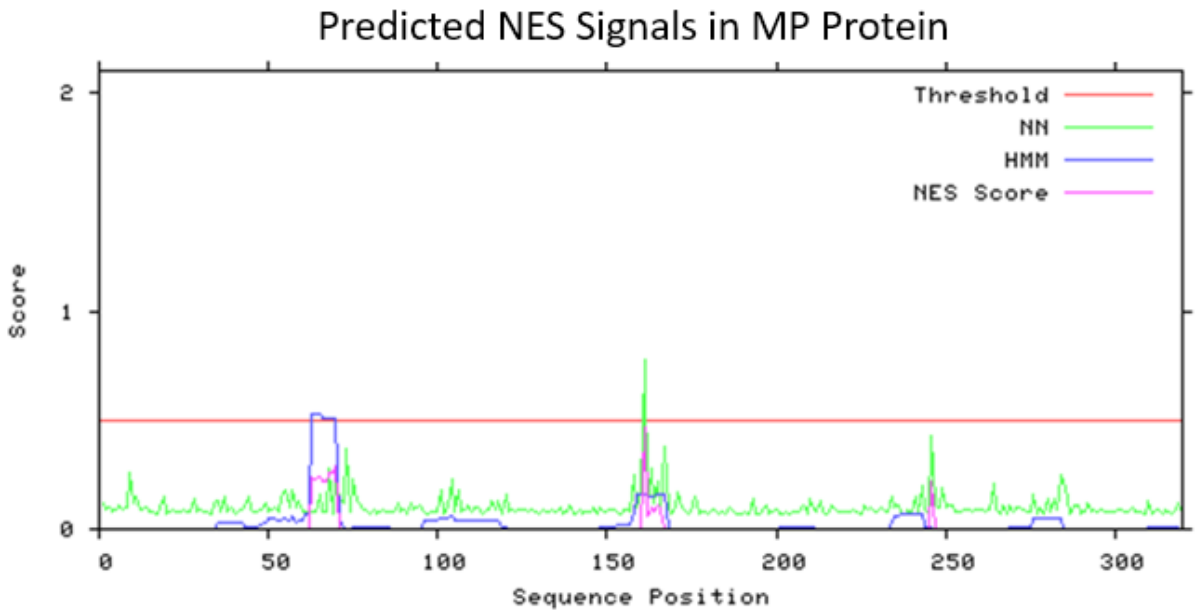
Predicted NES Signals in MP Protein
Threshold
NN
HMM
NES Score
Score
Sequence Position
0
1
2
0
50
100
150
200
250
300

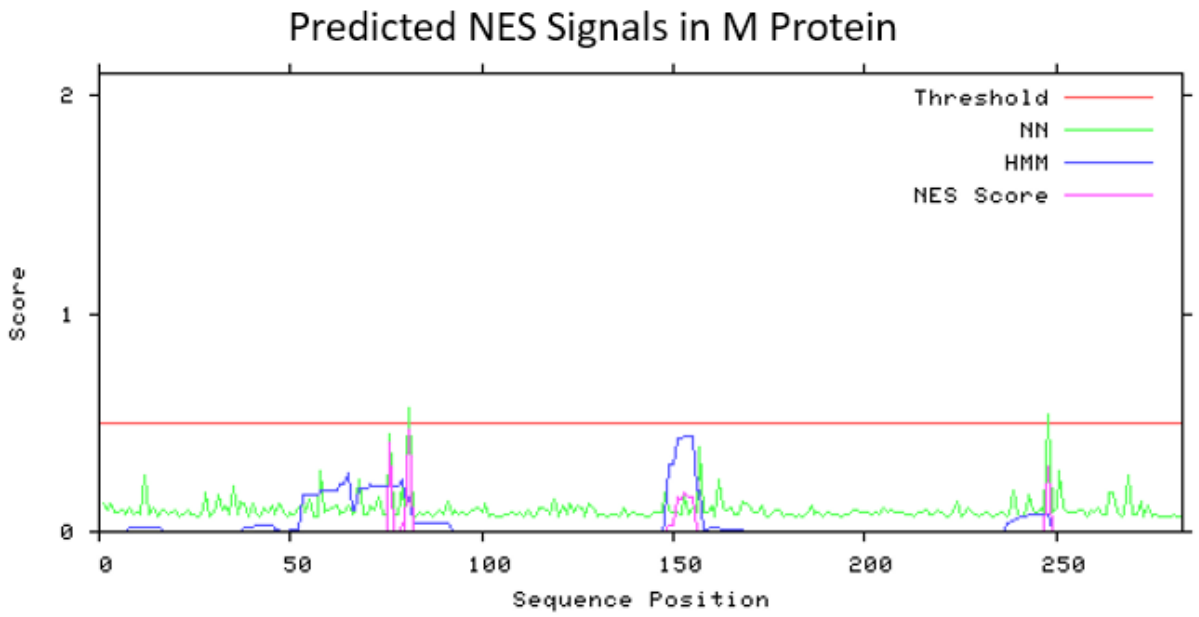
Predicted NES Signals in M Protein
Threshold
NN
HMM
NES Score
Score
Sequence Position
0
1
2
0
50
100
150
200
250

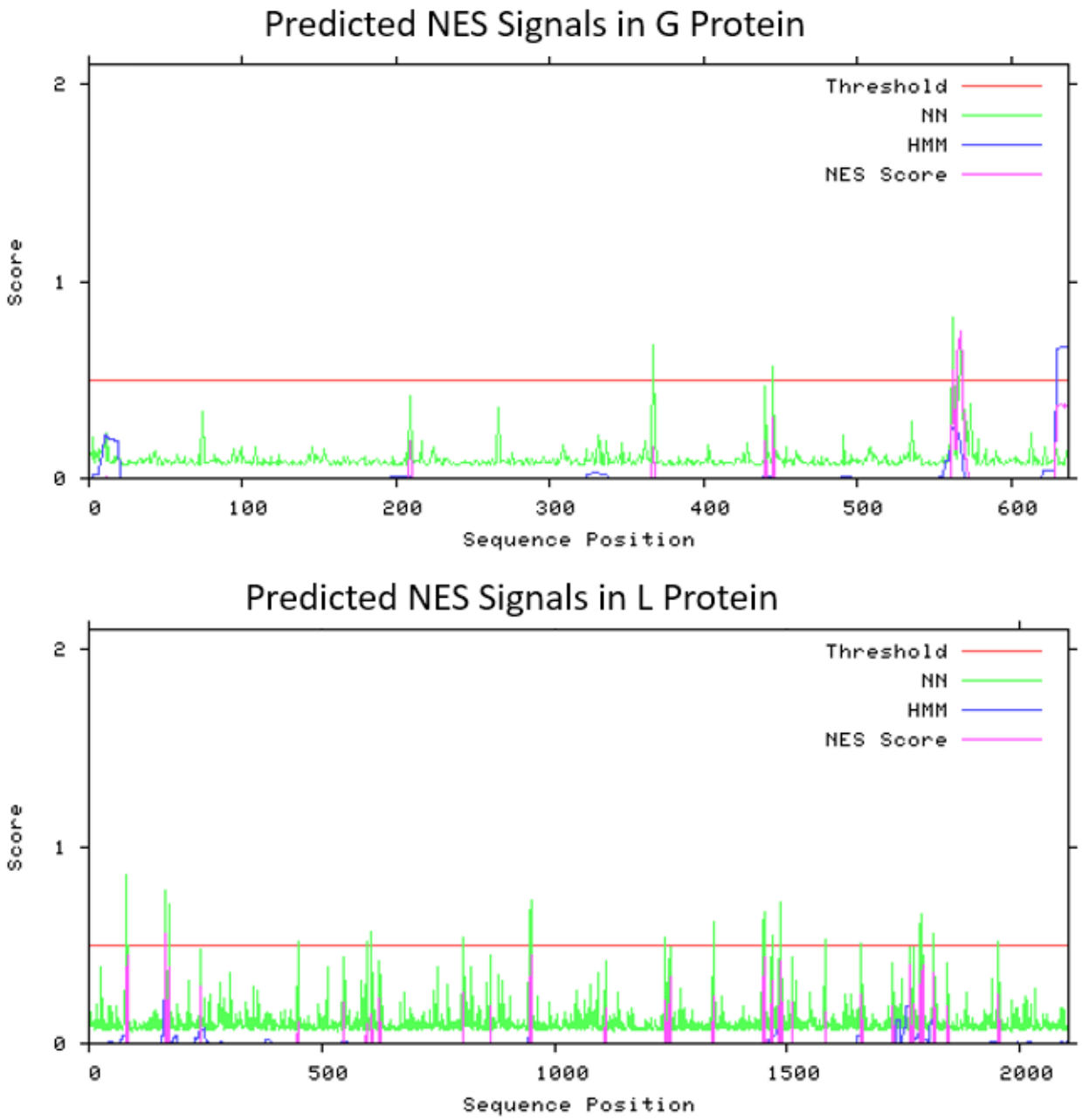

Supplementary Figure 4.1: Algorithmic analysis of predicted nuclear export signals (NES) in each SYVV protein.

COILS Output for P Protein

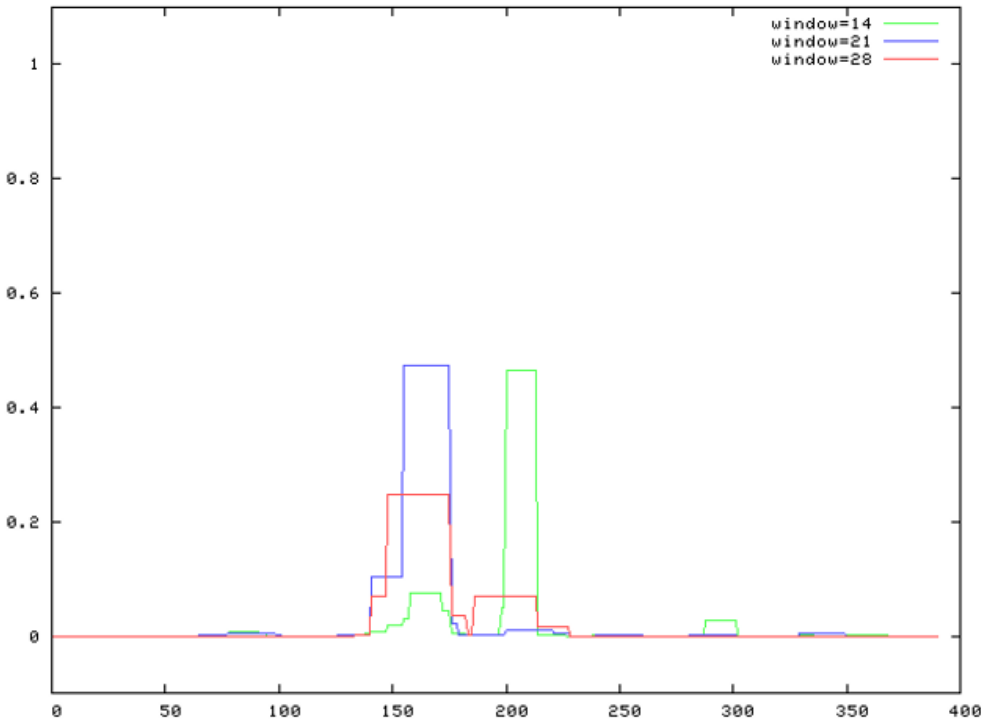

COILS Output for G Protein

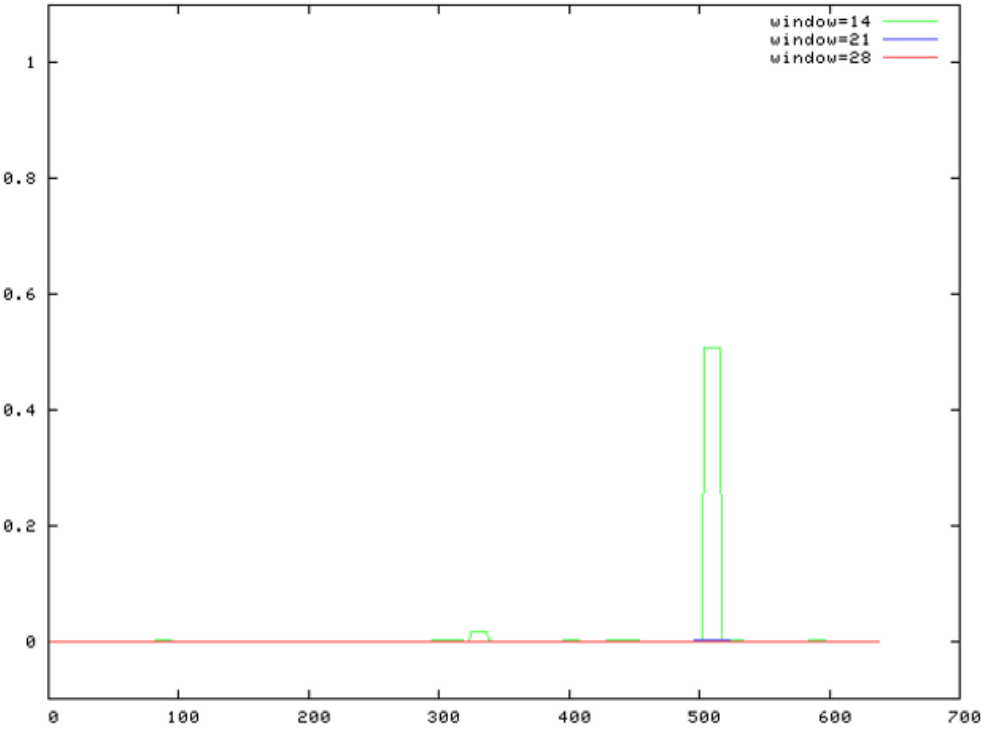

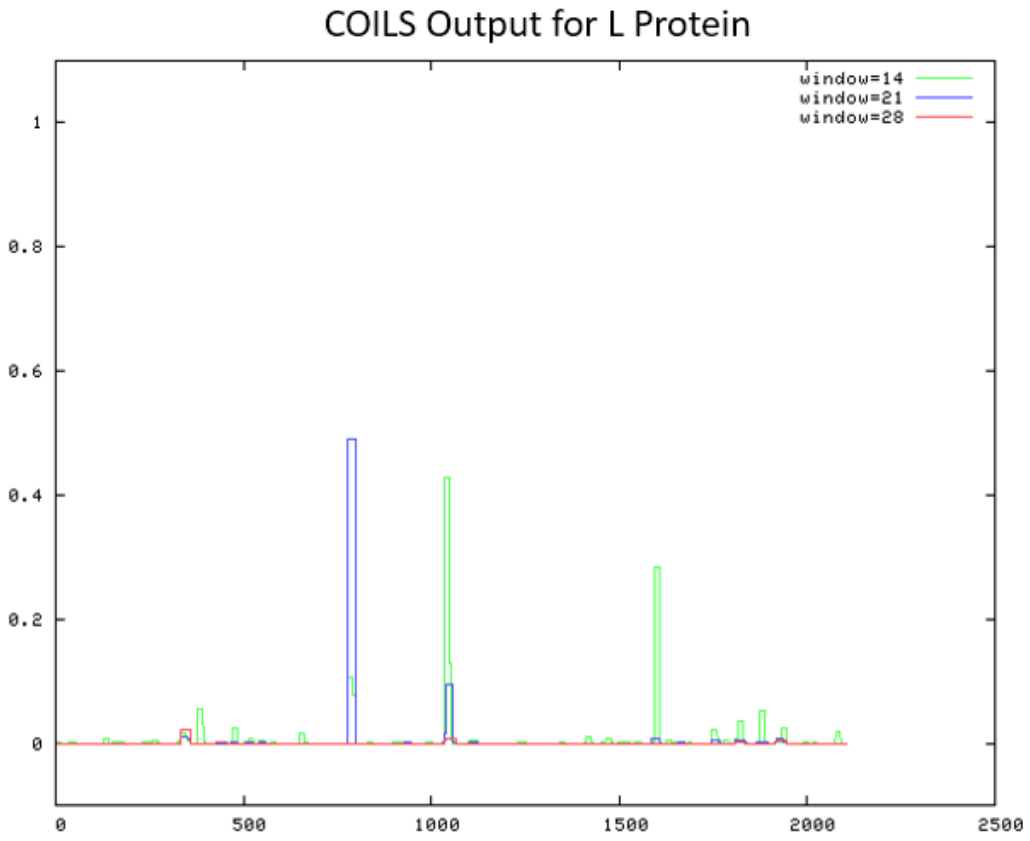

Supplementary Figure 4.2: Algorithmic analysis of predicted coiled-coil domains in the P, G, and L proteins of SYVV.

REFERENCES

1. Abraham, G., and Banerjee, A.K. (1976). Sequential transcription of the genes of vesicular stomatitis virus. Proceedings of the National Academy of Sciences *73*, 1504.
2. Ahmed, M., and Lyles, D.S. (1998). Effect of vesicular stomatitis virus matrix protein on transcription directed by host RNA polymerases I, II, and III. J Virol *72*, 8413-8419.
3. Ala-Poikela, M., Rajamäki, M.-L., and Valkonen, J.P.T. (2019). A Novel Interaction Network Used by Potyviruses in Virus–Host Interactions at the Protein Level. Viruses *11*, 1158.
4. Alaskhar Alhamwe, B., Khalaila, R., Wolf, J., von Bülow, V., Harb, H., Alhamdan, F., Hii, C.S., Prescott, S.L., Ferrante, A., Renz, H.*, et al.* (2018). Histone modifications and their role in epigenetics of atopy and allergic diseases. Allergy Asthma Clin Immunol *14*, 39.
5. Alber, F., Dokudovskaya, S., Veenhoff, L.M., Zhang, W., Kipper, J., Devos, D., Suprapto, A., Karni-Schmidt, O., Williams, R., Chait, B.T.*, et al.* (2007). The molecular architecture of the nuclear pore complex. Nature *450*, 695-701.
6. Allan, W.L., Clark, S.M., Hoover, G.J., and Shelp, B.J. (2009). Role of plant glyoxylate reductases during stress: a hypothesis. Biochem J *423*, 15-22.
7. Artlip, T., McDermaid, A., Ma, Q., and Wisniewski, M. (2019). Differential gene expression in non-transgenic and transgenic "M.26" apple overexpressing a peach CBF gene during the transition from eco-dormancy to bud break. Horticulture Research *6*, 86.
8. Aydin, I., and Schelhaas, M. (2016). Viral Genome Tethering to Host Cell Chromatin: Cause and Consequences. Traffic *17*, 327-340.
9. Babu, J.R., Jeganathan, K.B., Baker, D.J., Wu, X., Kang-Decker, N., and van Deursen, J.M. (2003). Rae1 is an essential mitotic checkpoint regulator that cooperates with Bub3 to prevent chromosome missegregation. J Cell Biol *160*, 341-353.
10. Balinsky, C.A., Schmeisser, H., Ganesan, S., Singh, K., Pierson, T.C., and Zoon, K.C. (2013). Nucleolin interacts with the dengue virus capsid protein and plays a role in formation of infectious virus particles. J Virol *87*, 13094-13106.
11. Bally, J., Jung, H., Mortimer, C., Naim, F., Philips, J.G., Hellens, R., Bombarely, A., Goodin, M.M., and Waterhouse, P.M. (2018). The Rise and Rise of Nicotiana benthamiana: A Plant for All Reasons. Annual Review of Phytopathology *56*, 405-426.
12. Bandyopadhyay, A., Kopperud, K., Anderson, G., Martin, K., and Goodin, M. (2010). An integrated protein localization and interaction map for Potato yellow dwarf virus, type species of the genus Nucleorhabdovirus. Virology *402*, 61-71.
13. Bardina, M.V., Lidsky, P.V., Sheval, E.V., Fominykh, K.V., van Kuppeveld, F.J., Polyakov, V.Y., and Agol, V.I. (2009). Mengovirus-induced rearrangement of the nuclear pore complex: hijacking cellular phosphorylation machinery. J Virol *83*, 3150-3161.
14. Barik, S., and Banerjee, A.K. (1992). Phosphorylation by cellular casein kinase II is essential for transcriptional activity of vesicular stomatitis virus phosphoprotein P. Proc

Natl Acad Sci U S A *89*, 6570-6574.

15. Barr, J.N., Whelan, S.P., and Wertz, G.W. (1997). cis-Acting signals involved in termination of vesicular stomatitis virus mRNA synthesis include the conserved AUAC and the U7 signal for polyadenylation. Journal of Virology *71*, 8718.
16. Barr, J.N., Whelan, S.P.J., and Wertz, G.W. (2002). Transcriptional control of the RNA-dependent RNA polymerase of vesicular stomatitis virus. Biochimica et Biophysica Acta (BBA) - Gene Structure and Expression *1577*, 337-353.
17. Beck, M., and Hurt, E. (2017). The nuclear pore complex: understanding its function through structural insight. Nature Reviews Molecular Cell Biology *18*, 73-89.
18. Ben-Efraim, I., and Gerace, L. (2001). Gradient of increasing affinity of importin beta for nucleoporins along the pathway of nuclear import. J Cell Biol *152*, 411-417.
19. Benfeitas, R., Uhlen, M., Nielsen, J., and Mardinoglu, A. (2017). New Challenges to Study Heterogeneity in Cancer Redox Metabolism. Front Cell Dev Biol *5*, 65.
20. Bierne, H., Hamon, M., and Cossart, P. (2012). Epigenetics and bacterial infections. Cold Spring Harb Perspect Med *2*, a010272.
21. Birnbaum, K., Shasha, D.E., Wang, J.Y., Jung, J.W., Lambert, G.M., Galbraith, D.W., and Benfey, P.N. (2003). A Gene Expression Map of the Arabidopsis Root. Science *302*, 1956-1960.
22. Blondel, D., Maarifi, G., Nisole, S., and Chelbi-Alix, M.K. (2015). Resistance to Rhabdoviridae Infection and Subversion of Antiviral Responses. Viruses *7*, 3675-3702.
23. Bobik, K., and Burch-Smith, T.M. (2015). Chloroplast signaling within, between and beyond cells. Frontiers in plant science *6*, 781-781.
24. Boeglin, M., Fuglsang, A.T., Luu, D.T., Sentenac, H., Gaillard, I., and Chérel, I. (2016). Reduced expression of AtNUP62 nucleoporin gene affects auxin response in Arabidopsis. BMC Plant Biol *16*, 2.
25. Boruc, J., Zhou, X., and Meier, I. (2012). Dynamics of the Plant Nuclear Envelope and Nuclear Pore. Plant Physiology *158*, 78.
26. Bouazizi, E., Gharbi, Y., and Triki, M.A. (2020). Differential gene expression patterns in two pear cultivars with differential susceptibility to the necrotrophic pathogen Erwinia amylovora. Acta Physiologiae Plantarum *42*, 92.
27. Bradish, C.J., Brooksby, J.B., and Dillon, J.F. (1956). Biophysical Studies of the Virus System of Vesicular Stomatitis. Microbiology *14*, 290-314.
28. Braun, P., Aubourg, S., Van Leene, J., De Jaeger, G., and Lurin, C. (2013). Plant protein interactomes. Annu Rev Plant Biol *64*, 161-187.
29. Brikis, C.J., Zarei, A., Trobacher, C.P., DeEll, J.R., Akama, K., Mullen, R.T., Bozzo, G.G., and Shelp, B.J. (2017). Ancient Plant Glyoxylate/Succinic Semialdehyde Reductases: GLYR1s Are Cytosolic, Whereas GLYR2s Are Localized to Both Mitochondria and Plastids. Frontiers in plant science *8*, 601-601.
30. Brito, A.F., and Pinney, J.W. (2017). Protein–Protein Interactions in Virus–Host Systems. Frontiers in Microbiology *8*.

31. Brohawn, S.G., Partridge, J.R., Whittle, J.R.R., and Schwartz, T.U. (2009). The Nuclear Pore Complex Has Entered the Atomic Age. Structure *17*, 1156-1168.

32. Burnham, A.J., Gong, L., and Hardy, R.W. (2007). Heterogeneous nuclear ribonuclear protein K interacts with Sindbis virus nonstructural proteins and viral subgenomic mRNA. Virology *367*, 212-221.

33. Burrell, C., Howard, C., and Murphy, F. (2017). Rhabdoviruses. In, pp. 383-394.

34. Caicedo, J.C., Cooper, S., Heigwer, F., Warchal, S., Qiu, P., Molnar, C., Vasilevich, A.S., Barry, J.D., Bansal, H.S., Kraus, O.*, et al.* (2017). Data-analysis strategies for image-based cell profiling. Nature Methods *14*, 849-863.

35. Calil, I.P., and Fontes, E.P.B. (2016). Plant immunity against viruses: antiviral immune receptors in focus. Ann Bot *119*, 711-723.

36. Canton, J., Fehr, A.R., Fernandez-Delgado, R., Gutierrez-Alvarez, F.J., Sanchez-Aparicio, M.T., García-Sastre, A., Perlman, S., Enjuanes, L., and Sola, I. (2018). MERS-CoV 4b protein interferes with the NF-κB-dependent innate immune response during infection. PLOS Pathogens *14*, e1006838.

37. Carrington, J.C., Kasschau, K.D., Mahajan, S.K., and Schaad, M.C. (1996). Cell-to-Cell and Long-Distance Transport of Viruses in Plants. Plant Cell *8*, 1669.

38. Castelló, A., Alvarez, E., and Carrasco, L. (2011). The multifaceted poliovirus 2A protease: regulation of gene expression by picornavirus proteases. J Biomed Biotechnol *2011*, 369648-369648.

39. Chakrabarty, R., Banerjee, R., Chung, S.-M., Farman, M., Citovsky, V., Hogenhout, S.A., Tzfira, T., and Goodin, M. (2007). pSITE Vectors for Stable Integration or Transient Expression of Autofluorescent Protein Fusions in Plants: Probing Nicotiana benthamiana-Virus Interactions. Molecular Plant-Microbe Interactions® *20*, 740-750.

40. Chan, K.X., Crisp, P.A., Estavillo, G.M., and Pogson, B.J. (2010). Chloroplast-to-nucleus communication: current knowledge, experimental strategies and relationship to drought stress signaling. Plant signaling & behavior *5*, 1575-1582.

41. Chaudhury, A., Chander, P., and Howe, P.H. (2010). Heterogeneous nuclear ribonucleoproteins (hnRNPs) in cellular processes: Focus on hnRNP E1's multifunctional regulatory roles. Rna *16*, 1449-1462.

42. Chiba, S., Hleibieh, K., Delbianco, A., Klein, E., Ratti, C., Ziegler-Graff, V., Bouzoubaa, S., and Gilmer, D. (2013). The Benyvirus RNA Silencing Suppressor Is Essential for Long-Distance Movement, Requires Both Zinc-Finger and NoLS Basic Residues but Not a Nucleolar Localization for Its Silencing-Suppression Activity. Molecular Plant-Microbe Interactions® *26*, 168-181.

43. Choi, H., Jo, Y., Yoon, J.Y., Choi, S.K., and Cho, W.K. (2015). Complete Genome Sequences of Chrysanthemum Stunt Viroid from a Single Chrysanthemum Cultivar. Genome Announc *3*.

44. Chow, T.L., Chow, F.H., and Hanson, R.P. (1954). Morphology of vesicular stomatitis virus. J Bacteriol *68*, 724-726.

45. Christie, S., Christie, R., and Edwardson, J. (1974). Transmission of a bacilliform virus of sowthistle and Bidens pilosa. Phytopathology *64*, 840-845.

46. Cohen, M., Tzur, Y.B., Neufeld, E., Feinstein, N., Delannoy, M.R., Wilson, K.L., and Gruenbaum, Y. (2002). Transmission electron microscope studies of the nuclear envelope in Caenorhabditis elegans embryos. Journal of Structural Biology *140*, 232-240.

47. Cohen, S., Au, S., and Panté, N. (2011). How viruses access the nucleus. Biochimica et Biophysica Acta (BBA) - Molecular Cell Research *1813*, 1634-1645.

48. Colariccio, A., Chaves, A.L.R., Eiras, M., Chagas, C.M., and Roggero, P. (2005). Detection of Varicosavirus and Ophiovirus in lettuce associated with lettuce big-vein symptoms in Brazil. Fitopatologia Brasileira *30*, 416-419.

49. Consortium, A.I.M. (2011). Evidence for network evolution in an Arabidopsis interactome map. Science *333*, 601-607.

50. Consortium, T.G. (2020). The GTEx Consortium atlas of genetic regulatory effects across human tissues. Science *369*, 1318.

51. Conti, E., and Izaurralde, E. (2001). Nucleocytoplasmic transport enters the atomic age. Current Opinion in Cell Biology *13*, 310-319.

52. Cook, H.V., and Jensen, L.J. (2018). An Integrative Approach to Virus–Host Protein–Protein Interactions. In Computational Cell Biology: Methods and Protocols, L. von Stechow, and A. Santos Delgado, eds. (New York, NY: Springer New York), pp. 175-196.

53. Costa-Mattioli, M., Svitkin, Y., and Sonenberg, N. (2004). La autoantigen is necessary for optimal function of the poliovirus and hepatitis C virus internal ribosome entry site in vivo and in vitro. Molecular and cellular biology *24*, 6861-6870.

54. Cros, J.F., García-Sastre, A., and Palese, P. (2005). An unconventional NLS is critical for the nuclear import of the influenza A virus nucleoprotein and ribonucleoprotein. Traffic *6*, 205-213.

55. Dang, C.V., and Lee, W.M. (1989). Nuclear and nucleolar targeting sequences of c-erb-A, c-myb, N-myc, p53, HSP70, and HIV tat proteins. J Biol Chem 264, 18019-18023.

56. D'Angelo, M.A., Anderson, D.J., Richard, E., and Hetzer, M.W. (2006). Nuclear pores form de novo from both sides of the nuclear envelope. Science *312*, 440-443.

57. Dechtawewat, T., Songprakhon, P., Limjindaporn, T., Puttikhunt, C., Kasinrerk, W., Saitornuang, S., Yenchitsomanus, P.T., and Noisakran, S. (2015). Role of human heterogeneous nuclear ribonucleoprotein C1/C2 in dengue virus replication. Virol J *12*, 14.

58. Deng, L., Zeng, Q., Wang, M., Cheng, A., Jia, R., Chen, S., Zhu, D., Liu, M., Yang, Q., Wu, Y.*, et al.* (2018). Suppression of NF-κB Activity: A Viral Immune Evasion Mechanism. Viruses *10*, 409.

59. Dereeper, A., Guignon, V., Blanc, G., Audic, S., Buffet, S., Chevenet, F., Dufayard, J.-F., Guindon, S., Lefort, V., and Lescot, M. (2008). Phylogeny. fr: robust phylogenetic analysis for the non-specialist. Nucleic Acids Res *36*, W465-W469.

60. Desveaux, D., Subramaniam, R., Després, C., Mess, J.-N., Lévesque, C., Fobert, P.R., Dangl, J.L., and Brisson, N. (2004). A "Whirly" Transcription Factor Is Required for Salicylic Acid-Dependent Disease Resistance in Arabidopsis. Developmental Cell *6*, 229-240.

61. Dharan, A., Talley, S., Tripathi, A., Mamede, J.I., Majetschak, M., Hope, T.J., and Campbell, E.M. (2016). KIF5B and Nup358 Cooperatively Mediate the Nuclear Import of HIV-1 during Infection. PLOS Pathogens *12*, e1005700.

62. Dhillon, P., Tandra, V.N., Chorghade, S.G., Namsa, N.D., Sahoo, L., and Rao, C.D. (2018). Cytoplasmic Relocalization and Colocalization with Viroplasms of Host Cell Proteins, and Their Role in Rotavirus Infection. Journal of virology *92*, e00612-00618.

63. Di Nunzio, F., Fricke, T., Miccio, A., Valle-Casuso, J.C., Perez, P., Souque, P., Rizzi, E., Severgnini, M., Mavilio, F., Charneau, P.*, et al.* (2013). Nup153 and Nup98 bind the HIV-1 core and contribute to the early steps of HIV-1 replication. Virology *440*, 8-18.

64. Dietzgen, R., Calisher, C., Kurath, G., Kuzman, I., Rodriguez, L., Stone, D., Tesh, R., Tordo, N., Walker, P., and Wetzel, T. (2011). Family rhabdoviridae.

65. Dietzgen, R.G., Freitas-Astúa, J., Chabi-Jesus, C., Ramos-González, P.L., Goodin, M.M., Kondo, H., Tassi, A.D., and Kitajima, E.W. (2018). Dichorhaviruses in their host plants and mite vectors. In Advances in Virus Research (Elsevier), pp. 119-148.

66. Dietzgen, R.G., Kondo, H., Goodin, M.M., Kurath, G., and Vasilakis, N. (2017). The family Rhabdoviridae: mono- and bipartite negative-sense RNA viruses with diverse genome organization and common evolutionary origins. Virus Res *227*, 158-170.

67. Dietzgen, R.G., Kuhn, J.H., Clawson, A.N., Freitas-Astúa, J., Goodin, M.M., Kitajima, E.W., Kondo, H., Wetzel, T., and Whitfield, A.E. (2014). Dichorhavirus: a proposed new genus for Brevipalpus mite-transmitted, nuclear, bacilliform, bipartite, negative-strand RNA plant viruses. Archives of virology *159*, 607-619.

68. Dingwall, C., Robbins, J., Dilworth, S.M., Roberts, B., and Richardson, W.D. (1988). The nucleoplasmin nuclear location sequence is larger and more complex than that of SV-40 large T antigen. J Cell Biol *107*, 841-849.

69. Diwaker, D., Mishra, K.P., Ganju, L., and Singh, S.B. (2016). Dengue virus non-structural 1 protein interacts with heterogeneous nuclear ribonucleoprotein H in human monocytic cells. Asian Pacific Journal of Tropical Medicine *9*, 112-118.

70. Dreyfuss, G., Matunis, M.J., Piñol-Roma, S., and Burd, C.G. (1993). hnRNP proteins and the biogenesis of mRNA. Annu Rev Biochem *62*, 289-321.

71. Duffus, J.E. (1963). Possible multiplication in the aphid vector of sowthistle yellow vein virus, a virus with an extremely long insect latent period. Virology *21*, 194-202.

72. Egger, D., Wölk, B., Gosert, R., Bianchi, L., Blum, H.E., Moradpour, D., and Bienz, K. (2002). Expression of Hepatitis C Virus Proteins Induces Distinct Membrane Alterations Including a Candidate Viral Replication Complex. Journal of Virology *76*, 5974.

73. Enninga, J., Levy, D.E., Blobel, G., and Fontoura, B.M. (2002). Role of nucleoporin induction in releasing an mRNA nuclear export block. Science *295*, 1523-1525.

74. Faria, P.A., Chakraborty, P., Levay, A., Barber, G.N., Ezelle, H.J., Enninga, J., Arana, C., van Deursen, J., and Fontoura, B.M. (2005). VSV disrupts the Rae1/mrnp41 mRNA nuclear export pathway. Mol Cell *17*, 93-102.

75. Fay, N., and Panté, N. (2015). Nuclear entry of DNA viruses. Frontiers in Microbiology *6*.

76. Feng, Z., Chen, X., Wu, X., and Zhang, M. (2019). Formation of biological condensates via phase separation: Characteristics, analytical methods, and physiological implications. The Journal of biological chemistry 294, 14823-14835.

77. Fichtman, B., Ramos, C., Rasala, B., Harel, A., and Forbes, D.J. (2010). Inner/Outer nuclear membrane fusion in nuclear pore assembly: biochemical demonstration and molecular analysis. Mol Biol Cell *21*, 4197-4211.

78. Fischer, N. (2020). Infection-induced epigenetic changes and their impact on the pathogenesis of diseases. Semin Immunopathol *42*, 127-130.

79. Fiserova, J., Kiseleva, E., and Goldberg, M.W. (2009). Nuclear envelope and nuclear pore complex structure and organization in tobacco BY-2 cells. The Plant Journal *59*, 243-255.

80. Flatt, J.W., and Greber, U.F. (2015). Misdelivery at the Nuclear Pore Complex-Stopping a Virus Dead in Its Tracks. Cells *4*, 277-296.

81. Freitas, N., and Cunha, C. (2009). Mechanisms and signals for the nuclear import of proteins. Curr Genomics *10*, 550-557.

82. Frieman, M., Yount, B., Heise, M., Kopecky-Bromberg, S.A., Palese, P., and Baric, R.S. (2007). Severe acute respiratory syndrome coronavirus ORF6 antagonizes STAT1 function by sequestering nuclear import factors on the rough endoplasmic reticulum/Golgi membrane. Journal of virology *81*, 9812-9824.

83. Gabriel, G., Klingel, K., Otte, A., Thiele, S., Hudjetz, B., Arman-Kalcek, G., Sauter, M., Shmidt, T., Rother, F., Baumgarte, S.*, et al.* (2011). Differential use of importin-α isoforms governs cell tropism and host adaptation of influenza virus. Nature communications *2*, 156-156.

84. Ganesan, U., Bragg, J.N., Deng, M., Marr, S., Lee, M.Y., Qian, S., Shi, M., Kappel, J., Peters, C., Lee, Y.*, et al.* (2013). Construction of a Sonchus Yellow Net Virus minireplicon: a step toward reverse genetic analysis of plant negative-strand RNA viruses. J Virol *87*, 10598-10611.

85. Gao, S., Song, L., Li, J., Zhang, Z., Peng, H., Jiang, W., Wang, Q., Kang, T., Chen, S., and Huang, W. (2012). Influenza A virus-encoded NS1 virulence factor protein inhibits innate immune response by targeting IKK. Cellular Microbiology *14*, 1849-1866.

86. Gerace, L., Ottaviano, Y., and Kondor-Koch, C. (1982). Identification of a major polypeptide of the nuclear pore complex. J Cell Biol *95*, 826-837.

87. Germain, M.-A., Chatel-Chaix, L., Gagné, B., Bonneil, É., Thibault, P., Pradezynski, F., de Chassey, B., Meyniel-Schicklin, L., Lotteau, V., Baril, M.*, et al.* (2014). Elucidating novel hepatitis C virus-host interactions using combined mass spectrometry and functional genomics approaches. Mol Cell Proteomics *13*, 184-203.

88. Ghildyal, R., Jordan, B., Li, D., Dagher, H., Bardin, P.G., Gern, J.E., and Jans, D.A. (2009). Rhinovirus 3C Protease Can Localize in the Nucleus and Alter Active and Passive Nucleocytoplasmic Transport. Journal of Virology *83*, 7349.

89. Goodin, M., Yelton, S., Ghosh, D., Mathews, S., and Lesnaw, J. (2005). Live-Cell Imaging of Rhabdovirus-Induced Morphological Changes in Plant Nuclear Membranes. Molecular Plant-Microbe Interactions® *18*, 703-709.

90. Goodin, M.M., Austin, J., Tobias, R., Fujita, M., Morales, C., and Jackson, A.O. (2001). Interactions and Nuclear Import of the N and P Proteins of Sonchus Yellow Net Virus, a Plant Nucleorhabdovirus. Journal of Virology *75*, 9393.

91. Goodin, M.M., Chakrabarty, R., Banerjee, R., Yelton, S., and DeBolt, S. (2007). New Gateways to Discovery. Plant Physiology *145*, 1100-1109.

92. Goodin, M.M., Dietzgen, R.G., Schichnes, D., Ruzin, S., and Jackson, A.O. (2002). pGD vectors: versatile tools for the expression of green and red fluorescent protein fusions in agroinfiltrated plant leaves. Plant J *31*, 375-383.

93. Gordon, D.E., Jang, G.M., Bouhaddou, M., Xu, J., Obernier, K., White, K.M., O'Meara, M.J., Rezelj, V.V., Guo, J.Z., Swaney, D.L.*, et al.* (2020). A SARS-CoV-2 protein interaction map reveals targets for drug repurposing. Nature *583*, 459-468.

94. Görlich, D., and Kutay, U. (1999). Transport Between the Cell Nucleus and the Cytoplasm. Annual Review of Cell and Developmental Biology *15*, 607-660.

95. Görlich, D., Prehn, S., Laskey, R.A., and Hartmann, E. (1994). Isolation of a protein that is essential for the first step of nuclear protein import. Cell *79*, 767-778.

96. Gorski, S., and Misteli, T. (2005). Systems biology in the cell nucleus. Journal of Cell Science *118*, 4083.

97. Greber, U.F., Senior, A., and Gerace, L. (1990). A major glycoprotein of the nuclear pore complex is a membrane-spanning polypeptide with a large lumenal domain and a small cytoplasmic tail. Embo j *9*, 1495-1502.

98. Guo, H., Song, X., Xie, C., Huo, Y., Zhang, F., Chen, X., Geng, Y., and Fang, R. (2013). Rice yellow stunt rhabdovirus protein 6 suppresses systemic RNA silencing by blocking RDR6-mediated secondary siRNA synthesis. Molecular plant-microbe interactions *26*, 927-936.

99. Guo, T., and Fang, Y. (2014). Functional organization and dynamics of the cell nucleus. Frontiers in plant science *5*, 378-378.

100. Gupta, A.K., Blondel, D., Choudhary, S., and Banerjee, A.K. (2000). The phosphoprotein of rabies virus is phosphorylated by a unique cellular protein kinase and specific isomers of protein kinase C. Journal of virology *74*, 91-98.

101. Gustin, K.E. (2003). Inhibition of nucleo-cytoplasmic trafficking by RNA viruses: targeting the nuclear pore complex. Virus research *95*, 35-44.

102. Gustin, K.E., and Sarnow, P. (2001). Effects of poliovirus infection on nucleo-cytoplasmic trafficking and nuclear pore complex composition. Embo j *20*, 240-249.

103. Hallberg, E., Wozniak, R.W., and Blobel, G. (1993). An integral membrane protein of the

pore membrane domain of the nuclear envelope contains a nucleoporin-like region. J Cell Biol *122*, 513-521.

104. Healy, D., Banyard, A., and Fooks, A. (2012). Rhabdoviruses. In.

105. Heaton, L.A., Hillman, B.I., Hunter, B.G., Zuidema, D., and Jackson, A.O. (1989). Physical map of the genome of sonchus yellow net virus, a plant rhabdovirus with six genes and conserved gene junction sequences. Proceedings of the National Academy of Sciences *86*, 8665-8668.

106. Herranz, M.C., Pallas, V., and Aparicio, F. (2012). Multifunctional roles for the N-terminal basic motif of Alfalfa mosaic virus coat protein: nucleolar/cytoplasmic shuttling, modulation of RNA-binding activity, and virion formation. Mol Plant Microbe Interact *25*, 1093-1103.

107. Hikmet, F., Méar, L., Edvinsson, Å., Micke, P., Uhlén, M., and Lindskog, C. (2020). The protein expression profile of ACE2 in human tissues. bioRxiv, 2020.2003.2031.016048.

108. Hilario, E., and Mackay, J. (2007). Protocols for nucleic acid analysis by nonradioactive probes, Vol 353 (Springer Science & Business Media).

109. Hipper, C., Brault, V., Ziegler-Graff, V., and Revers, F. (2013). Viral and Cellular Factors Involved in Phloem Transport of Plant Viruses. Frontiers in Plant Science *4*.

110. Hiscox, J.A. (2007). RNA viruses: hijacking the dynamic nucleolus. Nat Rev Microbiol *5*, 119-127.

111. Hogenhout, S.A., Redinbaugh, M.G., and Ammar, E.-D. (2003). Plant and animal rhabdovirus host range: a bug's view. Trends in Microbiology *11*, 264-271.

112. Hondele, M., Heinrich, S., De Los Rios, P., and Weis, K. (2020). Membraneless organelles: phasing out of equilibrium. Emerging Topics in Life Sciences.

113. Huh, W.K., Falvo, J.V., Gerke, L.C., Carroll, A.S., Howson, R.W., Weissman, J.S., and O'Shea, E.K. (2003). Global analysis of protein localization in budding yeast. Nature *425*, 686-691.

114. Hui, W., Yang, Y., Wu, G., Wang, Y., Zaky Zayed, M., and Chen, X. (2018). Differential gene expression analyses related to fruit yield of Jatropha curcas L. using RNA-seq. Biotechnology & Biotechnological Equipment *32*, 1126-1133.

115. Hull, R. (2009). Mechanical Inoculation of Plant Viruses. Current Protocols in Microbiology *13*, 16B.16.11-16B.16.14

116. Hull, R. (2014). Chapter 10 - Movement of Viruses Within Plants. In Plant Virology (Fifth Edition), R. Hull, ed. (Boston: Academic Press), pp. 531-603.

117. Hummeler, K., Koprowski, H., and Wiktor, T.J. (1967). Structure and development of rabies virus in tissue culture. J Virol *1*, 152-170.

118. Hyodo, K., and Okuno, T. (2020). Chapter Two - Hijacking of host cellular components as proviral factors by plant-infecting viruses. In Advances in Virus Research, J.P. Carr, and M.J. Roossinck, eds. (Academic Press), pp. 37-86.

119. Ivanov, I., Yabukarski, F., Ruigrok, R.W., and Jamin, M. (2011). Structural insights into the rhabdovirus transcription/replication complex. Virus Res *162*, 126-137.

120. Iverson, L.E., and Rose, J.K. (1981). Localized attenuation and discontinuous synthesis during vesicular stomatitis virus transcription. Cell *23*, 477-484.

121. Izumi, R.E., Valdez, B., Banerjee, R., Srivastava, M., and Dasgupta, A. (2001). Nucleolin stimulates viral internal ribosome entry site-mediated translation. Virus Research *76*, 17-29.

122. Jackson, A.O., Dietzgen, R.G., Goodin, M.M., Bragg, J.N., and Deng, M. (2005). Biology of plant rhabdoviruses. Annu Rev Phytopathol *43*, 623-660.

123. Jackson, A.O., and Li, Z. (2016). Developments in plant negative-strand RNA virus reverse genetics. Annual review of phytopathology *54*, 469-498.

124. Jayakar, H.R., and Whitt, M.A. (2002). Identification of two additional translation products from the matrix (M) gene that contribute to vesicular stomatitis virus cytopathology. Journal of virology *76*, 8011-8018.

125. Jean-Philippe, J., Paz, S., and Caputi, M. (2013). hnRNP A1: the Swiss army knife of gene expression. Int J Mol Sci *14*, 18999-19024.

126. Jiang, X.-S., Tang, L.-Y., Dai, J., Zhou, H., Li, S.-J., Xia, Q.-C., Wu, J.-R., and Zeng, R. (2005). Quantitative Analysis of Severe Acute Respiratory Syndrome (SARS)-associated Coronavirus-infected Cells Using Proteomic Approaches. Molecular & Cellular Proteomics *4*, 902.

127. Jones, J.D., and Dangl, J.L. (2006). The plant immune system. Nature *444*, 323-329.

128. Kabachinski, G., and Schwartz, T.U. (2015). The nuclear pore complex – structure and function at a glance. Journal of Cell Science *128*, 423.

129. Kaerlein, M., and Horak, I. (1976). Phosphorylation of ribosomal proteins in HeLa cells infected with vaccinia virus. Nature *259*, 150-151.

130. Kalderon, D., Roberts, B.L., Richardson, W.D., and Smith, A.E. (1984). A short amino acid sequence able to specify nuclear location. Cell *39*, 499-509.

131. Kalinina, N.O., Makarova, S., Makhotenko, A., Love, A.J., and Taliansky, M. (2018). The Multiple Functions of the Nucleolus in Plant Development, Disease and Stress Responses. Front Plant Sci *9*, 132.

132. Kambham, R.p., Chuang, C., and Nagy, P. (2017). Co-opting ATP-generating glycolytic enzyme PGK1 phosphoglycerate kinase facilitates the assembly of viral replicase complexes. PLOS Pathogens *13*, e1006689.

133. Kane, M., Rebensburg, S.V., Takata, M.A., Zang, T.M., Yamashita, M., Kvaratskhelia, M., and Bieniasz, P.D. (2018). Nuclear pore heterogeneity influences HIV-1 infection and the antiviral activity of MX2. eLife *7*, e35738.

134. Karlas, A., Machuy, N., Shin, Y., Pleissner, K.-P., Artarini, A., Heuer, D., Becker, D., Khalil, H., Ogilvie, L.A., Hess, S.*, et al.* (2010). Genome-wide RNAi screen identifies human host factors crucial for influenza virus replication. Nature *463*, 818-822.

135. Kaur, R., and Lal, S.K. (2020). The multifarious roles of heterogeneous ribonucleoprotein A1 in viral infections. Reviews in Medical Virology *30*, e2097.

136. Keating, J.A., and Striker, R. (2012). Phosphorylation events during viral infections

provide potential therapeutic targets. Reviews in medical virology *22*, 166-181.

137. Keen, J., and Moore, H. (2015). The Genotype-Tissue Expression (GTEx) Project: Linking Clinical Data with Molecular Analysis to Advance Personalized Medicine. Journal of Personalized Medicine *5*, 22-29.

138. Kennedy, I.M., Stevely, W.S., and Leader, D.P. (1981). Phosphorylation of ribosomal proteins in hamster fibroblasts infected with pseudorabies virus or herpes simplex virus. Journal of Virology *39*, 359-366.

139. Khoonsari, P.E., Shevchenko, G., Herman, S., Remnestål, J., Giedraitis, V., Brundin, R., Degerman Gunnarsson, M., Kilander, L., Zetterberg, H., Nilsson, P.*, et al.* (2019). Improved Differential Diagnosis of Alzheimer's Disease by Integrating ELISA and Mass Spectrometry-Based Cerebrospinal Fluid Biomarkers. J Alzheimers Dis *67*, 639-651.

140. Kim, S.H., Macfarlane, S., Kalinina, N.O., Rakitina, D.V., Ryabov, E.V., Gillespie, T., Haupt, S., Brown, J.W.S., and Taliansky, M. (2007). Interaction of a plant virus-encoded protein with the major nucleolar protein fibrillarin is required for systemic virus infection. Proc Natl Acad Sci U S A *104*, 11115-11120.

141. Kim, S.J., Fernandez-Martinez, J., Nudelman, I., Shi, Y., Zhang, W., Raveh, B., Herricks, T., Slaughter, B.D., Hogan, J.A., Upla, P.*, et al.* (2018). Integrative structure and functional anatomy of a nuclear pore complex. Nature *555*, 475-482.

142. Klepikova, A.V., and Penin, A.A. (2019). Gene Expression Maps in Plants: Current State and Prospects. Plants (Basel) *8*, 309.

143. Kobiler, O., Drayman, N., Butin-Israeli, V., and Oppenheim, A. (2012). Virus strategies for passing the nuclear envelope barrier. Nucleus *3*, 526-539.

144. König, R., Stertz, S., Zhou, Y., Inoue, A., Hoffmann, H.H., Bhattacharyya, S., Alamares, J.G., Tscherne, D.M., Ortigoza, M.B., Liang, Y.*, et al.* (2010). Human host factors required for influenza virus replication. Nature *463*, 813-817.

145. Krause, K., Oetke, S., and Krupinska, K. (2012). Dual targeting and retrograde translocation: regulators of plant nuclear gene expression can be sequestered by plastids. Int J Mol Sci *13*, 11085-11101.

146. Krupinska, K., Blanco, N.E., Oetke, S., and Zottini, M. (2020). Genome communication in plants mediated by organelle-n-ucleus-located proteins. Philos Trans R Soc Lond B Biol Sci *375*, 20190397.

147. Kumar, K.R.R., and Kirti, P.B. (2011). Differential gene expression in Arachis diogoi upon interaction with peanut late leaf spot pathogen, Phaeoisariopsis personata and characterization of a pathogen induced cyclophilin. Plant Molecular Biology *75*, 497-513.

148. Kuss, S.K., Mata, M.A., Zhang, L., and Fontoura, B.M.A. (2013). Nuclear imprisonment: viral strategies to arrest host mRNA nuclear export. Viruses *5*, 1824-1849.

149. Laliberté, J.-F., and Sanfaçon, H. (2010). Cellular Remodeling During Plant Virus Infection. Annual Review of Phytopathology *48*, 69-91.

150. Lafontaine, D.L.J., Riback, J.A., Bascetin, R., and Brangwynne, C.P. (2020). The nucleolus as a multiphase liquid condensate. Nature Reviews Molecular Cell Biology.

151. Lam, Y.W., Lamond, A.I., Mann, M., and Andersen, J.S. (2007). Analysis of nucleolar protein dynamics reveals the nuclear degradation of ribosomal proteins. Curr Biol *17*, 749-760.

152. Lam, Y.W., Trinkle-Mulcahy, L., and Lamond, A.I. (2005). The nucleolus. Journal of Cell Science *118*, 1335.

153. Lange, A., Mills, R.E., Lange, C.J., Stewart, M., Devine, S.E., and Corbett, A.H. (2007). Classical nuclear localization signals: definition, function, and interaction with importin alpha. J Biol Chem *282*, 5101-5105.

154. LaPointe, A.T., Gebhart, N.N., Meller, M.E., Hardy, R.W., and Sokoloski, K.J. (2018). Identification and Characterization of Sindbis Virus RNA-Host Protein Interactions. Journal of Virology *92*, e02171-02117.

155. Le Sage, V., and Mouland, A.J. (2013). Viral subversion of the nuclear pore complex. Viruses *5*, 2019-2042.

156. Leastro, M.O., Kitajima, E.W., Silva, M.S., Resende, R.O., and Freitas-Astúa, J. (2018). Dissecting the Subcellular Localization, Intracellular Trafficking, Interactions, Membrane Association, and Topology of Citrus Leprosis Virus C Proteins. Frontiers in Plant Science *9*.

157. Lee, S., Zhang, C., Arif, M., Liu, Z., Benfeitas, R., Bidkhori, G., Deshmukh, S., Al Shobky, M., Lovric, A., Boren, J.*, et al.* (2018). TCSBN: a database of tissue and cancer specific biological networks. Nucleic Acids Res *46*, D595-d600.

158. Levin, A., Neufeldt, C.J., Pang, D., Wilson, K., Loewen-Dobler, D., Joyce, M.A., Wozniak, R.W., and Tyrrell, D.L.J. (2014). Functional characterization of nuclear localization and export signals in hepatitis C virus proteins and their role in the membranous web. PLoS One *9*, e114629-e114629.

159. Levy, A., Zheng, J.Y., and Lazarowitz, S.G. (2013). The tobamovirus Turnip Vein Clearing Virus 30-kilodalton movement protein localizes to novel nuclear filaments to enhance virus infection. J Virol *87*, 6428-6440.

160. Lewis, P.F., and Emerman, M. (1994). Passage through mitosis is required for oncoretroviruses but not for the human immunodeficiency virus. Journal of virology *68*, 510-516.

161. Li, H. (2018). Minimap2: pairwise alignment for nucleotide sequences. Bioinformatics *34*, 3094-3100.

162. Li, H., Handsaker, B., Wysoker, A., Fennell, T., Ruan, J., Homer, N., Marth, G., Abecasis, G., and Durbin, R. (2009). 1000 Genome Project Data Processing Subgroup. 2009. The sequence alignment/map format and samtools. Bioinformatics *25*, 2078-2079.

163. Li, M., Ramage, H., and Cherry, S. (2020). Deciphering flavivirus-host interactions using quantitative proteomics. Curr Opin Immunol *66*, 90-97.

164. Li, S. (2019). Regulation of Ribosomal Proteins on Viral Infection. Cells *8*, 508.

165. Libault, M., Farmer, A., Brechenmacher, L., Drnevich, J., Langley, R.J., Bilgin, D.D., Radwan, O., Neece, D.J., Clough, S.J., May, G.D.*, et al.* (2010). Complete transcriptome

of the soybean root hair cell, a single-cell model, and its alteration in response to Bradyrhizobium japonicum infection. Plant Physiol *152*, 541-552.

166. Lin, D.H., and Hoelz, A. (2019). The Structure of the Nuclear Pore Complex (An Update). Annual Review of Biochemistry *88*, 725-783.

167. Liu, T., Zhang, L., Joo, D., and Sun, S.-C. (2017). NF-κB signaling in inflammation. Signal Transduction and Targeted Therapy *2*, 17023.

168. Lobaina, Y., and Perera, Y. (2019). Implication of B23/NPM1 in Viral Infections, Potential Uses of B23/NPM1 Inhibitors as Antiviral Therapy. Infect Disord Drug Targets *19*, 2-16.

169. Lucy, A.P., Guo, H.-S., Li, W.-X., and Ding, S.-W. (2000). Suppression of post-transcriptional gene silencing by a plant viral protein localized in the nucleus. The EMBO Journal *19*, 1672-1680.

170. Lukhovitskaya, N.I., Cowan, G.H., Vetukuri, R.R., Tilsner, J., Torrance, L., and Savenkov, E.I. (2015). Importin-α-Mediated Nucleolar Localization of Potato Mop-Top Virus TRIPLE GENE BLOCK1 (TGB1) Protein Facilitates Virus Systemic Movement, Whereas TGB1 Self-Interaction Is Required for Cell-to-Cell Movement in *Nicotiana benthamiana*. Plant Physiology *167*, 738-752.

171. Lukic, Z., Dharan, A., Fricke, T., Diaz-Griffero, F., and Campbell, E.M. (2014). HIV-1 uncoating is facilitated by dynein and kinesin 1. Journal of virology *88*, 13613-13625.

172. Luo, J.L., Kamata, H., and Karin, M. (2005). IKK/NF-kappaB signaling: balancing life and death--a new approach to cancer therapy. J Clin Invest *115*, 2625-2632.

173. Lyles, D.S. (2000). Cytopathogenesis and inhibition of host gene expression by RNA viruses. Microbiol Mol Biol Rev *64*, 709-724.

174. Macara, I.G. (2001). Transport into and out of the Nucleus. Microbiology and Molecular Biology Reviews *65*, 570.

175. Maeto, C., Knott, M., Linero, F., Ellenberg, P., Scolaro, L., and Castilla, V. (2011). Differential effect of acute and persistent Junin virus infections on the nucleo-cytoplasmic trafficking and expression of heterogeneous nuclear ribonucleoproteins type A and B. The Journal of general virology *92*, 2181-2190.

176. Mann, K.S., Johnson, K.N., and Dietzgen, R.G. (2015). Cytorhabdovirus phosphoprotein shows RNA silencing suppressor activity in plants, but not in insect cells. Virology *476*, 413-418.

177. Martin, K., and Helenius, A. (1991). Nuclear transport of influenza virus ribonucleoproteins: the viral matrix protein (M1) promotes export and inhibits import. Cell *67*, 117-130.

178. Martin, K., Kopperud, K., Chakrabarty, R., Banerjee, R., Brooks, R., and Goodin, M.M. (2009). Transient expression in Nicotiana benthamiana fluorescent marker lines provides enhanced definition of protein localization, movement and interactions in planta. The Plant Journal *59*, 150-162.

179. Martin, K.M., Dietzgen, R.G., Wang, R., and Goodin, M.M. (2012). Lettuce necrotic

yellows cytorhabdovirus protein localization and interaction map, and comparison with nucleorhabdoviruses. Journal of General Virology *93*, 906-914.

180. Martin, R.M., Ter-Avetisyan, G., Herce, H.D., Ludwig, A.K., Lättig-Tünnemann, G., and Cardoso, M.C. (2015). Principles of protein targeting to the nucleolus. Nucleus *6*, 314-325.

181. Mateo, M., Reid, S.P., Leung, L.W., Basler, C.F., and Volchkov, V.E. (2010). Ebolavirus VP24 Binding to Karyopherins Is Required for Inhibition of Interferon Signaling. Journal of Virology *84*, 1169.

182. Meier, I., and Brkljacic, J. (2009). Adding pieces to the puzzling plant nuclear envelope. Current Opinion in Plant Biology *12*, 752-759.

183. Meier, I., Richards, E.J., and Evans, D.E. (2017). Cell Biology of the Plant Nucleus. Annu Rev Plant Biol *68*, 139-172.

184. Meng, W., Wang, X.-J., and Wang, H.-C.R. (2019). Targeting nuclear proteins for control of viral replication. Critical Reviews in Microbiology *45*, 495-513.

185. Menzel, W., Richert-Poggeler, K., Winter, S., and Knierim, D. (2018). Characterization of a nucleorhabdovirus from Physostegia. Acta horticulturae.

186. Meyuhas, O. (2008). Chapter 1 Physiological Roles of Ribosomal Protein S6: One of Its Kind. In Int Rev Cell Mol Biol (Academic Press), pp. 1-37.

187. Miyake, Y., Keusch, J.J., Decamps, L., Ho-Xuan, H., Iketani, S., Gut, H., Kutay, U., Helenius, A., and Yamauchi, Y. (2019). Influenza virus uses transportin 1 for vRNP debundling during cell entry. Nat Microbiol *4*, 578-586.

188. Monette, A., Ajamian, L., López-Lastra, M., and Mouland, A.J. (2009). Human immunodeficiency virus type 1 (HIV-1) induces the cytoplasmic retention of heterogeneous nuclear ribonucleoprotein A1 by disrupting nuclear import: implications for HIV-1 gene expression. The Journal of biological chemistry *284*, 31350-31362.

189. Monette, A., Panté, N., and Mouland, A.J. (2011). HIV-1 remodels the nuclear pore complex. J Cell Biol *193*, 619-631.

190. Mori, Y., Okabayashi, T., Yamashita, T., Zhao, Z., Wakita, T., Yasui, K., Hasebe, F., Tadano, M., Konishi, E., Moriishi, K.*, et al.* (2005). Nuclear localization of Japanese encephalitis virus core protein enhances viral replication. J Virol *79*, 3448-3458.

191. Morin, E., Sjöberg, E., Tjomsland, V., Testini, C., Lindskog, C., Franklin, O., Sund, M., Öhlund, D., Kiflemariam, S., Sjöblom, T.*, et al.* (2018). VEGF receptor-2/neuropilin 1 trans-complex formation between endothelial and tumor cells is an independent predictor of pancreatic cancer survival. J Pathol *246*, 311-322.

192. Morita, M., Kuba, K., Ichikawa, A., Nakayama, M., Katahira, J., Iwamoto, R., Watanebe, T., Sakabe, S., Daidoji, T., Nakamura, S.*, et al.* (2013). The Lipid Mediator Protectin D1 Inhibits Influenza Virus Replication and Improves Severe Influenza. Cell *153*, 112-125.

193. Munier, S., Rolland, T., Diot, C., Jacob, Y., and Naffakh, N. (2013). Exploration of Binary Virus–Host Interactions Using an Infectious Protein Complementation Assay. Molecular & Cellular Proteomics *12*, 2845.

194. Nagy, P.D., and Lin, W. (2020). Taking over Cellular Energy-Metabolism for TBSV Replication: The High ATP Requirement of an RNA Virus within the Viral Replication Organelle. Viruses *12*.

195. Nagy, P.D., and Pogany, J. (2011). The dependence of viral RNA replication on co-opted host factors. Nat Rev Microbiol *10*, 137-149.

196. Nakada, R., Hirano, H., and Matsuura, Y. (2015). Structure of importin-α bound to a non-classical nuclear localization signal of the influenza A virus nucleoprotein. Scientific reports *5*, 15055-15055.

197. Nakai, T., and Howatson, A.F. (1968). The fine structure of vesicular stomatitis virus. Virology *35*, 268-281.

198. Navarro, J.A., Sanchez-Navarro, J.A., and Pallas, V. (2019). Chapter One - Key checkpoints in the movement of plant viruses through the host. In Advances in Virus Research, M. Kielian, T.C. Mettenleiter, and M.J. Roossinck, eds. (Academic Press), pp. 1-64.

199. Nehme, Z., Pasquereau, S., and Herbein, G. (2019). Control of viral infections by epigenetic-targeted therapy. Clinical Epigenetics *11*, 55.

200. Neufeldt, C.J., Joyce, M.A., Levin, A., Steenbergen, R.H., Pang, D., Shields, J., Tyrrell, D.L.J., and Wozniak, R.W. (2013). Hepatitis C virus-induced cytoplasmic organelles use the nuclear transport machinery to establish an environment conducive to virus replication. PLoS pathogens *9*, e1003744-e1003744.

201. Newton, K., Petfalski, E., Tollervey, D., and Cáceres, J.F. (2003). Fibrillarin Is Essential for Early Development and Required for Accumulation of an Intron-Encoded Small Nucleolar RNA in the Mouse. Molecular and Cellular Biology *23*, 8519.

202. Nobuta, K., Venu, R.C., Lu, C., Beló, A., Vemaraju, K., Kulkarni, K., Wang, W., Pillay, M., Green, P.J., Wang, G.L.*, et al.* (2007). An expression atlas of rice mRNAs and small RNAs. Nat Biotechnol *25*, 473-477.

203. O'Neill, R.E., Jaskunas, R., Blobel, G., Palese, P., and Moroianu, J. (1995). Nuclear import of influenza virus RNA can be mediated by viral nucleoprotein and transport factors required for protein import. J Biol Chem *270*, 22701-22704.

204. Onischenko, E., and Weis, K. (2011). Nuclear pore complex-a coat specifically tailored for the nuclear envelope. Current opinion in cell biology *23*, 293-301.

205. Ooi, Y.S., Majzoub, K., Flynn, R.A., Mata, M.A., Diep, J., Li, J.K., van Buuren, N., Rumachik, N., Johnson, A.G., Puschnik, A.S.*, et al.* (2019). An RNA-centric dissection of host complexes controlling flavivirus infection. Nature Microbiology *4*, 2369-2382.

206. Ori, A., Banterle, N., Iskar, M., Andrés-Pons, A., Escher, C., Khanh Bui, H., Sparks, L., Solis-Mezarino, V., Rinner, O., Bork, P.*, et al.* (2013). Cell type-specific nuclear pores: a case in point for context-dependent stoichiometry of molecular machines. Mol Syst Biol *9*, 648-648.

207. Osterbaan, L., and Fuchs, M. (2019). Dynamic interactions between plant viruses and their hosts for symptom development. Journal of Plant Pathology *101*.

208. Panté, N., and Aebi, U. (1993). The nuclear pore complex. J Cell Biol *122*, 977-984.

209. Park, N., Katikaneni, P., Skern, T., and Gustin, K.E. (2008). Differential Targeting of Nuclear Pore Complex Proteins in Poliovirus-Infected Cells. Journal of Virology *82*, 1647.

210. Paschal, B.M., and Gerace, L. (1995). Identification of NTF2, a cytosolic factor for nuclear import that interacts with nuclear pore complex protein p62. J Cell Biol *129*, 925-937.

211. Pasdeloup, D., Blondel, D., Isidro, A.L., and Rixon, F.J. (2009). Herpesvirus capsid association with the nuclear pore complex and viral DNA release involve the nucleoporin CAN/Nup214 and the capsid protein pUL25. Journal of virology *83*, 6610-6623.

212. Pattnaik, A.K., Hwang, L., Li, T., Englund, N., Mathur, M., Das, T., and Banerjee, A.K. (1997). Phosphorylation within the amino-terminal acidic domain I of the phosphoprotein of vesicular stomatitis virus is required for transcription but not for replication. Journal of Virology *71*, 8167.

213. Pawlotsky, J.M., Chevaliez, S., and McHutchison, J.G. (2007). The Hepatitis C Virus Life Cycle as a Target for New Antiviral Therapies. Gastroenterology *132*, 1979-1998.

214. Payne, S. (2017). Chapter 19 - Family Rhabdoviridae. In Viruses, S. Payne, ed. (Academic Press), pp. 165-172.

215. Pesti, R., Kontra, L., Paul, K., Vass, I., Csorba, T., Havelda, Z., and Várallyay, É. (2019). Differential gene expression and physiological changes during acute or persistent plant virus interactions may contribute to viral symptom differences. PLoS One *14*, e0216618.

216. Peters, D., and Black, L. (1970). Infection of primary cultures of aphid cells with a plant virus. Virology *40*, 847-853.

217. Peters, D., and Kitajima, E. (1970). Purification and electron microscopy of sowthistle yellow vein virus. Virology *41*, 135-150.

218. Pettit Kneller, E.L., Connor, J.H., and Lyles, D.S. (2009). hnRNPs Relocalize to the Cytoplasm following Infection with Vesicular Stomatitis Virus. Journal of Virology *83*, 770-780.

219. Porter, F.W., Brown, B., and Palmenberg, A.C. (2010). Nucleoporin phosphorylation triggered by the encephalomyocarditis virus leader protein is mediated by mitogen-activated protein kinases. Journal of virology *84*, 12538-12548.

220. Porter, F.W., and Palmenberg, A.C. (2009). Leader-induced phosphorylation of nucleoporins correlates with nuclear trafficking inhibition by cardioviruses. Journal of virology *83*, 1941-1951.

221. Quan, B., Seo, H.-S., Blobel, G., and Ren, Y. (2014). Vesiculoviral matrix (M) protein occupies nucleic acid binding site at nucleoporin pair (Rae1•Nup98). Proceedings of the National Academy of Sciences *111*, 9127.

222. Rajamäki, M.-L., Sikorskaite-Gudziuniene, S., Sarmah, N., Varjosalo, M., and Valkonen, J.P.T. (2020). Nuclear proteome of virus-infected and healthy potato leaves. BMC plant biology *20*, 355-355.

223. Rajamäki, M.-L., and Valkonen, J.P.T. (2009). Control of nuclear and nucleolar localization of nuclear inclusion protein a of picorna-like Potato virus A in Nicotiana species. Plant Cell *21*, 2485-2502.

224. Rajani, K.R., Pettit Kneller, E.L., McKenzie, M.O., Horita, D.A., Chou, J.W., and Lyles, D.S. (2012). Complexes of vesicular stomatitis virus matrix protein with host Rae1 and Nup98 involved in inhibition of host transcription. PLoS Pathog *8*, e1002929.

225. Rajoo, S., Vallotton, P., Onischenko, E., and Weis, K. (2018). Stoichiometry and compositional plasticity of the yeast nuclear pore complex revealed by quantitative fluorescence microscopy. Proc Natl Acad Sci U S A *115*, E3969-E3977.

226. Ramalho, T., Figueira, A., Sotero, A., Wang, R., Duarte, P.G., Farman, M., and Goodin, M. (2014). Characterization of Coffee ringspot virus-Lavras: A model for an emerging threat to coffee production and quality. Virology *464*, 385-396.

227. Ramírez-González, R.H., Borrill, P., Lang, D., Harrington, S.A., Brinton, J., Venturini, L., Davey, M., Jacobs, J., van Ex, F., Pasha, A.*, et al.* (2018). The transcriptional landscape of polyploid wheat. Science *361*.

228. Redinbaugh, M.G., and Hogenhout, S.A. (2005). Plant rhabdoviruses. Curr Top Microbiol Immunol *292*, 143-163.

229. Redondo, N., Madan, V., Alvarez, E., and Carrasco, L. (2015). Impact of Vesicular Stomatitis Virus M Proteins on Different Cellular Functions. PLoS One *10*, e0131137-e0131137.

230. Regev, A., Teichmann, S.A., Lander, E.S., Amit, I., Benoist, C., Birney, E., Bodenmiller, B., Campbell, P., Carninci, P., Clatworthy, M.*, et al.* (2017). The Human Cell Atlas. eLife *6*, e27041.

231. Reid, S.P., Leung, L.W., Hartman, A.L., Martinez, O., Shaw, M.L., Carbonnelle, C., Volchkov, V.E., Nichol, S.T., and Basler, C.F. (2006). Ebola virus VP24 binds karyopherin alpha1 and blocks STAT1 nuclear accumulation. J Virol *80*, 5156-5167.

232. Rein, A. (2013). Murine leukemia virus p12 functions include hitchhiking into the nucleus. Proceedings of the National Academy of Sciences *110*, 9195.

233. Rhee, S.Y., Birnbaum, K.D., and Ehrhardt, D.W. (2019). Towards Building a Plant Cell Atlas. Trends in Plant Science *24*, 303-310.

234. Ribbeck, K., and Görlich, D. (2001). Kinetic analysis of translocation through nuclear pore complexes. The EMBO Journal *20*, 1320-1330.

235. Richardson, J., and Sylvester, E.S. (1968). Further evidence of multiplication of sowthistle yellow vein virus in its aphid vector, Hyperomyzus lactucae. Virology *35*, 347-355.

236. Ricour, C., Delhaye, S., Hato, S.V., Olenyik, T.D., Michel, B., van Kuppeveld, F.J.M., Gustin, K.E., and Michiels, T. (2009). Inhibition of mRNA export and dimerization of interferon regulatory factor 3 by Theiler's virus leader protein. The Journal of general virology *90*, 177-186.

237. Riddick, G., and Macara, I.G. (2005). A systems analysis of importin-{alpha}-{beta}

mediated nuclear protein import. J Cell Biol *168*, 1027-1038.

238. Roberts, K., and Northcote, D.H. (1970). Structure of the Nuclear Pore in Higher Plants. Nature *228*, 385-386.

239. Rowland, R.R., Schneider, P., Fang, Y., Wootton, S., Yoo, D., and Benfield, D.A. (2003). Peptide domains involved in the localization of the porcine reproductive and respiratory syndrome virus nucleocapsid protein to the nucleolus. Virology *316*, 135-145.

240. Ruiz, M.T., Voinnet, O., and Baulcombe, D.C. (1998). Initiation and maintenance of virus-induced gene silencing. Plant Cell *10*, 937-946.

241. Ruiz-Ruiz, S., Soler, N., Sánchez-Navarro, J., Fagoaga, C., López, C., Navarro, L., Moreno, P., Peña, L., and Flores, R. (2013). Citrus tristeza virus p23: determinants for nucleolar localization and their influence on suppression of RNA silencing and pathogenesis. Mol Plant Microbe Interact *26*, 306-318.

242. Rupprecht, C., Kuzmin, I., and Meslin, F. (2017). Lyssaviruses and rabies: current conundrums, concerns, contradictions and controversies. F1000Res *6*, 184.

243. Ryan, E.L., Hollingworth, R., and Grand, R.J. (2016). Activation of the DNA Damage Response by RNA Viruses. Biomolecules *6*, 2.

244. Saha, N., and Tomar, R.S. (2018). Epigenetics and Infectious Pathogens: Interactions, Ploy and Perspectives. In Infectious Diseases and Your Health, P.P. Singh, ed. (Singapore: Springer Singapore), pp. 359-388.

245. Sanchez, E.L., and Lagunoff, M. (2015). Viral activation of cellular metabolism. Virology *479-480*, 609-618.

246. Schmid, M., Speiseder, T., Dobner, T., and Gonzalez, R.A. (2014). DNA virus replication compartments. Journal of virology *88*, 1404-1420.

247. Schnell, M.J., Buonocore, L., Whitt, M.A., and Rose, J.K. (1996). The minimal conserved transcription stop-start signal promotes stable expression of a foreign gene in vesicular stomatitis virus. Journal of virology *70*, 2318-2323.

248. Schoelz, J.E., Harries, P.A., and Nelson, R.S. (2011). Intracellular Transport of Plant Viruses: Finding the Door out of the Cell. Molecular Plant *4*, 813-831.

249. Scholthof, K.-B.G., Hillman, B.I., Modrell, B., Heaton, L.A., and Jackson, A.O. (1994). Characterization and Detection of sc4: A Sixth Gene Encoded by Sonchus Yellow Net Virus. Virology *204*, 279-288.

250. Schreiber, A.W., Sutton, T., Caldo, R.A., Kalashyan, E., Lovell, B., Mayo, G., Muehlbauer, G.J., Druka, A., Waugh, R., Wise, R.P.*, et al.* (2009). Comparative transcriptomics in the Triticeae. BMC Genomics *10*, 285.

251. Schultz, M., and Harrap, K. (1976). The structural polypeptides of sowthistle yellow vein virus (SYVV). Archives of virology *50*, 173-176.

252. Scott, M.S., Boisvert, F.-M., McDowall, M.D., Lamond, A.I., and Barton, G.J. (2010). Characterization and prediction of protein nucleolar localization sequences. Nucleic Acids Res *38*, 7388-7399.

253. Sekhon, R.S., Lin, H., Childs, K.L., Hansey, C.N., Buell, C.R., de Leon, N., and

Kaeppler, S.M. (2011). Genome-wide atlas of transcription during maize development. Plant J *66*, 553-563.

254. Sen Gupta, A., Joshi, G., Pawar, S., and Sengupta, K. (2018). Nucleolin modulates compartmentalization and dynamics of histone 2B-ECFP in the nucleolus. Nucleus *9*, 350-367.

255. Sen, R., and Baltimore, D. (1986). Multiple nuclear factors interact with the immunoglobulin enhancer sequences. Cell *46*, 705-716.

256. Severin, A.J., Woody, J.L., Bolon, Y.T., Joseph, B., Diers, B.W., Farmer, A.D., Muehlbauer, G.J., Nelson, R.T., Grant, D., Specht, J.E.*, et al.* (2010). RNA-Seq Atlas of Glycine max: a guide to the soybean transcriptome. BMC Plant Biol *10*, 160.

257. Shakoor, N., Nair, R., Crasta, O., Morris, G., Feltus, A., and Kresovich, S. (2014). A Sorghum bicolor expression atlas reveals dynamic genotype-specific expression profiles for vegetative tissues of grain, sweet and bioenergy sorghums. BMC Plant Biol *14*, 35.

258. Sheth, B.P., and Thaker, V.S. (2014). Plant systems biology: insights, advances and challenges. Planta *240*, 33-54.

259. Shiroki, K., Isoyama, T., Kuge, S., Ishii, T., Ohmi, S., Hata, S., Suzuki, K., Takasaki, Y., and Nomoto, A. (1999). Intracellular redistribution of truncated La protein produced by poliovirus 3Cpro-mediated cleavage. Journal of virology *73*, 2193-2200.

260. Simpson, J.P., Di Leo, R., Dhanoa, P.K., Allan, W.L., Makhmoudova, A., Clark, S.M., Hoover, G.J., Mullen, R.T., and Shelp, B.J. (2008). Identification and characterization of a plastid-localized Arabidopsis glyoxylate reductase isoform: comparison with a cytosolic isoform and implications for cellular redox homeostasis and aldehyde detoxification. Journal of experimental botany *59*, 2545-2554.

261. Singh, A.P., Galland, R., Finch-Edmondson, M.L., Grenci, G., Sibarita, J.-B., Studer, V., Viasnoff, V., and Saunders, T.E. (2017). 3D Protein Dynamics in the Cell Nucleus. Biophys J *112*, 133-142.

262. Sirri, V., Urcuqui-Inchima, S., Roussel, P., and Hernandez-Verdun, D. (2008). Nucleolus: the fascinating nuclear body. Histochem Cell Biol *129*, 13-31.

263. Sitterlin, D. (2004). Characterization of the Drosophila Rae1 protein as a G1 phase regulator of the cell cycle. Gene *326*, 107-116.

264. Sjöstedt, E., Zhong, W., Fagerberg, L., Karlsson, M., Mitsios, N., Adori, C., Oksvold, P., Edfors, F., Limiszewska, A., Hikmet, F.*, et al.* (2020). An atlas of the protein-coding genes in the human, pig, and mouse brain. Science *367*, eaay5947.

265. Slotte, T., Holm, K., McIntyre, L.M., Lagercrantz, U., and Lascoux, M. (2007). Differential Expression of Genes Important for Adaptation in *Capsella bursa-pastoris* (Brassicaceae). Plant Physiology *145*, 160-173.

266. Stelpflug, S.C., Sekhon, R.S., Vaillancourt, B., Hirsch, C.N., Buell, C.R., de Leon, N., and Kaeppler, S.M. (2016). An Expanded Maize Gene Expression Atlas based on RNA Sequencing and its Use to Explore Root Development. Plant Genome *9*.

267. Stenger, D., Richardson, J., Sylvester, E., Jackson, A., and Moriss, T. (1988). Analysis of

sowthistle yellow vein virus specific RNAs in infected hosts. Phytopathology *78*, 1473-1477.

268. Stenger, D.C., Burbank, L.P., Krugner, R., and Sisterson, M.S. (2019). Individual field-collected glassy-winged sharpshooter vectors harbor sequences from two Xylella fastidiosa subspecies. European Journal of Plant Pathology *155*, 329-338.

269. Stillman, E.A., and Whitt, M.A. (1997). Mutational analyses of the intergenic dinucleotide and the transcriptional start sequence of vesicular stomatitis virus (VSV) define sequences required for efficient termination and initiation of VSV transcripts. Journal of Virology *71*, 2127.

270. Strunze, S., Engelke, Martin F., Wang, I.H., Puntener, D., Boucke, K., Schleich, S., Way, M., Schoenenberger, P., Burckhardt, Christoph J., and Greber, Urs F. (2011). Kinesin-1-Mediated Capsid Disassembly and Disruption of the Nuclear Pore Complex Promote Virus Infection. Cell Host & Microbe *10*, 210-223.

271. Sun, S.C. (2011). Non-canonical NF-κB signaling pathway. Cell Res *21*, 71-85.

272. Sylvester, E., Richardson, J., and Behncken, G. (1970). Effect of dosage on the incubation period of sowthistle yellow vein virus in the aphid Hyperomyzus lactucae. Virology *40*, 590-594.

273. Sylvester, E.S. (1969). Evidence of transovarial passage of the sowthistle yellow vein virus in the aphid Hyperomyzus lactucae. Virology *38*, 440-446.

274. Sylvester, E.S. (1973). Reduction of excretion, reproduction, and survival in Hyperomyzus lactucae fed on plants infected with isolates of sowthistle yellow vein virus. Virology *56*, 632-635.

275. Sylvester, E.S., and Richardson, J. (1969). Additional evidence of multiplication of the sowthistle yellow vein virus in an aphid vector—serial passage. Virology *37*, 26-31.

276. Sylvester, E.S., and Richardson, J. (1970). Infection of Hyperomyzus lactucae by sowthistle yellow vein virus. Virology *42*, 1023-1042.

277. Sylvester, E.S., and Richardson, J. (1971). Decreased survival of Hyperomyzus lactucae inoculated with serially passed sowthistle yellow vein virus. Virology *46*, 310-317.

278. Sylvester, E.S., and Richardson, J. (1992). Aphid-borne rhabdoviruses—relationships with their vectors. In Advances in disease vector research (Springer), pp. 313-341.

279. Tajrishi, M.M., Tuteja, R., and Tuteja, N. (2011). Nucleolin: The most abundant multifunctional phosphoprotein of nucleolus. Commun Integr Biol *4*, 267-275.

280. Taliansky, M., Torrance, L., and Kalinina, N.O. (2008). Role of Plant Virus Movement Proteins. In Plant Virology Protocols: From Viral Sequence to Protein Function, G.D. Foster, I.E. Johansen, Y. Hong, and P.D. Nagy, eds. (Totowa, NJ: Humana Press), pp. 33-54.

281. Tamura, K., Fukao, Y., Iwamoto, M., Haraguchi, T., and Hara-Nishimura, I. (2010). Identification and Characterization of Nuclear Pore Complex Components in *Arabidopsis thaliana*. Plant Cell *22*, 4084-4097.

282. Tamura, K., and Hara-Nishimura, I. (2012). The molecular architecture of the plant

nuclear pore complex. Journal of Experimental Botany *64*, 823-832.

283. Tang, Y., Huang, A., and Gu, Y. (2020). Global profiling of plant nuclear membrane proteome in Arabidopsis. Nat Plants *6*, 838-847.

284. Tsuda, Y., Mori, Y., Abe, T., Yamashita, T., Okamoto, T., Ichimura, T., Moriishi, K., and Matsuura, Y. (2006). Nucleolar Protein B23 Interacts with Japanese Encephalitis Virus Core Protein and Participates in Viral Replication. Microbiology and Immunology *50*, 225-234.

285. Ueki, S., and Citovsky, V. (2007). Spread Throughout the Plant: Systemic Transport of Viruses. In Viral Transport in Plants, E. Waigmann, and M. Heinlein, eds. (Berlin, Heidelberg: Springer Berlin Heidelberg), pp. 85-118.

286. Uhlén, M., Björling, E., Agaton, C., Szigyarto, C.A., Amini, B., Andersen, E., Andersson, A.C., Angelidou, P., Asplund, A., Asplund, C.*, et al.* (2005). A human protein atlas for normal and cancer tissues based on antibody proteomics. Mol Cell Proteomics *4*, 1920-1932.

287. Uhlén, M., Fagerberg, L., Hallström, B.M., Lindskog, C., Oksvold, P., Mardinoglu, A., Sivertsson, Å., Kampf, C., Sjöstedt, E., Asplund, A.*, et al.* (2015). Proteomics. Tissue-based map of the human proteome. Science *347*, 1260419.

288. Uhlén, M., Karlsson, M.J., Hober, A., Svensson, A.S., Scheffel, J., Kotol, D., Zhong, W., Tebani, A., Strandberg, L., Edfors, F.*, et al.* (2019). The human secretome. Sci Signal *12*.

289. Uhlen, M., Karlsson, M.J., Zhong, W., Tebani, A., Pou, C., Mikes, J., Lakshmikanth, T., Forsström, B., Edfors, F., Odeberg, J.*, et al.* (2019). A genome-wide transcriptomic analysis of protein-coding genes in human blood cells. Science *366*.

290. Uhlen, M., Zhang, C., Lee, S., Sjöstedt, E., Fagerberg, L., Bidkhori, G., Benfeitas, R., Arif, M., Liu, Z., Edfors, F.*, et al.* (2017). A pathology atlas of the human cancer transcriptome. Science *357*.

291. Vandereyken, K., Van Leene, J., De Coninck, B., and Cammue, B.P.A. (2018). Hub Protein Controversy: Taking a Closer Look at Plant Stress Response Hubs. Front Plant Sci *9*, 694.

292. Vasu, S.K., and Forbes, D.J. (2001). Nuclear pores and nuclear assembly. Current Opinion in Cell Biology *13*, 363-375.

293. Vaucheret, H., Béclin, C., and Fagard, M. (2001). Post-transcriptional gene silencing in plants. Journal of Cell Science *114*, 3083.

294. von Kobbe, C., van Deursen, J.M.A., Rodrigues, J.P., Sitterlin, D., Bachi, A., Wu, X., Wilm, M., Carmo-Fonseca, M., and Izaurralde, E. (2000). Vesicular Stomatitis Virus Matrix Protein Inhibits Host Cell Gene Expression by Targeting the Nucleoporin Nup98. Molecular Cell *6*, 1243-1252.

295. Wagner, R.R. (1987). Rhabdovirus biology and infection. In The Rhabdoviruses (Springer), pp. 9-74.

296. Walker, E.J., Jensen, L.M., Croft, S., and Ghildyal, R. (2015). Variation in the nuclear effects of infection by different human rhinovirus serotypes. Frontiers in Microbiology *6*.

297. Walker, E.J., Younessi, P., Fulcher, A.J., McCuaig, R., Thomas, B.J., Bardin, P.G., Jans, D.A., and Ghildyal, R. (2013). Rhinovirus 3C Protease Facilitates Specific Nucleoporin Cleavage and Mislocalisation of Nuclear Proteins in Infected Host Cells. PLoS One *8*, e71316.

298. Walker, P., Dietzgen, R., Joubert, D., and Blasdell, K. (2011). Rhabdovirus accessory genes. Virus research *162*, 110-125.

299. Walker, P.J., Blasdell, K.R., Calisher, C.H., Dietzgen, R.G., Kondo, H., Kurath, G., Longdon, B., Stone, D.M., Tesh, R.B., Tordo, N.*, et al.* (2018). ICTV Virus Taxonomy Profile: Rhabdoviridae. Journal of General Virology *99*, 447-448.

300. chryWalley, J.W., Sartor, R.C., Shen, Z., Schmitz, R.J., Wu, K.J., Urich, M.A., Nery, J.R., Smith, L.G., Schnable, J.C., Ecker, J.R.*, et al.* (2016). Integration of omic networks in a developmental atlas of maize. Science *353*, 814-818.

301. Wang, P., Palese, P., and O'Neill, R.E. (1997). The NPI-1/NPI-3 (karyopherin alpha) binding site on the influenza a virus nucleoprotein NP is a nonconventional nuclear localization signal. J Virol *71*, 1850-1856.

302. Wang, X., Li, M., Zheng, H., Muster, T., Palese, P., Beg, A.A., and García-Sastre, A. (2000). Influenza A Virus NS1 Protein Prevents Activation of NF-κB and Induction of Alpha/Beta Interferon. Journal of Virology *74*, 11566-11573.

303. Weis, K. (2007). The nuclear pore complex: oily spaghetti or gummy bear? Cell *130*, 405-407.

304. Wetzel, T., Dietzgen, R., and Dale, J. (1994). Genomic organization of lettuce necrotic yellows rhabdovirus. Virology *200*, 401-412.

305. Whitfield, A.E., Huot, O.B., Martin, K.M., Kondo, H., and Dietzgen, R.G. (2018). Plant rhabdoviruses—their origins and vector interactions. Current Opinion in Virology *33*, 198-207.

306. Whitham, S.A., Yang, C., and Goodin, M.M. (2006). Global Impact: Elucidating Plant Responses to Viral Infection. Molecular Plant-Microbe Interactions® *19*, 1207-1215.

307. Whittaker, G., Bui, M., and Helenius, A. (1996). Nuclear trafficking of influenza virus ribonuleoproteins in heterokaryons. Journal of virology *70*, 2743-2756.

308. Wiermer, M., Cheng, Y.T., Imkampe, J., Li, M., Wang, D., Lipka, V., and Li, X. (2012). Putative members of the Arabidopsis Nup107-160 nuclear pore sub-complex contribute to pathogen defense. The Plant Journal *70*, 796-808.

309. Willie, K., and Stewart, L.R. (2017). Complete Genome sequence of a new maize-associated cytorhabdovirus. Genome announcements *5*.

310. Wolf, C., and Mofrad, M.R.K. (2008). On the Octagonal Structure of the Nuclear Pore Complex: Insights from Coarse-Grained Models. Biophys J *95*, 2073-2085.

311. Wollmann, G., Davis, J.N., Bosenberg, M.W., and van den Pol, A.N. (2013). Vesicular stomatitis virus variants selectively infect and kill human melanomas but not normal melanocytes. Journal of virology *87*, 6644-6659.

312. Wozniak, R.W., Blobel, G., and Rout, M.P. (1994). POM152 is an integral protein of the

pore membrane domain of the yeast nuclear envelope. J Cell Biol *125*, 31-42.

313. Wright, K.M., Cowan, G.H., Lukhovitskaya, N.I., Tilsner, J., Roberts, A.G., Savenkov, E.I., and Torrance, L. (2010). The N-terminal domain of PMTV TGB1 movement protein is required for nucleolar localization, microtubule association, and long-distance movement. Mol Plant Microbe Interact *23*, 1486-1497.

314. Wu, W., Sankhala, R.S., Florio, T.J., Zhou, L., Nguyen, N.L.T., Lokareddy, R.K., Cingolani, G., and Panté, N. (2017). Synergy of two low-affinity NLSs determines the high avidity of influenza A virus nucleoprotein NP for human importin α isoforms. Scientific reports *7*, 11381-11381.

315. Wu, X., Valli, A., García, J.A., Zhou, X., and Cheng, X. (2019). The Tug-of-War between Plants and Viruses: Great Progress and Many Remaining Questions. Viruses *11*.

316. Xu, W., Edwards, Megan R., Borek, Dominika M., Feagins, Alicia R., Mittal, A., Alinger, Joshua B., Berry, Kayla N., Yen, B., Hamilton, J., Brett, Tom J.*, et al.* (2014). Ebola Virus VP24 Targets a Unique NLS Binding Site on Karyopherin Alpha 5 to Selectively Compete with Nuclear Import of Phosphorylated STAT1. Cell Host & Microbe *16*, 187-200.

317. Xu, X.M., and Meier, I. (2008). The nuclear pore comes to the fore. Trends in Plant Science *13*, 20-27.

318. Yarbrough, M.L., Mata, M.A., Sakthivel, R., and Fontoura, B.M. (2014). Viral subversion of nucleocytoplasmic trafficking. Traffic *15*, 127-140.

319. Yoo, D., Wootton, S.K., Li, G., Song, C., and Rowland, R.R. (2003). Colocalization and interaction of the porcine arterivirus nucleocapsid protein with the small nucleolar RNA-associated protein fibrillarin. J Virol *77*, 12173-12183.

320. Zarei, A., Brikis, C.J., Bajwa, V.S., Chiu, G.Z., Simpson, J.P., DeEll, J.R., Bozzo, G.G., and Shelp, B.J. (2017). Plant Glyoxylate/Succinic Semialdehyde Reductases: Comparative Biochemical Properties, Function during Chilling Stress, and Subcellular Localization. Frontiers in Plant Science *8*.

321. Zhang, G., Guo, G., Hu, X., Zhang, Y., Li, Q., Li, R., Zhuang, R., Lu, Z., He, Z., Fang, X.*, et al.* (2010). Deep RNA sequencing at single base-pair resolution reveals high complexity of the rice transcriptome. Genome Res *20*, 646-654.

322. Zhang, W., Yan, J., Li, X., Xing, Q., Chethana, K.W.T., and Zhao, W. (2019). Transcriptional response of grapevine to infection with the fungal pathogen Lasiodiplodia theobromae. Scientific Reports *9*, 5387.

323. Zheng, L., Du, Z., Lin, C., Mao, Q., Wu, K., Wu, J., Wei, T., Wu, Z., and Xie, L. (2015). Rice stripe tenuivirus p2 may recruit or manipulate nucleolar functions through an interaction with fibrillarin to promote virus systemic movement. Molecular Plant Pathology *16*, 921-930.

324. Zheng, L., He, J., Ding, Z., Zhang, C., and Meng, R. (2018). Identification of Functional Domain(s) of Fibrillarin Interacted with p2 of Rice stripe virus. Can J Infect Dis Med Microbiol *2018*, 8402839.

325. Zhou, X., Lin, W., Sun, K., Wang, S., Zhou, X., Jackson, A.O., and Li, Z. (2019).

Specificity of Plant Rhabdovirus Cell-to-Cell Movement. Journal of Virology *93*, e00296-00219.

326. Zhou, J., Cao, K., Zhang, Z., Wang, L., and Li, S. (2020). Identification and characterization of a novel rhabdovirus infecting peach in China. Virus Research, 197905.

327. Ziemiecki, A., and Peters, D. (1976). The proteins of sowthistle yellow vein virus: characterization and location. Journal of General Virology *32*, 369-381.

VITA

A. Education

Bachelor of Science, Plant Pathology with Research Distinction, Minor in Agronomy. The Ohio State University, Columbus, OH. May 2018

B. Professional positions held

Teaching assistant, ABT 120: Genetics and Society. University of Kentucky. Jan 2019-May 2019.

C. Scholastic and professional honors

Graduate school travel award recipient. March 2020.

D. Professional publications

Stenger, D.C., Burbank, L.P., Wang, R., Stewart, A.A., **Mathias, C.,** and Goodin, M.M. (2020). Lost and found: Rediscovery and genomic characterization of sowthistle yellow vein virus after a 30+ year hiatus. Virus Research 284, 197987.

Caleb Mathias